IN VIVO ULTRASOUND ASSESSMENT OF CAROTID ARTERY WALLS AND PLAQUES

Integrating morphological and mechanical characteristics

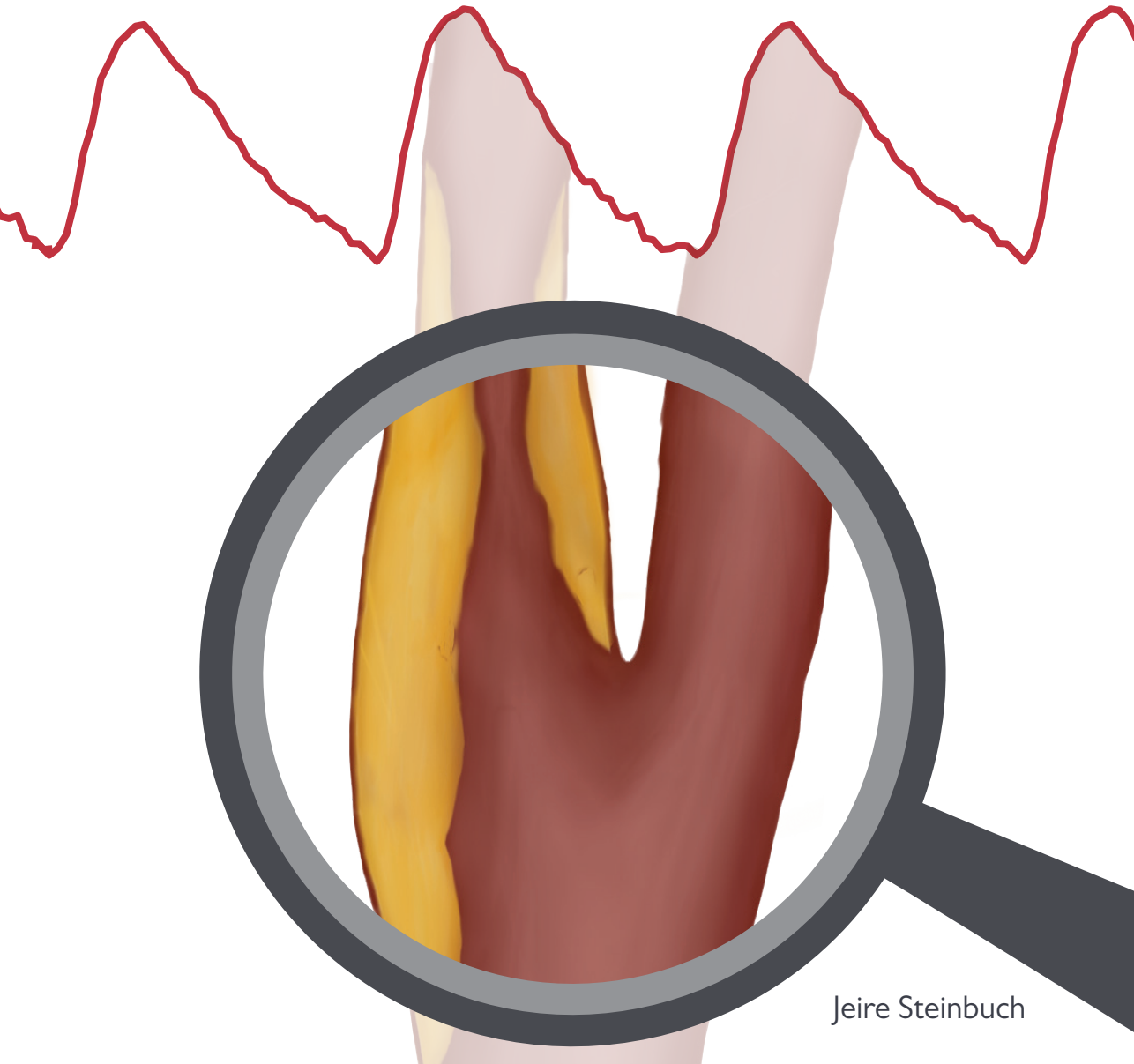

Jeire Steinbuch

ISBN 978 94 6159 693 2

Cover design and lay-out by Cynthia Vermeulen, www.cynthiavermeulen.nl

Printed by Datawyse / Universitaire Pers, Maastricht, The Netherlands

In vivo ultrasound assessment of carotid artery walls and plaques

Integrating morphological and mechanical characteristics

PROEFSCHRIFT

ter verkrijging van de graad van doctor aan de Universiteit Maastricht,

op gezag van de Rector Magnificus, Prof. dr. Rianne M. Letschert

volgens het besluit van het College van Decanen,

in het openbaar te verdedigen

op vrijdag 2 juni 2017 om 10.00

Door:

Jeire Steinbuch
geboren op 3 januari 1988,
te Heeze, Nederland

Promotor
Prof. dr. W.H. Mess

Copromotor
Dr. ir. K.D. Reesink

Beoordelingscommissie
Prof. dr. A.A. Kroon (voorzitter)
Prof. dr. P. Boutouyrie (l'Hôpital Européen Georges Pompidou, Frankrijk)
Prof. dr. C.L. De Korte (Radboudumc Nijmegen)
Prof. dr. G.W.H. Schurink
Dr. J. Staals

This research was performed within the framework of the Center of Translational Molecular Medicine, project PARISK (grant 01C-202), and was supported by a grant of the Dutch Heart Foundation (DHF-2008-T094).

Financial support by the Dutch Heart Foundation for the publication of this thesis is gratefully acknowledged.

In addition, financial support by Maastricht University, Pie Medical Imaging, Stichting Hartsvrienden RESCAR, and Yacht for the publication of this thesis is gratefully acknowledged.

CONTENTS

1

General introduction

Clinical problem

In Europe, around 1 million people die annually of stroke which is the second most common cause of death (Nichols et al. 2012). This leads to high costs, not only during stroke (direct health care costs) but also because of productivity losses and informal care of stroke patients. Consequently, the total estimated cost for European Union economy due to stroke is over 38 billion Euro a year (Nichols et al. 2012). The most common type of stroke is an ischemic stroke, caused by an occluded artery due to a thrombosis or embolism. In the Netherlands, around 6000 people die annually of ischemic stroke and around 33000 people are hospitalized annually due to ischemic stroke, excluding day hospitalization (Koopman et al. 2014). 15-20% of ischemic strokes are caused by the rupture of a vulnerable atherosclerotic plaque in the carotid bifurcation or internal carotid artery (ICA) (Chaturvedi et al. 2005), resulting in thrombus formation and the release of thrombogenic material.

To prevent stroke from plaque rupture, a plaque can be removed. Currently, only the lumen reduction of the carotid artery as caused by the plaque and expressed as the degree of stenosis, is considered when selecting patients for a carotid endarterectomy (CEA). The risk for any stroke or death within 30 days after the CEA is around 4-6% (Hobson et al. 2004; Mas et al. 2006; Ringleb et al. 2006; Halm et al. 2009; Sidawy et al. 2009). Since the number needed to treat (NNT) to prevent one ipsilateral stroke in the next 5 years is relatively low (NNT=6), it is common practice to operate on patients with a recent ischemic stroke or transient ischemic attack (TIA) and a plaque causing a lumen reduction of at least 70% (according to the NASCET criterion, see below) in the carotid bifurcation (North American Symptomatic Carotid Endarterectomy Trial 1991; Barnett et al. 1998; European Carotid Surgery Trialists' Collaborative 1998; Rothwell et al. 2003). Patients with a 50-70% degree of stenosis only have a moderate beneficial effect of CEA (Barnett et al. 1998; Rothwell et al. 2003). Furthermore, there is a marked gender difference for the NNT (men 12 and women 67; (Barnett et al. 1998)) so that in daily practice only males with a 50-70% stenosis are operated on. Patients with a degree of stenosis below 50% do not profit from a CEA (NNT=26) (Barnett et al. 1998; Rothwell et al. 2003). The benefit of surgery does not only depend on the degree of stenosis, but is also related to age and the time between the ischemic stroke or TIA and the CEA (Rothwell et al. 2004a; Rothwell et al. 2004b). Taken together, Dutch guidelines recommend that men with a symptomatic stenosis above 50% and women with symptomatic stenosis above 70% will undergo CEA preferably within two weeks after the clinical event (Nederlandse vereniging voor Neurologie 2008). All other patients with a symptomatic stenosis will receive treatment, consisting of cholesterol synthesis inhibitors (statins) and anti-thrombotic therapy to prevent recurrent stroke or TIA (Nederlandse vereniging voor Neurologie 2008). However, it has been reported that 15% of the medically treated women with a moderate stenosis (50-69%) will experience a recurrent ipsilateral stroke within five years after the first event (Barnett et al. 1998). Between 1960 and 2009, the risk of stroke has been reduced with 1% per decade due to improved blood pressure control and antiplatelet therapy (Hong et al. 2011). Nowadays, the risk of recurrent stroke is lower due to better medical treatment (Park and Ovbiagele 2015) challenging the effectiveness of CEA and demanding the best possible selection of patients who will undergo surgery.

Anatomy of the arterial wall and carotid plaque development

To understand the development of plaque, an overview of a healthy arterial wall composition is provided. The wall of the carotid artery consists of three main layers: tunica intima, tunica media and tunica adventitia (Figure 1A).

The tunica intima is the inner layer of the arterial wall. It is composed of one layer of endothelial cells supported by a subendothelial layer consisting of a basement membrane and loose connective tissue (Marieb and Hoehn 2007). In healthy subjects, the intima thickness is approximately only 0.02 mm (Salonen and Salonen 1993) and is not relevant for the mechanical properties of the arterial wall (Holzapfel et al. 2000). The internal elastic lamina, composed mainly of elastin, separates the tunica intima from the tunica media. The tunica media consists mostly of smooth muscle cells and elastin fibers (Marieb and Hoehn 2007). In healthy subjects, the media has the most significant contribution to the mechanical properties of the arterial wall (Wolinsky and Glagov 1964; Holzapfel et al. 2000). An external elastic lamina separates the tunica media from the tunica adventitia which is the outer layer. The tunica adventitia mainly consists of collagen fibers, which reinforce the arterial wall and protect the wall against overextension (Marieb and Hoehn 2007).

The arterial diameter varies across different arteries, from the proximal aorta with an internal diameter of approximately 25 mm to the smallest capillaries with an internal diameter of 3 µm. The smooth muscle cells within the arterial wall have similar load-bearing properties and, hence, the wall tension T should be similar independent of the caliber or location of the artery. The Lamé equation (Liang et al. 2001; Nichols et al. 2011) relates the wall tension to wall thickness h, diameter d and transmural blood pressure p; $2T=pd/h$. Since T/p hardly varies, the diameter/thickness ratio should also be similar. The wall thickness of the aorta is 2 mm (about 10% of diameter) and declines gradually towards the smallest capillaries (1 µm). The tissue composition of the artery wall depends on vessel function. Elastic arteries are thick-walled large arteries (10-25 mm in diameter) located near the heart, such as the aorta and carotid arteries. These arteries conduct the blood from the heart to medium-sized arteries and act

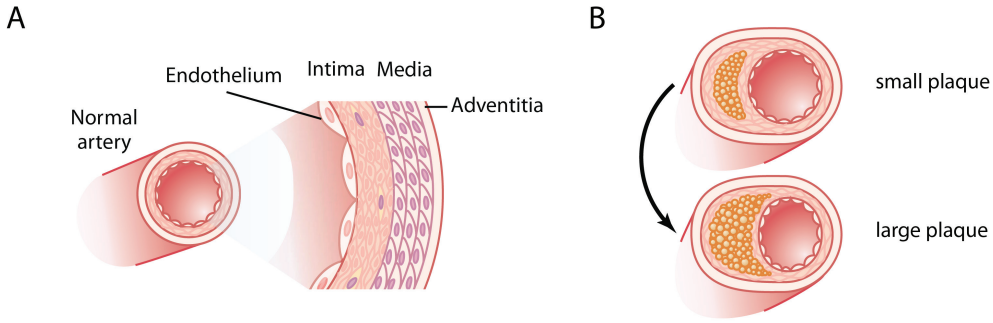

Figure 1

Carotid artery wall consists of three layers: intima, media and adventitia (A). Plaque formation in the carotid artery wall containing lipid pools (B). Adapted from Hall and Guyton (2011).

as a volume reservoir to attenuate the pressure pulse. Hence, these arteries contain a high fraction of elastin. The muscular arteries (3-10 mm in diameter) deliver blood to the organs and control the blood supply by vasoconstriction. Consequently, these arteries contain a thick tunica media and a high fraction of smooth muscle cells (Marieb and Hoehn 2007).

Atherosclerosis is a chronic inflammatory disease which starts with pathological thickening of the intima layer and developing lipid pools (Figure1B) (Finn et al. 2010). Early lesions consist of subendothelial accumulation of foam cells, i.e. cholesterol-rich macrophages (Lusis 2000). Possibly due to infiltration of macrophages into the lipid pools, a lipid-rich necrotic core develops (Finn et al. 2010). More advanced lesions additionally contain smooth muscle cells, calcifications and hemorrhage (Lusis 2000; Finn et al. 2010). The so-called vulnerable plaques, i.e., plaques prone to rupture, have a lipid-rich necrotic core with a thin fibrous cap (<65 μm), accumulation of macrophages and lack of smooth muscle cells (Lusis 2000; Virmani et al. 2000; Virmani et al. 2006). According to the Mannheim consensus, advanced atherosclerotic lesions are defined as plaques when the local wall segment is 1) protruding into the lumen more than 500 μm, 2) larger than 50% of the surrounding intima-media thickness (IMT) and/or 3) larger than 1500 μm (Touboul et al. 2012).

Plaques are preferentially located in junctions and curved vessels, for example in the carotid bifurcation. The carotid arteries are located in the neck at each side, supplying the brain and other tissues with blood. The common carotid artery (CCA) branches into the internal carotid artery (ICA) and external carotid artery (ECA). The carotid artery expands at the carotid bifurcation to approximately 120% of the CCA cross-sectional area (Truskey et al. 2004), which minimizes pulse wave reflections. This widening mainly occurs in the inlet of the ICA, called the bulb or bifurcation, which contains the baro- and chemoreceptors for signaling changes in blood pressure and carbon-dioxide concentration. The cross-sectional area of the downstream ICA and ECA equals 50% and 32% of the CCA cross-sectional area. 70% of the CCA blood flows towards the ICA, going into the circle of Willis within the brains, whereas 30% flows into the ECA supplying blood to the facial muscles and other tissues (Truskey et al. 2004).

Degree of stenosis

To quantify the lumen narrowing due to plaque formation in the carotid artery bifurcation or ICA, the degree of stenosis is determined using imaging techniques (angiography, which is now obsolete; CT angiography or MR angiography) according to the European Carotid Surgery Trial (ECST) criterion (European Carotid Surgery Trialists' Collaborative 1998) or the North American Symptomatic Carotid Endarterectomy Trial (NASCET) criterion (North American Symptomatic Carotid Endarterectomy Trial 1991). The ECST criterion uses the ratio of the lumen diameter at the site of the plaque by the assumed original vessel diameter at the same location to characterise the atherosclerotic burden. The NASCET criterion considers the ratio of the lumen diameter at the site of the plaque by the vessel diameter just distally to the plaque location. Because the bulb normally narrows towards the ICA, the NASCET criterion for plaques in the bulb region underestimates the atherosclerotic burden (Staikov et al. 2000). Despite this limitation, the NASCET criterion is used in clinical guidelines and practice. Another means to classify the degree of stenosis is by Doppler ultrasound. As described by the Bernoulli equation, the narrowing of the lumen by a plaque will lead to a local increase in blood flow velocity (Nichols et al. 2011). The criteria defined by the Society of Radiologists in Ultrasound (Grant et al. 2003) linking the peak Doppler velocities with the degree of stenosis according to NASCET criteria are shown in Table 1.

In the Netherlands, patients suspected of having a symptomatic stenosis in the carotid artery, i.e., a ruptured plaque which led to a stroke or TIA, are screened with duplex ultrasound (combined B- and Doppler modes, see **Chapter 2**) to establish whether a plaque is present in the carotid artery and if so, which degree of stenosis is caused by that plaque. Patients with a highest peak systolic velocity around the border criteria (125 cm/s for men and 230 cm/s for women) are referred to Magnetic Resonance Angiography (MRA) or sometimes Computed Tomographic Angiography (CTA) for confirmation (Nederlandse vereniging voor Neurologie 2008).

Table 1

Criteria to determine the degree of stenosis based on the highest peak systolic velocity, measured by Doppler ultrasound.

Peak systolic velocity	Degree of stenosis (NASCET)
<125 cm/s	<50%
125 - 230 cm/s	50-69%
>230 cm/s	>70%

Mechanical properties of the arterial wall

In addition to the degree of stenosis and plaque composition, mechanical properties of the arterial wall and of the plaque in combination with the mechanical load (dynamic blood pressure) play an important role in plaque rupture.

Common carotid artery

Atherosclerosis is associated with changes in mechanical properties of the CCA (Leone et al. 2008). The end-diastolic diameter of the CCA is about 5 - 8 mm depending on sex, age and subject size (Engelen et al. 2015). It should be realized that the CCA diameter as measured with ultrasound techniques is based on the estimated distance between the echoes originating from the anterior and posterior adventitia-media transitions. Hence the quoted diameter is larger than the true lumen diameter. This is also the case for diameters measured with angiographic techniques, of which the limited spatial resolution will extend opacification beyond the lumen boundaries. The intima-media thickness (IMT) represents the thickness of the intima and media layer and ranges from 300 μm for a young subject up to 1000 μm for an old subject (Engelen et al. 2013). Since wall thickness also includes the adventitia layer (250 μm), IMT ranges from 60-70% of the vessel wall thickness.

In a large asymptomatic population, a high IMT of the CCA is associated with an increased risk of myocardial infarction and stroke (O'Leary et al. 1999; Silvestrini et al. 2010). In addition, enlarged mean and maximal IMT of the CCA is a predictor of recurrent stroke in a stroke population (Tsivgoulis et al. 2006; Roquer et al. 2011). Although IMT seems to predict the risk of cardiovascular events, this is only true for a large population. Accordingly, including mean IMT in the traditional cardiovascular risk prediction models does not improve the prediction for individual subjects (Lorenz et al. 2010; den Ruijter et al. 2013; van den Oord et al. 2013; Bots et al. 2014).

As stated earlier, the artery wall is composed of elastic material that responds to a transmural blood pressure increase by circumferential elongation, i.e., an increase in artery diameter. The absolute distension of the CCA, i.e., the difference between the end-diastolic and systolic diameter, is within the range of 0.2-1.0 mm and depends on the diastolic diameter and elastic properties of the artery. Due to stiffening of the arteries, distension decreases with age (Engelen et al. 2015). In subjects with severe ICA stenosis and no stenosis at the contralateral ICA, the distension of the CCA and ICA at the ipsilateral side is significantly lower compared to that of the contralateral side (Giannattasio et al. 2001), indicating a stiffer vessel due to the atherosclerosis.

CCA plaques

Although CCA plaques are rare and less prone to rupture than ICA plaques, some studies focused on CCA plaques (Paini et al. 2007; Beaussier et al. 2008; Beaussier et al. 2011). CCA plaques are easily accessible for ultrasound due to their superficial location (depth 20 mm) and the straight appearance of the CCA parallel to the skin. Type 2 diabetes, dyslipidemia and hypertension are associated with a locally stiffer artery at the plaque in the CCA, i.e., exhibiting a lower distension than the adjacent proximal CCA (Paini et al. 2007; Beaussier et

al. 2008). Furthermore, a decreased distension at the plaque location is associated with an advanced plaque phenotype, i.e. containing a lipid core, intra-plaque hemorrhage, calcifications or thrombus (Beaussier et al. 2011).

Plaque dynamics

Since the cross-sectional area at the site of the stenosis may be reduced, the local blood flow velocity will be increased correspondingly (while volume flow is constant). Due to the Venturi effect, described by the Bernoulli equation, the increase in local blood flow velocity (kinetic energy) is at the expense of potential energy, i.e. local blood pressure (Holen et al. 1987; Xu et al. 2016). Within the stenosis, the decreased luminal blood pressure in combination with the higher blood pressure within the local vasa vasorum affect the transmural blood pressure gradient, which may even change direction. Additionally in case of a severe stenosis, the increased hemodynamic impedance will reflect the blood pressure waves, thereby increasing the proximal pulse pressure and the cyclic mechanical stress acting on the proximal site of stenosis. Therefore, plaque deformation may depend on plaque composition, pulse pressure and wave reflections, and the degree of stenosis in combination with the Venturi effect. These pressure dynamics and plaque features may eventually contribute to plaque rupture (Hoeks et al. 2008; Xu et al. 2016).

PARISK study

The possibility to assess the risk of rupture of a plaque will have tremendous impact on clinical decision making and may help to reduce healthcare costs. Identifying patients at high risk for a stroke or TIA could not only prevent a substantial number of strokes, especially in patients with mild-to-moderate stenosis (30-70%), but could also avoid unnecessary interventions in patients with a substantial stenosis (>70%). Previous studies to evaluate the feasibility of imaging to assess plaque vulnerability have shown a good correlation between imaging and histology and/or clinical characteristics, but employed only one or two image modalities in small cohorts and focused primarily on morphological plaque parameters (Biasi et al. 1999; Gronholdt et al. 2001; Mathiesen et al. 2001; Yuan et al. 2002; Fayad et al. 2004; Takaya et al. 2006; Altaf et al. 2008; Cappendijk et al. 2008; Henneman et al. 2008; Li et al. 2008; Underhill et al. 2008; Wintermark et al. 2008; Topakian et al. 2011) . Furthermore, these studies may not have delivered the necessary sensitivity and specificity and/or lack adequate clinical validation to change the current clinical guidelines. Therefore, in daily practice currently only the degree of stenosis is used as clinical guideline to assess plaques at risk.

The Plaque At RISK (PARISK) study (clinical trials.gov NCT01208025) aims to evaluate plaques at risk with multiple non-invasive imaging techniques to improve, in a final application stage, identification of patients at increased risk of stroke, even before a first stroke or TIA has occurred (Truijman et al. 2014). To minimize exposure to radiation and ease the procedure for the patient, PARISK focuses on multiple non-invasive imaging techniques such as Magnetic Resonance Imaging (MRI), multidetector CTA (MDCTA), ultrasound (US) and Transcranial Doppler (TCD).

PARISK is an ongoing, multicenter 2-year follow-up study. Four hospitals in the Netherlands participate in the PARISK study, i.e., Maastricht University Medical Center (MUMC), Erasmus Medical Center (EMC), University Medical Center Utrecht (UMCU) and Amsterdam Medical Center (AMC). Patients who recently had an ischemic stroke or TIA and had a mild-to-moderate stenosis (30-70%) in the ipsilateral ICA are included within three months after the clinical event. They receive medical treatment and are enrolled in a 2-year follow-up study. Since in these patients stroke or TIA occur more often than in the population at large, it will be easier to improve identification of imaging features preceding a (recurrent) cerebrovascular event. Image modality recordings are performed after inclusion and are repeated after two years.

PARISK aims to increase the sensitivity and specificity of the applied imaging techniques to identify suitable plaque parameters, including morphology, composition and mechanical parameters. The study involves cross-sectional as well as longitudinal clinical validation of these techniques. Therefore, eventually PARISK will enable to 1) diagnose plaques at an early stage and monitor progression, 2) assess individual risk for stroke or TIA, 3) assess efficacy of individual drug therapy and intervention for (asymptomatic) patients at risk for a (recurrent) stroke or TIA and 4) develop surrogate endpoints of non-invasive imaging techniques in novel drug development.

Image modalities

Several non-invasive image modalities, i.e., MRI, MDCTA and ultrasound, will be evaluated for feasibility to assess plaque vulnerability. All image modalities have their own spatial resolution, i.e., the minimum distance at which two objects can be distinguished, which may also depend on orientation (i.e. in different directions resolution might be different as well). To determine wall and plaque dynamics, the temporal resolution (the minimum time interval between two independent successive images) is also important. A brief description of the non-invasive image modalities used in the PARISK study is given below.

Magnetic Resonance Imaging

MRI can identify and quantify the size and contents of a carotid atherosclerotic plaque, i.e., a lipid-rich necrotic core (LRNC), intraplaque hemorrhage (IPH) and the fibrous cap status. In-plane resolution is specified by the voxel size (approximately 0.6*0.6 mm^2 with a 2 mm slice thickness according to PARISK study protocol (Truijman et al. 2014)) which may vary across pulse sequences used for acquiring the MRI images. IPH and LRNC can be determined with MRI with high sensitivity and specificity (Cappendijk et al. 2005). The presence of a thin or ruptured fibrous cap is associated with previous stroke or TIA (Yuan et al. 2002). Plaques with a lipid rich necrotic core (LRNC), intraplaque hemorrhage (IPH) and a thin/ruptured fibrous cap are associated with an increased risk of future ischemic events (Takaya et al. 2006; Gupta et al. 2013). Finite element modelling shows that a thin fibrous cap and large lumen curvature increase plaque stress, thereby increasing plaque vulnerability (Li et al. 2008). However, an MRI scanner is expensive, involves waiting lines, the scanning procedure is usually long and noisy, while post processing prevents interactive application. Furthermore, patients who are claustrophobic or have metal objects/devices implanted are excluded from MRI. In addition, detailed assessment of vessel wall and plaque dynamics is problematic, because of a long acquisition time (>heart beat) of an MRI image sequence. Imaging within a heartbeat is only possible when images over multiple heartbeats are averaged, but this is a very time-consuming process and only allows for average heart beat information.

Multidetector computed tomographic angiography (MDCTA)

MDCTA is an accurate, noninvasive image modality to determine the degree of stenosis caused by a plaque (Koelemay et al. 2004). Plane-resolution of MDCTA is approximately 0.2-0.3 mm with 1 mm slice thickness according to PARISK study protocol (Truijman et al. 2014). MDCTA can distinguish and quantify total, calcified and fibrous plaque area in good correlation with histology (de Weert et al. 2006). Symptomatic carotid plaques are associated with a lower degree of calcifications determined by either MDCTA, MRI or US grey-scale values than asymptomatic carotid plaques (Kwee 2010). Carotid plaque ulcerations can also be determined by MDCTA and is associated with nonlacunar ischemic stroke (Homburg et al. 2010). However, CT involves exposure to radiation and the contrast fluid used to enhance the vessel lumen can damage kidney function. Since real time beat to beat recording is not an option because of radiation exposure restrictions, wall and plaque dynamics can not be determined with CT.

Ultrasound

Ultrasound (US) is a non-invasive, safe and interactive image modality which uses high-frequency sound waves to produce echo images of structure boundaries within the body (cf. **Chapter 2**). The main advantages of ultrasound are its affordability and accessibility, and its ability to provide immediate information on both geometry and deformation. Ultrasound imaging techniques cope well with tissue motion caused by blood pressure pulsations due to its high sustained frame rate (25 up to 500 fps) and associated temporal resolution. Therefore, ultrasound is an excellent imaging modality to study the dynamic mechanical properties of the carotid artery, through diameter waveform characteristics, distension and intima-media thickness. Furthermore, ultrasound can also provide information about plaque morphology and mechanical characteristics, and about its constituents, based on the relative grey values of the plaque within an image.

A major disadvantage of ultrasound imaging is that it is based on the reflections originating from transitions in acoustic impedance; a homogeneous structure does not reflect ultrasound (**Chapter 2**). The shorter the emitted pulse, requiring a higher emission frequency, the higher the spatial resolution will be. However, the absorption by tissue is reciprocally related to frequency and hence penetration depth decreases with ultrasound frequency (**Chapter 2**). For superficially located arteries, i.e. at a depth of 10 to 30 mm an emission frequency of about 6 MHz with a bandwidth of 50% (3 MHz) is feasible, facilitating a depth resolution of 0.25 to 0.3 mm, which is just below the thickness of the intima-media layer (see above).

Morphological features like diameter, intima-media thickness, plaque location and plaque size, can be reliable extracted from standard sequence of echo ultrasound images (25-40 fps) in daily clinical practice. Grey-scale median values of standard echo ultrasound images can be used to determine the plaque constituents. Echolucent plaques are associated with increased risk of cerebrovascular events (Biasi et al. 1999; Gronholdt et al. 2001; Mathiesen et al. 2001; Topakian et al. 2011). However, plaque echogenicity alone is not powerful enough to select patients for CEA (Gupta et al. 2015). The dynamic distension of the CCA, is commonly extracted with radiofrequency phase tracking within echo images recorded at high frame rate (>300 fps), which exchanges image width and/or line density for frame rate (Meinders et al. 2001). It requires a more expensive and dedicated ultrasound machine to apply radiofrequency phase tracking and its use is therefore restricted to a small number of specialized hospitals.

Transcranial Doppler recordings (TCD)

Transcranial Doppler (TCD) recordings of the middle cerebral artery (MCA) measure the blood velocity and Doppler amplitude using the Doppler principle (**cf Chapter 2**). Short transient increases of the Doppler amplitude signal, called microembolic signals (MES), are indicative for the presence of microemboli, possibly caused by the ongoing release of thrombogenetic material and stressing the necessity of carotid endarterectomy (CEA). Due to a high temporal variability in microemboli, it is advised to record TCD as long as possible (Forteza et al. 1996). In the PARISK study, patients were recorded with TCD for maximal four hours, depending on patient comfort. In an asymptomatic population with at least 60% stenosis (accor-

ding to the NASCET criterion), the presence of microemboli and cardiovascular events was significantly reduced in patients with intensive medical therapy, i.e. use of statins and optimal blood pressure control, compared to patients without intensive medical therapy (Spence et al. 2010). Furthermore, MES are more frequently detected soon after cerebrovascular events (Forteza et al. 1996). Since the PARISK TCD recordings are extensively discussed in a separate thesis (Truijman 2016), TCD recordings are not part of this thesis.

Aim

In conclusion, each of the non-invasive imaging techniques discussed above shows potential to identify the vulnerability of plaques and has their own (dis)advantages. On the other hand, plaque development, and eventually plaque rupture, is not yet fully understood. Previous studies employed only one or two non-invasive imaging techniques in relatively small cohorts which did not deliver the necessary sensitivity to change the current clinical guidelines (Nederlandse vereniging voor Neurologie 2008). Therefore, it remains unclear which imaging technique, or more specifically which plaque feature(s), is best to assess plaques at risk. The patients within the PARISK study have a high prevalence for recurrent stroke (up to 5% within 2 years) (Rothwell et al. 2004b; Truijman et al. 2014), facilitating identification of plaque features related to an increased risk of recurrent stroke. Since ultrasound imaging is cheap and versatile, widely accessible and can be used quickly after observation of complaints, this thesis focuses on the implementation of ultrasound techniques to identify at an early stage plaques at risk.

The main aim of this thesis is to develop and validate new ultrasound techniques to extract mechanical properties of the carotid artery and plaques to improve non-invasive characterization of plaque at risk. The first part of this thesis will address morphological and mechanical properties of the common carotid artery (CCA) in association with distal plaques. The second part of this thesis will focus on plaque properties. Plaque distortion is subject to carotid distensibility, blood pressure, plaque composition and compressibility.

Outline thesis

This thesis works towards identification of plaques at risk with ultrasound and pertains to the baseline ultrasound recordings (2010-2014) of the 2-year follow up PARISK study. For this purpose, we will develop and validate a program to extract mechanical properties of the carotid artery, such as diameter, distension and intima-media thickness (IMT), with a novel edge detection technique applied to standard ultrasound echo images as recorded in the clinic, favoring widespread application.

Chapter 2 of this thesis provides an overview of ultrasound principles. The basics of ultrasound and technical aspects involved are described in more detail.

Since the internal carotid artery (ICA) is located deeply and is usually curved, we will validate our method first for the relatively straight common carotid artery (CCA). In **Chapter 3** of this thesis we explore whether the distension extracted with edge tracking applied to standard echo ultrasound recordings (frame rate of ±37 fps) of the CCA is as precise and accurate as the distension obtained with radiofrequency phase tracking from high frame rate echo ultrasound recordings. If it can be shown that the technique based on standard equipment is applicable for the CCA of an old patient, and hence relevant, population, it allows more widespread use of distension recordings.

Mean or maximal intima-media thickness (IMT) are not suitable to predict the risk of (future) cardiovascular events for an individual patient (Lorenz et al. 2010; den Ruijter et al. 2013; van den Oord et al. 2013; Bots et al. 2014). However, irregularities of the vessel wall, i.e., the IMT inhomogeneity, could be a promising alternative. In **Chapter 4** the inhomogeneity of IMT will be correlated with the mechanical properties of the common carotid artery, as extracted with our method, and the degree of ICA stenosis, as extracted from CT recordings.

In **Chapter 5**, we compare multiple wall thickness parameters of the CCA in relation to the degree of ipsilateral ICA stenosis. We will investigate whether mainly CCA plaques with respect to other wall thickness parameters are associated with the degree of ipsilateral ICA stenosis. Furthermore, we consider absolute as well as normalized maximal wall thickness. Risk classification based on CCA wall thickness for having a moderate ICA stenosis (>50%) might be affected when wall thickness in relation to artery diameter is considered rather than its absolute value.

CCA rise time characteristics, i.e. the rise time of the upstroke of the distension waveform, may be influenced by wave reflections and, hence, by ICA plaque size and composition. The associations between the rise time characteristics of the CCA, the degree of ICA stenosis and the MRI plaque features are investigated in **Chapter 6**. We will investigate whether a soft distal plaque (substantial proximal lipids and thin/ruptured fibrous cap), compared to a stable, hard ICA plaque, may cushion the impinging blood pressure wave and thereby reduce the magnitude of the reflected pressure wave, which otherwise would interfere with the incident wave. Consequently, we anticipate that this will have consequences for the rise time inhomogeneity of the CCA distension distribution.

To make a step towards wall tracking of a carotid bifurcation with plaques, we consider in **Chapter 7** CCA plaques. Since automatic edge detection is challenging in the presence of plaques, vessel wall and CCA plaques are manually segmented. We consider the intra- and inter-observer precision of the distension and plaque compression characteristics and subsequently the association between plaque compression and echogenicity.

In **Chapter 8**, the discussion of the major findings and the final conclusion of this thesis will be presented.

References

Altaf N, Daniels L, Morgan PS, Auer D, MacSweeney ST, Moody AR, Gladman JR. Detection of intraplaque hemorrhage by magnetic resonance imaging in symptomatic patients with mild to moderate carotid stenosis predicts recurrent neurological events. J Vasc Surg 2008;47:337-342.

Barnett HJ, Taylor DW, Eliasziw M, Fox AJ, Ferguson GG, Haynes RB, Rankin RN, Clagett GP, Hachinski VC, Sackett DL, Thorpe KE, Meldrum HE, Spence JD. Benefit of carotid endarterectomy in patients with symptomatic moderate or severe stenosis. North American Symptomatic Carotid Endarterectomy Trial Collaborators. N Engl J Med 1998;339:1415-1425.

Beaussier H, Masson I, Collin C, Bozec E, Laloux B, Calvet D, Zidi M, Boutouyrie P, Laurent S. Carotid plaque, arterial stiffness gradient, and remodeling in hypertension. Hypertension 2008;52:729-736.

Beaussier H, Naggara O, Calvet D, Joannides R, Guegan-Massardier E, Gerardin E, Iacob M, Laloux B, Bozec E, Bellien J, Touze E, Masson I, Thuillez C, Oppenheim C, Boutouyrie P, Laurent S. Mechanical and structural characteristics of carotid plaques by combined analysis with echotracking system and MR imaging. JACC Cardiovasc Imaging 2011;4:468-477.

Biasi GM, Sampaolo A, Mingazzini P, De Amicis P, El-Barghouty N, Nicolaides AN. Computer analysis of ultrasonic plaque echolucency in identifying high risk carotid bifurcation lesions. Eur J Vasc Endovasc Surg 1999;17:476-479.

Bots ML, Groenewegen KA, Anderson TJ, Britton AR, Dekker JM, Engstrom G, Evans GW, de Graaf J, Grobbee DE, Hedblad B, Hofman A, Holewijn S, Ikeda A, Kavousi M, Kitagawa K, Kitamura A, Ikram MA, Lonn EM, Lorenz MW, Mathiesen EB, Nijpels G, Okazaki S, O'Leary DH, Polak JF, Price JF, Robertson C, Rembold CM, Rosvall M, Rundek T, Salonen JT, Sitzer M, Stehouwer CD, Franco OH, Peters SA, den Ruijter HM. Common carotid intima-media thickness measurements do not improve cardiovascular risk prediction in individuals with elevated blood pressure: the USE-IMT collaboration. Hypertension 2014;63:1173-1181.

Cappendijk VC, Cleutjens KB, Kessels AG, Heeneman S, Schurink GW, Welten RJ, Mess WH, Daemen MJ, van Engelshoven JM, Kooi ME. Assessment of human atherosclerotic carotid plaque components with multisequence MR imaging: initial experience. Radiology 2005;234:487-492.

Cappendijk VC, Heeneman S, Kessels AG, Cleutjens KB, Schurink GW, Welten RJ, Mess WH, van Suylen RJ, Leiner T, Daemen MJ, van Engelshoven JM, Kooi ME. Comparison of single-sequence T1w TFE MRI with multisequence MRI for the quantification of lipid-rich necrotic core in atherosclerotic plaque. J Magn Reson Imaging 2008;27:1347-1355.

Chaturvedi S, Bruno A, Feasby T, Holloway R, Benavente O, Cohen SN, Cote R, Hess D, Saver J, Spence JD, Stern B, Wilterdink J, Therapeutics, Technology Assessment Subcommittee of the American Academy of N. Carotid endarterectomy--an evidence-based review: report of the Therapeutics and Technology Assessment Subcommittee of the American Academy of Neurology. Neurology 2005;65:794-801.

de Weert TT, Ouhlous M, Meijering E, Zondervan PE, Hendriks JM, van Sambeek MR, Dippel DW, van der Lugt A. In vivo characterization and quantification of atherosclerotic carotid plaque components with multidetector computed tomography and histopathological correlation. Arterioscler Thromb Vasc Biol 2006;26:2366-2372.

den Ruijter HM, Peters SA, Groenewegen KA, Anderson TJ, Britton AR, Dekker JM, Engstrom G, Eijkemans MJ, Evans GW, de Graaf J, Grobbee DE, Hedblad B, Hofman A, Holewijn S, Ikeda A, Kavousi M, Kitagawa K, Kitamura A, Koffijberg H, Ikram MA, Lonn EM, Lorenz MW, Mathiesen EB, Nijpels G, Okazaki S, O'Leary DH, Polak JF, Price JF, Robertson C, Rembold CM, Rosvall M, Rundek T, Salonen JT, Sitzer M, Stehouwer CD, Witteman JC, Moons KG, Bots ML. Common carotid intima-media thickness does not add to Framingham risk score in individuals with diabetes mellitus: the USE-IMT initiative. Diabetologia 2013;56:1494-1502.

Engelen L, Bossuyt J, Ferreira I, van Bortel LM, Reesink KD, Segers P, Stehouwer CD, Laurent S, Boutouyrie P. Reference values for local arterial stiffness. Part A. Journal of Hypertension 2015;33:1981-1996.

Engelen L, Ferreira I, Stehouwer CD, Boutouyrie P, Laurent S, Reference Values for Arterial Measurements C. Reference intervals for common carotid intima-media thickness measured with echotracking: relation with risk factors. Eur Heart J 2013;34:2368-2380.

European Carotid Surgery Trialists' Collaborative G. Randomised trial of endarterectomy for recently symptomatic carotid stenosis: final results of the MRC European Carotid Surgery Trial (ECST). The Lancet 1998;351:1379-1387.

Fayad ZA, Sirol M, Nikolaou K, Choudhury RP, Fuster V. Magnetic resonance imaging and computed tomography in assessment of atherosclerotic plaque. Curr Atheroscler Rep 2004;6:232-242.

Finn AV, Kolodgie FD, Virmani R. Correlation between carotid intimal/medial thickness and atherosclerosis: a point of view from pathology. Arterioscler Thromb Vasc Biol 2010;30:177-181.

Forteza AM, Babikian VL, Hyde C, Winter M, Pochay V. Effect of time and cerebrovascular symptoms of the prevalence of microembolic signals in patients with cervical carotid stenosis. Stroke 1996;27:687-690.

Giannattasio C, Failla M, Emanuelli G, Grappiolo A, Boffi L, Corsi D, Mancia G. Local effects of atherosclerotic plaque on arterial distensibility. Hypertension 2001;38:1177-1180.

Grant EG, Benson CB, Moneta GL, Alexandrov AV, Baker JD, Bluth EI, Carroll BA, Eliasziw M, Gocke J, Hertzberg BS, Katarick S, Needleman L, Pellerito J, Polak JF, Rholl KS, Wooster DL, Zierler E, Society of Radiologists in U. Carotid artery stenosis: grayscale and Doppler ultrasound diagnosis--Society of Radiologists in Ultrasound consensus conference. Ultrasound Q 2003;19:190-198.

Gronholdt ML, Nordestgaard BG, Schroeder TV, Vorstrup S, Sillesen H. Ultrasonic echolucent carotid plaques predict future strokes. Circulation 2001;104:68-73.

Gupta A, Baradaran H, Schweitzer AD, Kamel H, Pandya A, Delgado D, Dunning A, Mushlin AI, Sanelli PC. Carotid plaque MRI and stroke risk: a systematic review and meta-analysis. Stroke 2013;44:3071-3077.

Gupta A, Kesavabhotla K, Baradaran H, Kamel H, Pandya A, Giambrone AE, Wright D, Pain KJ, Mtui EE, Suri JS, Sanelli PC, Mushlin AI. Plaque echolucency and stroke risk in asymptomatic carotid stenosis: a systematic review and meta-analysis. Stroke 2015;46:91-97.

Hall JE, Guyton AC. Guyton and Hall textbook of medical physiology. 12th. Saunders/Elsevier, Philadelphia, Pa., 2011.

Halm EA, Tuhrim S, Wang JJ, Rockman C, Riles TS, Chassin MR. Risk factors for perioperative death and stroke after carotid endarterectomy: results of the new york carotid artery surgery study. Stroke 2009;40:221-229.

Henneman MM, Schuijf JD, Pundziute G, van Werkhoven JM, van der Wall EE, Jukema JW, Bax JJ. Noninvasive evaluation with multislice computed tomography in suspected acute coronary syndrome: plaque morphology on multislice computed tomography versus coronary calcium score. J Am Coll Cardiol 2008;52:216-222.

Hobson RW, 2nd, Howard VJ, Roubin GS, Brott TG, Ferguson RD, Popma JJ, Graham DL, Howard G, Investigators C. Carotid artery stenting is associated with increased complications in octogenarians: 30-day stroke and death rates in the CREST lead-in phase. J Vasc Surg 2004;40:1106-1111.

Hoeks AP, Reesink KD, Hermeling E, Reneman RS. Local blood pressure rather than shear stress should be blamed for plaque rupture. J Am Coll Cardiol 2008;52:1107-1108; author reply 1108-1109.

Holen J, Waag RC, Gramiak R. Doppler ultrasound in aortic stenosis: in vitro studies of pressure gradient determination. Ultrasound Med Biol 1987;13:321-328.

Holzapfel GA, Gasser TC, Ogden RW. A New Constitutive Framework for Arterial Wall Mechanics and a Comparative Study of Material Models. Journal of elasticity and the physical science of solids 2000;61:1-48.

Homburg PJ, Rozie S, van Gils MJ, Jansen T, de Weert TT, Dippel DW, van der Lugt A. Atherosclerotic plaque ulceration in the symptomatic internal carotid artery is associated with nonlacunar ischemic stroke. Stroke 2010;41:1151-1156.

Hong KS, Yegiaian S, Lee M, Lee J, Saver JL. Declining stroke and vascular event recurrence rates in secondary prevention trials over the past 50 years and consequences for current trial design. Circulation 2011;123:2111-2119.

Koelemay MJ, Nederkoorn PJ, Reitsma JB, Majoie CB. Systematic review of computed tomographic angiography for assessment of carotid artery disease. Stroke 2004;35:2306-2312.

Koopman C, van Dis I, Vaartjes I, Visseren FLJ, Bots ML. Hart- en vaatziekten in Nederland 2014, cijfers over kwaliteit van leven, ziekte en sterfte. 2014

Kwee RM. Systematic review on the association between calcification in carotid plaques and clinical ischemic symptoms. Journal of Vascular Surgery 2010;51:1015-1025.

Leone N, Ducimetiere P, Gariepy J, Courbon D, Tzourio C, Dartigues JF, Ritchie K, Alperovitch A, Amouyel P, Safar ME, Zureik M. Distension of the carotid artery and risk of coronary events: the three-city study. Arterioscler Thromb Vasc Biol 2008;28:1392-1397.

Li ZY, Tang T, J UK-I, Graves M, Sutcliffe M, Gillard JH. Assessment of carotid plaque vulnerability using structural and geometrical determinants. Circ J 2008;72:1092-1099.

Liang YL, Shiel LM, Teede H, Kotsopoulos D, McNeil J, Cameron JD, McGrath BP. Effects of Blood Pressure, Smoking, and Their Interaction on Carotid Artery Structure and Function. Hypertension 2001;37:6-11.

Lorenz MW, Schaefer C, Steinmetz H, Sitzer M. Is carotid intima media thickness useful for individual prediction of cardiovascular risk? Ten-year results from the Carotid Atherosclerosis Progression Study (CAPS). Eur Heart J 2010;31:2041-2048.

Lusis AJ. Atherosclerosis. Nature 2000;407:233-241.

Marieb E, Hoehn K. Human anatomy & physiology. 7th edition. Pearson Education, San Francisco, United States of America, 2007.

Mas JL, Chatellier G, Beyssen B, Branchereau A, Moulin T, Becquemin JP, Larrue V, Lievre M, Leys D, Bonneville JF, Watelet J, Pruvo JP, Albucher JF, Viguier A, Piquet P, Garnier P, Viader F, Touze E, Giroud M, Hosseini H, Pillet JC, Favrole P, Neau JP, Ducrocq X, Investigators E-S. Endarterectomy versus stenting in patients with symptomatic severe carotid stenosis. N Engl J Med 2006;355:1660-1671.

Mathiesen EB, Bonaa KH, Joakimsen O. Echolucent plaques are associated with high risk of ischemic cerebrovascular events in carotid stenosis: the tromso study. Circulation 2001;103:2171-2175.

Meinders JM, Brands PJ, Willigers JM, Kornet L, Hoeks AP. Assessment of the spatial homogeneity of artery dimension parameters with high frame rate 2-D B-mode. Ultrasound Med Biol 2001;27:785-794.

Nederlandse vereniging voor Neurologie. Richtlijn Diagnostiek, behandeling en zorg voor patienten met een beroerte. 2008

Nichols M, Townsend N, Luengo-Fernandez R, Leal J, Gray A, Scarborough P, Rayner M. European cardiovascular disease statistics 2012. European Heart Network, Brussels, European Society of Cardiology, Sophia Antipolis 2012;

Nichols WW, O'Rourke MF, Vlachopoulos C. McDonald's blood flow in arteries : theoretic, experimental, and clinical principles. 6th. Hodder Arnold, London, 2011.

North American Symptomatic Carotid Endarterectomy Trial C. Beneficial effect of carotid endarterectomy in symptomatic patients with high-grade carotid stenosis. N Engl J Med 1991;325:445-453.

O'Leary DH, Polak JF, Kronmal RA, Manolio TA, Burke GL, Wolfson SK, Jr. Carotid-artery intima and media thickness as a risk factor for myocardial infarction and stroke in older adults. Cardiovascular Health Study Collaborative Research Group. N Engl J Med 1999;340:14-22.

Paini A, Boutouyrie P, Calvet D, Zidi M, Agabiti-Rosei E, Laurent S. Multiaxial mechanical characteristics of carotid plaque: analysis by multiarray echotracking system. Stroke 2007;38:117-123.

Park JH, Ovbiagele B. Optimal combination secondary prevention drug treatment and stroke outcomes. Neurology 2015;84:50-56.

Ringleb PA, Allenberg J, Bruckmann H, Eckstein HH, Fraedrich G, Hartmann M, Hennerici M, Jansen O, Klein G, Kunze A, Marx P, Niederkorn K, Schmiedt W, Solymosi L, Stingele R, Zeumer H, Hacke W. 30 day results from the SPACE trial of stent-protected angioplasty versus carotid endarterectomy in symptomatic patients: a randomised non-inferiority trial. Lancet 2006;368:1239-1247.

Roquer J, Segura T, Serena J, Cuadrado-Godia E, Blanco M, Garcia-Garcia J, Castillo J, Study A. Value of carotid intima-media thickness and significant carotid stenosis as markers of stroke recurrence. Stroke 2011;42:3099-3104.

Rothwell PM, Eliasziw M, Gutnikov SA, Fox AJ, Taylor DW, Mayberg MR, Warlow CP, Barnett HJM. Analysis of pooled data from the randomised controlled trials of endarterectomy for symptomatic carotid stenosis. The Lancet 2003;361:107-116.

Rothwell PM, Eliasziw M, Gutnikov SA, Warlow CP, Barnett HJ. Sex difference in the effect of time from symptoms to surgery on benefit from carotid endarterectomy for transient ischemic attack and non-disabling stroke. Stroke 2004a;35:2855-2861.

Rothwell PM, Eliasziw M, Gutnikov SA, Warlow CP, Barnett HJM. Endarterectomy for symptomatic carotid stenosis in relation to clinical subgroups and timing of surgery. The Lancet 2004b;363:915-924.

Salonen JT, Salonen R. Ultrasound B-mode imaging in observational studies of atherosclerotic progression. Circulation 1993;87:II56-65.

Sidawy AN, Zwolak RM, White RA, Siami FS, Schermerhorn ML, Sicard GA, Outcomes Committee for the Society for Vascular S. Risk-adjusted 30-day outcomes of carotid stenting and endarterectomy: results from the SVS Vascular Registry. J Vasc Surg 2009;49:71-79.

Silvestrini M, Cagnetti C, Pasqualetti P, Albanesi C, Altamura C, Lanciotti C, Bartolini M, Mattei F, Provinciali L, Vernieri F. Carotid wall thickness and stroke risk in patients with asymptomatic internal carotid stenosis. Atherosclerosis 2010;210:452-457.

Spence JD, Coates V, Li H, Tamayo A, Munoz C, Hackam DG, DiCicco M, DesRoches J, Bogiatzi C, Klein J, Madrenas J, Hegele RA. Effects of intensive medical therapy on microemboli and cardiovascular risk in asymptomatic carotid stenosis. Arch Neurol 2010;67:180-186.

Staikov IN, Arnold M, Mattle HP, Remonda L, Sturzenegger M, Baumgartner RW, Schroth G. Comparison of the ECST, CC, and NASCET grading methods and ultrasound for assessing carotid stenosis. European Carotid Surgery Trial. North American Symptomatic Carotid Endarterectomy Trial. J Neurol 2000;247:681-686.

Takaya N, Yuan C, Chu B, Saam T, Underhill H, Cai J, Tran N, Polissar NL, Isaac C, Ferguson MS, Garden GA, Cramer SC, Maravilla KR, Hashimoto B, Hatsukami TS. Association between carotid plaque characteristics and subsequent ischemic cerebrovascular events: a prospective assessment with MRI--initial results. Stroke 2006;37:818-823.

Topakian R, King A, Kwon SU, Schaafsma A, Shipley M, Markus HS, Investigators A. Ultrasonic plaque echolucency and emboli signals predict stroke in asymptomatic carotid stenosis. Neurology 2011;77:751-758.

Touboul PJ, Hennerici MG, Meairs S, Adams H, Amarenco P, Bornstein N, Csiba L, Desvarieux M, Ebrahim S, Hernandez Hernandez R, Jaff M, Kownator S, Naqvi T, Prati P, Rundek T, Sitzer M, Schminke U, Tardif JC, Taylor A, Vicaut E, Woo KS. Mannheim carotid intima-media thickness and plaque consensus (2004-2006-2011). An update on behalf of the advisory board of the 3rd, 4th and 5th watching the risk symposia, at the 13th, 15th and 20th European Stroke Conferences, Mannheim, Germany, 2004, Brussels, Belgium, 2006, and Hamburg, Germany, 2011. Cerebrovasc Dis 2012;34:290-296.

Truijman MT, Kooi ME, van Dijk AC, de Rotte AA, van der Kolk AG, Liem MI, Schreuder FH, Boersma E, Mess WH, van Oostenbrugge RJ, Koudstaal PJ, Kappelle LJ, Nederkoorn PJ, Nederveen AJ, Hendrikse J, van der Steen AF, Daemen MJ, van der Lugt A. Plaque At RISK (PARISK): prospective multicenter study to improve diagnosis of high-risk carotid plaques. Int J Stroke 2014;9:747-754.

Truijman MTB. Plaque vulnerability in stroke patients: a multimodality imaging approach. 2016

Truskey GA, Yuan F, Katz DF. Transport Phenomena in Biological Systems. Pearson Education, New Jersey, United States of America, 2004.

Tsivgoulis G, Vemmos K, Papamichael C, Spengos K, Manios E, Stamatelopoulos K, Vassilopoulos D, Zakopoulos N. Common carotid artery intima-media thickness and the risk of stroke recurrence. Stroke 2006;37:1913-1916.

Underhill HR, Yarnykh VL, Hatsukami TS, Wang J, Balu N, Hayes CE, Oikawa M, Yu W, Xu D, Chu B, Wyman BT, Polissar NL, Yuan C. Carotid plaque morphology and composition: initial comparison between 1.5- and 3.0-T magnetic field strengths. Radiology 2008;248:550-560.

van den Oord SC, Sijbrands EJ, ten Kate GL, van Klaveren D, van Domburg RT, van der Steen AF, Schinkel AF. Carotid intima-media thickness for cardiovascular risk assessment: systematic review and meta-analysis. Atherosclerosis 2013;228:1-11.

Virmani R, Burke AP, Farb A, Kolodgie FD. Pathology of the vulnerable plaque. J Am Coll Cardiol 2006;47:C13-18.

Virmani R, Kolodgie FD, Burke AP, Farb A, Schwartz SM. Lessons from sudden coronary death: a comprehensive morphological classification scheme for atherosclerotic lesions. Arterioscler Thromb Vasc Biol 2000;20:1262-1275.

Wintermark M, Arora S, Tong E, Vittinghoff E, Lau BC, Chien JD, Dillon WP, Saloner D. Carotid plaque computed tomography imaging in stroke and nonstroke patients. Ann Neurol 2008;64:149-157.

Wolinsky H, Glagov S. Structural Basis for the Static Mechanical Properties of the Aortic Media. Circ Res 1964;14:400-413.

Xu C, Yuan C, Stutzman E, Canton G, Comess KA, Beach KW. Quest for the Vulnerable Atheroma: Carotid Stenosis and Diametric Strain-A Feasibility Study. Ultrasound Med Biol 2016;42:699-716.

Yuan C, Zhang SX, Polissar NL, Echelard D, Ortiz G, Davis JW, Ellington E, Ferguson MS, Hatsukami TS. Identification of fibrous cap rupture with magnetic resonance imaging is highly associated with recent transient ischemic attack or stroke. Circulation 2002;105:181-185.

2

Ultrasound principles

Basics of ultrasound

The description of the ultrasound theory in this chapter is aimed at facilitating a thorough understanding of the next chapters of this thesis. Ultrasound is sound with a frequency above the human hearing limit (approximately 20 kHz). For ultrasound recordings, the transducer of an ultrasound system converts electrical energy into acoustic energy and thereby transmits a pressure wave into the human body which is reflected by acoustic inhomogeneities (see below) and received by the transducer. The instantaneous propagation speed of the ultrasound wave depends on elastic properties and density of the tissue. The ultrasound wave propagates very slowly in air (330 m/s), fast in bone (3500 m/s), while for most body tissues and fluids the propagation speed c is about 1540 m/s. The wavelength λ of the ultrasound wave is inversely proportional to the sound frequency f:

$$\lambda = \frac{c}{f} \tag{1.1}$$

For the same propagation speed, a higher frequency implies a shorter wavelength.

Reflection, transmission and scattering

At tissue boundaries, ultrasound pressure waves can be reflected, transmitted (refracted) and/or scattered, depending on the acoustic impedance properties and dimensions of both tissues. The acoustic impedance Z [Rayl=kg/(m²s)] is a material property and describes the local interaction of sound pressure and particle velocity (differs from sound velocity). It can be expressed as the product of the mass density ρ and propagation speed c (Cobbold 2007; Nichols et al. 2011):

$$Z = \rho c \tag{1.2}$$

At transients in acoustic impedance, typically at tissue interfaces, the ultrasound wave is partially reflected and transmitted (Figure 1). Reflection of the ultrasound wave predominantly occurs at interfaces with a dimension substantially larger than the wavelength. The angle of the reflected wave is similar to the angle of the incident wave. Tissue interfaces perpendicular to the transducer, i.e., incident angle is zero, are therefore reflected directly back towards the transducer. The relation between the angle of the transmitted wave θ_t and incident wave θ_i is described by Snell's law (Cobbold 2007):

$$\frac{\sin\theta_i}{\sin\theta_t} = \frac{c_1}{c_2} \tag{1.3}$$

The wave direction will change when propagation speeds differ, i.e., the ultrasound wave is refracted. In case the incident angle is zero ($\theta_i=\theta_t=0$), reflection and transmission coefficients (R and T), describing the fraction of impinging energy that is reflected or transmitted (R+T=1) are given by (Cobbold 2007):

$$R = \left[\frac{Z_2 - Z_1}{Z_2 + Z_1}\right]^2 \tag{1.4}$$

$$T = \frac{4Z_1Z_2}{\left[Z_2 + Z_1\right]^2} \tag{1.5}$$

Reflection does not occur within a homogeneous tissue (no change in impedance), whereas the reflection coefficient R increases for a larger acoustic impedance mismatch.

With decreasing size of the reflector, expressed in wavelengths, the pattern of the reflected wave gradually widens and becomes omnidirectional for interfaces with a much smaller dimension than the wavelength, a process called scattering. When insonating human tissue, it is likely that interfaces are rough, curved, and have a wide range of dimensions. Hence, the signal received by the transducer will be a mixture of scattered and reflected signals.

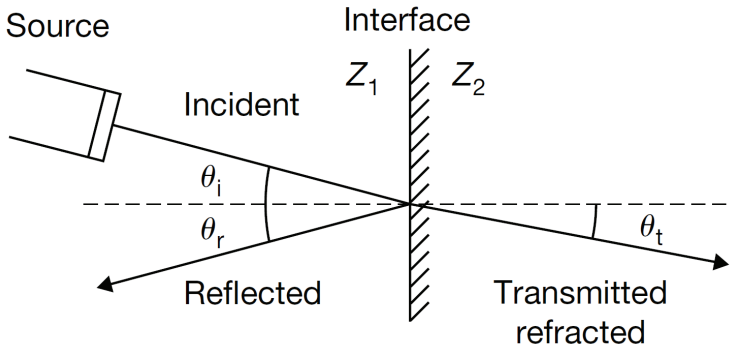

Figure 1

At transients in acoustic impedance (Z_1 and Z_2), typically at tissue interfaces, the ultrasound wave with incident angle θ_i is partially reflected and transmitted with reflected angle θ_r and transmitted angle θ_t; adapted from Baumgartner (2006).

Attenuation of waves

When an ultrasound wave travels through a medium, energy loss will occur and hence wave attenuation. Energy loss is caused by absorption (Cobbold 2007) and involves conversion of ultrasound energy into other energy forms, mostly heat (Cobbold 2007). The attenuation of ultrasound has an exponential decay and depends on both tissue properties and ultrasound frequency. The attenuation coefficient α is calculated according to:

$$\alpha = -10 \log_{10} \frac{I(x)}{I(0)} \tag{1.6}$$

where I(0) and I(x) are the incident intensity [W/m²] at location x=0 and x, respectively. The attenuation coefficient varies between 0.5 and 1 dB/(cm·MHz). So, a larger distance covered by the ultrasound wave and a higher frequency lead to a stronger attenuation. Therefore, superficial tissues can be investigated with a relatively higher ultrasound frequency (7-15 MHz), whereas deeper lying tissues, like the abdomen, require a lower ultrasound frequency (3-5 MHz).

Bone has a high attenuation coefficient of 10 dB/(cm MHz), implying after 1 cm transmission with an emission frequency of 1 MHz a decrease in intensity to 1/10 of the original intensity. Consequently, since the distance covered at reception is twice the depth at which the reflection occurred, the intensity at reception is decreased to 1/100 of the original intensity. Due to a high acoustic impedance mismatch at the tissue-bone interface, the transmitted waves will have a low amplitude. The reflected signal will encounter the interface again, causing further attenuation. Hence, it is only possible to gain information of tissue interfaces behind the bone when the emission frequency is low and bone thickness is thin, which is the case for transcranial brain investigation through the temporal bone. Similar to the tissue-bone interface, the large acoustic mismatch between air and tissue greatly limits transmission. Moreover, air has a very high attenuation coefficient. Therefore, ultrasound recordings in human beings are always made with a water based gel between the transducer and the skin.

Transducers

Bandwidth of the ultrasound pulse

Transducers, consisting of piezoelectric elements, convert electrical energy into acoustic energy and acoustic energy back into electrical energy, involving the piezoelectric effect. The effective bandwidth of an ultrasound pressure pulse is defined as width of the spectral distribution whereas the spectral amplitude is half the peak amplitude. The effective bandwidth B is related to the effective time duration T of the corresponding ultrasound pulse and is limited by $B \cdot T \geq 0.5$ (Gabor 1946), i.e., a larger bandwidth requires a shorter pulse duration. The minimum bandwidth-time product (0.5) is attained for a Gaussian shaped spectral distribution but in daily practice, it can be simplified to $B \cdot T = 1$ (Hoeks and Reneman 2005; Nichols et al. 2011). Transducers are made of piezoceramic material which usually exhibits a narrow, hence unsuitable bandwidth, but this is enlarged by transducer backing (to prevent ringing) and front layer impedance matching (Kremkau 1998) to bridge the impedance mismatch between transducer material (Z=30 MRayl) and water (Z=1.5 MRayl) (Kremkau 1998; Cobbold 2007). The relative bandwidth B_r is defined as the effective bandwidth divided by the emission frequency ($B_r = B/f$). Likewise, expressing the pulse duration as the number of emitted periods τ divided by the emission frequency ($T = \tau/f$), the effective number of emitted periods is inversely related to the relative bandwidth ($\tau = 1/B_r$), i.e. a relative bandwidth of 50% corresponds to a pulse length of two periods. The effective emitted pulse length sets the lower limit for the axial resolution, as discussed later in this Chapter.

Focusing of the ultrasound beam

The shape of the ultrasound beam depends on the dimensions of the transducer and activation of the transducer elements (Nichols et al. 2011). The ultrasound beam can be narrowed by focusing in the plane perpendicular to the scan plane as well as within the scan plane.

- Focusing in the perpendicular scan plane
  - Focusing in the perpendicular scan plane can be achieved mechanically by an acoustic lens with a propagation speed of sound deviating from the propagation speed of sound in tissues, creating a time delay depending on velocity difference and path length.
- Focusing within the scan plan
  - Focusing within the scan plan at emission is achieved by applying different time delays to the activation of a group of adjacent transducers elements, resulting in a curved excitation wavefront (Figure 2). Due to focusing, the ultrasound beam will converge at a specific depth, called focal point, where all ultrasound signals will arrive in phase, assuming that the speed of sound for all impinging directions is the same. Focusing is only possible in the near field of the transducer. Since the ultrasound beam will diverge further away from the focal point, the beam width will vary with depth.
  - More importantly, focusing within the scan plane is also achieved at reception, shifting dynamically the focal point (dynamic focusing) by adjusting the applied time delays according to the anticipated depth the signals are returned from.

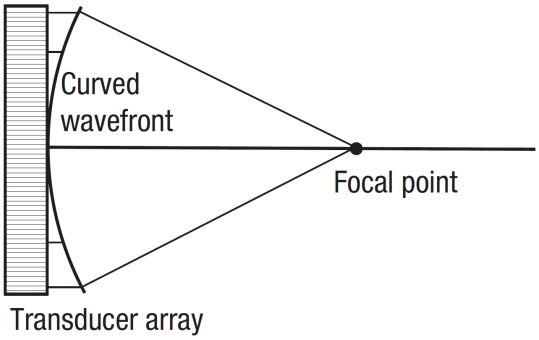

Figure 2

Applying different time delays to the activation of a group of adjacent transducers elements results in a curved excitation wavefront (Nichols et al. 2011). Assuming that the speed of sound for all impinging directions is the same, all ultrasound signals will arrive in phase at the focal point.

Axial and lateral resolution

Assuming similar propagation speed (c=1540 m/s) through tissues, the time delay (Δt) between transmission and reception of the ultrasound pulse can be converted to the depth (d) of the reflecting tissue interface by:

$$2d = \Delta tc \tag{1.7}$$

The round trip distance travelled by the ultrasound pulse is twice the depth of the tissue interface, which explains the factor 2 in the expression. The axial resolution is the smallest distance between two tissue interfaces for which the received signals can be discerned, which is equal to half the effective spatial pulse length (Kremkau 1998). High resolution ultrasound systems usually have a relative bandwidth of 50% and thus emit pulses containing effectively two periods (BT=1), resulting in a round-trip axial resolution of one wavelength (Nichols et al. 2011), which is 257 μm for an emission frequency of 6 MHz (c=1540 m/s). Since wavelength depends on the emission frequency and emission frequency determines attenuation (see above), a trade off needs to be made between axial resolution and penetration depth.

The lateral resolution is defined as the smallest distance at which two objects can be distinguished in the direction perpendicular to the axial direction. The lateral resolution depends on the beam width in the scan plane of the ultrasound wave and is considerably larger than the axial resolution. By focusing of the ultrasound beam, a narrower beam width typically around 5 wavelengths, and consequently better lateral resolution (about 1.3 mm at 6 MHz) can be accomplished (Nichols et al. 2011).

Imaging arrays

An ultrasound probe commonly contains numerous transducer elements arranged in a phased or linear array. A phased array (height and width on the order of 30 wavelengths) is divided into small elements (approximately 64 elements) with an element width less than a wavelength to facilitate for each element a disperse radiation pattern (Nichols et al. 2011). The elements together transmit and receive an ultrasound pulse. This pulse can be steered into different directions and focused by properly setting and adjusting the applied time delays at emission and reception, respectively. An advantage of a phased array is the small footprint of the probe. This renders phased arrays useful for imaging through a limited physiological window, for example between the ribs for cardiac applications. A linear or curved array (40 mm width for superficial applications) is composed of 128-256 elements. Typically, the element width is on the order of one wavelength (Nichols et al. 2011) which allows some steering of the beam direction. A subgroup of neighboring elements (16-32 elements), called aperture, is used to transmit and receive an ultrasound pulse and focus the ultrasound beam at emission and reception. After an ultrasound signal has sufficiently died away due to attenuation, a subgroup of neighboring elements shifted over one element position emits a new pulse. This process continues for the current and is repeated for the subsequent scan lines. Straight linear array probes are used for imaging at superficial locations while curved linear arrays (wider scan lines for the same footprint) are preferred for deeper lying locations, such as abdominal applications.

The sum signal received by the transducer elements is called the radiofrequency (RF) signal and is composed of reflected and scattered ultrasound signals with a gradually decaying amplitude as function of delay time (i.e. depth). Since the ultrasound speed hardly varies for biological tissues (except for bone), the time axis can be readily converted to a depth axis assuming an average sound speed (1540 m/s) by expression 1.7. At a greater depth, the signal amplitude reaches the noise level and a new pulse can be emitted without interaction (without attenuation the echoes would never fade away). Consequently, the pulse repetition frequency (PRF) can be high for a high ultrasound frequency or for highly attenuating media, i.e., for limited penetration depths. Therefore, the employed PRF, and hence the maximum image frame rate, depends on the selected ultrasound frequency (Kremkau 1998).

Ultrasound imaging modes

The display of the amplitude of the RF signal (envelope) is called amplitude mode, commonly referred to as an echoline in A-mode (A for amplitude). Commonly, for display, the amplitude is converted to grey scale levels based on an 8-bit data range, resulting in 256 grey levels. The display of subsequent A-mode echolines as function of time is called motion (M-) mode. With M-mode the brightness distribution in depth and over time reveals the location and dynamic behavior of tissue interfaces. Steering the path of the subsequent ultrasound pulses either with different sets of elements (aperture) or by varying the phase delay pattern of activation produces a two-dimensional (2D) scan plane and results, after grey scale conversion, into a 2-dimensional B-mode image (B for brightness) which is sector shaped for a phased array and rectangular for a linear array (Figure 3). Repeating the procedure produces a sequence of B-mode images over time. In the clinic, B-mode images in superficial applications (ultrasound frequency about 6-8 MHz) typically contain about 200 echolines covering 40 mm and have a frame rate in the range of 25 to 50 frames per second. Fast B-mode (Figure 3) is a special case in which a high frame rate (>300 Hz) is achieved by reducing the line density at the expense of spatial information (Meinders et al. 2001). Recording echo images at a high frame rate requires a dedicated RF acquisition system, restricting its use to research centers or specialized hospitals.

Compound imaging

Speckle is a grainy pattern on the ultrasound image caused by the phase interference of signals originating from reflectors and scatterers at an interspacing of less than the resolution. Therefore, the axial and lateral resolution of the ultrasound system within and beyond the focal region are directly reflected in the speckle size (Nichols et al. 2011). To reduce speckle artifacts and thereby improving image quality, multiple frames (usually 3) are recorded under slightly different (oblique) angles and averaged to build up a final B-mode image. This technique, called compound imaging, reduces the frame rate but enhances image quality by reducing speckle artefacts. In addition, compound imaging makes reflections less susceptible for the angle of incidence, which is relevant for curved tissue interfaces, e.g., artery walls inclined with respect to the ultrasound probe (Entrekin et al. 2001).

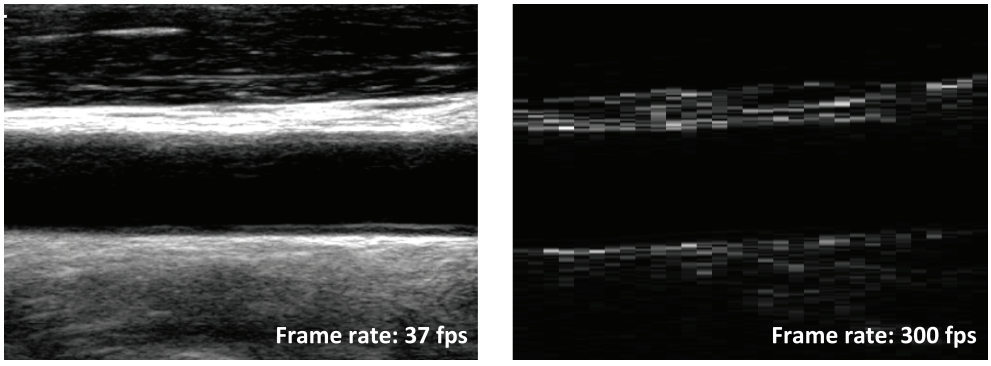

Figure 3

B-mode recording obtained with a linear array (left) and radiofrequent recording in fast B-mode (right) of the common carotid artery.

Image processing: from US scan frames to video display

Due to attenuation the amplitude of the RF signal degrades with depth. To ensure a similar amplitude level over depth, systems enforce an RF signal amplification that gradually increases with depth, also known as time gain compensation (TGC). Manual fine tuning for specific depth ranges is facilitated by slider controls. To avoid signal saturation the ultrasound system keeps the maximum signal level within limits. To avoid that relatively bright structures dominate an image, their amplitudes are, prior to grey scale conversion, selectively reduced by compression, a non-linear operation. Subsequently, the amplitude of the RF signal is sampled at around one third of the axial resolution in the depth direction and interpolated in lateral direction to arrive at square samples by a digital scan converter. The amplitude of each sample is converted to a grey scale value and stored at corresponding pixel locations in a digital memory, representing an echo image of M x N pixels (for example 400 by 400 pixels). Since the echo image is surrounded by supporting information, i.e., ultrasound settings, patient name etc., the ultrasound screen monitor should accommodate larger echo images (about 1000 by 800 pixels). After grey scale conversion, post-processing techniques which vary across ultrasound systems, i.e., smoothing techniques and edge enhancement are applied to B-mode images to enhance the image quality.

Ultrasound recordings can be stored either in DICOM (Digital Imaging and Communications in Medicine) or in AVI format. An advantage of the DICOM format is the preservation of the original frame rate and image size in pixels whereas AVI format has a fixed poor image format (600 by 400 pixels compared to 1000 by 800 pixels) and a standard frame rate of 25 fps.

Artifacts

Reverberations

Parallel interfaces perpendicular to the ultrasound beam direction cause a repetitive reflection of the ultrasound pulse by both interfaces, for example between blood vessel walls. This process is called reverberation and results in a trail of gradually decaying ghost echoes below the second interface. Although these subsequent reflections have lower amplitude than the original ultrasound echo, reverberations cause problems if the trail of echoes extends into echolucent regions. Reverberations can be reduced interactively by slightly angling the ultrasound probe.

Speed of sound and refraction artifacts

Focusing and image conversion are executed under the assumption that the speed of sound through tissues is constant (1540 m/s) and the ultrasound pulse follows a straight path. Violation of these assumption leads to blurring and improper location of tissue interfaces. Ultrasound pulse direction is affected by refraction effects leading also to improper location of tissue interfaces.

Attenuation artefacts

To compensate for attenuation by time-gain control (TGC), an average attenuation rate through the tissue is assumed. Underestimating or overestimating the local rate of attenuation leads to shadowing and flaring effects (Baumgartner 2006). For example, because of the impedance mismatch ultrasound pulses hardly penetrate a calcified plaque and attenuate more rapidly within plaques. Because of inadequate gain compensation, the region behind the leading tissue-plaque interface appears echolucent, referred to as a shadow (Figure 4). A cyst in tissue has the opposite effect. Because the fluid inside a cyst has a much lower attenuation rate than expected, the attenuation compensation is overexpressed, leading to a relatively bright region behind the cyst (Baumgartner 2006).

Out of plane motion artefacts

Due to breathing, swallowing and/or blood pressure pulsations, a blood vessel or plaque may be translated partly and temporarily moved out of the plane of observation. If the intended recording time is short, the patient can be asked to hold their breath to overcome this problem. Techniques for vessel wall detection are challenged by the lateral and/or axial (usually in case of a nearby vein) and/or out of plane motion of a blood vessel. The longer the time interval between observations (lower frame rate), the more problematic it will be to identify properly corresponding locations.

Doppler ultrasound imaging

Velocities of small moving objects, like red blood cells (with a dimension in the range of 5-8 μm which is far smaller than the wavelength causing scattering), can be determined by ultrasound employing the Doppler principle (Hoeks and Reneman 2005; Nichols et al. 2011). The Doppler approach can be applied to moving structures as well, but requires perpendicular insonification to ensure reception of the reflected sound signal. Moving objects induce a frequency shift f_d between the emitted and reflected ultrasound pressure waves, called the Doppler shift. The relative Doppler shift equals the relative velocity (Evans et al. 1989; Hoeks and Reneman 2005):

$$\frac{f_d}{f_e} = \frac{2v\cos\alpha}{c} \tag{1.8}$$

with f_e the emitted frequency, and $2v\cos\alpha$ the velocity of the object along the line of observation. Emission frequencies for Doppler applications usually range from 1 to 10 MHz (Evans et al. 1989). The Doppler shift measured with ultrasound is generally not caused by a single red blood cell, but rather by an ensemble of red blood cells passing the insonated vessel with unlikely the same velocity. Therefore, the received Doppler signal consists of a spectrum of frequencies (Reneman and Spencer 1979; Evans et al. 1989).

Assuming a blood flow velocity of 1 m/s, a speed of sound of 1540 m/s and an emitted frequency of 5 MHz, the Doppler shift is about 6.1 kHz which is in the audible range (Hoeks and Reneman 2005; Nichols et al. 2011). Generally, average blood velocities will be below 1 m/s. At a stenosis, average blood velocities can increase up to 5 m/s (Hoeks and Reneman 2005; Nichols et al. 2011) and large Doppler shifts are detected (Reneman and Spencer 1979). Since BT=1 (Hoeks and Reneman 2005), the observation interval T directly dictates the spectral resolution of the Doppler shift, which can be converted to the velocity resolution using the Doppler equation. For a given observation interval, the velocity resolution can be improved by higher emission frequency (though attenuation imposes an upper limit) or a more obtuse angle α between the ultrasound pulse and the object direction (Hoeks and Reneman 2005).

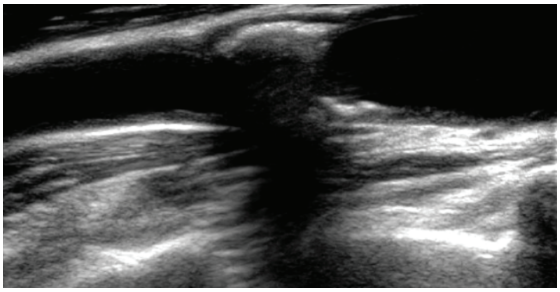

Figure 4

B-mode image of an echogenic plaque in the internal carotid artery. Because of inadequate gain compensation, the region behind the leading tissue-plaque interface appears echolucent, referred to as a shadow.

Doppler systems can be either categorized into continuous wave (CW), continuously transmitting and receiving ultrasound pulses, or pulsed wave (PW), transmitting and receiving ultrasound pulses at regular intervals enabling detection of velocities at a specific depth (Evans et al. 1989). Pulsed Doppler imaging requires at least 2 emission/reception cycles within a short time window. The displacement in between observations should not exceed a quarter of a wavelength to avoid observation of a false velocity direction (aliasing), setting a lower limit for the pulse repetition frequency (as discussed earlier attenuation imposes an upper limit). A high number of emission/reception cycles reduces velocity noise but a large temporal window (sample volume) will conflict with the dynamic nature of pulsatile flow. Changing intermittently the beam direction and/or beam position allows the acquisition of a 2D-velocity distribution. Color flow systems superimpose the 2D velocity information, obtained by scanning pulsed wave Doppler, in color on a B-mode image, enabling a combined presentation of anatomical and functional (blood flow) information. Traditionally, blood flow towards the ultrasound probe is colored red, whereas blood flow away from the probe is colored blue. Color flow imaging enables identification of jets within and distal to severe stenoses (Figure 5) and isolates echolucent plaques which will be missed in standard B-mode imaging (Figure 5).

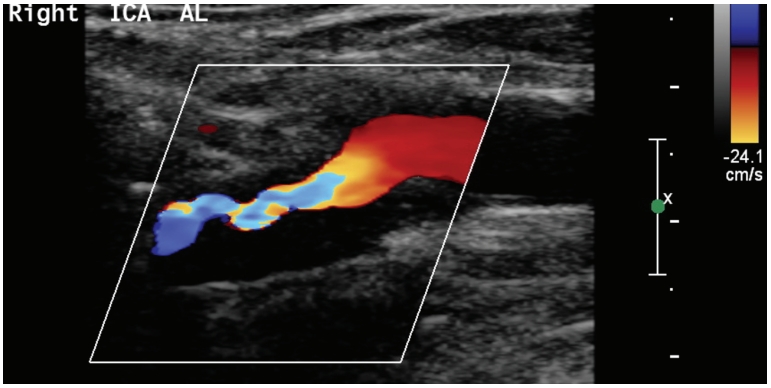

Figure 5

Color Doppler image of an echolucent plaque causing a severe stenosis (>70%) in the internal carotid artery. A jet (the area of blue colour as a consequence of aliasing) is formed near and distal to the stenosis. The echolucent plaque is apparent only by a partial lack of colour within the vessel lumen.

PARISK ultrasound recordings

In the PARISK study, ultrasound examinations of the common and internal carotid artery were performed bilaterally. The entire ultrasound protocol is listed in the Appendix. A short description of the PARISK ultrasound protocol is given below.

During the examinations, patients were in supine position with their head slightly tilted to the opposite side. Examinations were performed with a Philips iU22 scanner (Philips Medical Systems, Bothell, USA) using compound imaging and post-processing techniques at a frame rate of approximately 40 Hz. Different linear probes were used depending on the depth location of the carotid artery (17-5 MHz, 12-5 MHz or 9-3 MHz). To get a quasi 3D impression of 2D recordings, recordings of the carotid artery were acquired in the longitudinal plane at anterolateral and posterolateral angles perpendicular to each other (Figure 6). Recording duration was at least 5 seconds to cover 3-6 heart beats. In addition to B-mode recordings, color flow images were recorded to enable identification of echolucent plaques. To determine the degree of stenosis, the highest peak Doppler velocities at or distal of the stenosis were measured. To assess the inter-recording variation and preserve original frame rate, each recording was repeated once and stored in DICOM format.

In addition to the standard B-mode ultrasound examination, radiofrequency fast B-mode examinations of the symptomatic CCA and ICA were performed on a Mylab70 scanner (Esaote Europe, Maastricht, The Netherlands) using a 13-4 MHz linear probe (width 40 mm). Fast B-mode recordings commonly have a high frame rate (around 500 Hz) with consequently a reduced number of recording positions (e.g., 19 lines, spaced at 0.9 mm, covering 17 mm). Since plaque length is usually larger than 17 mm, in the PARISK study fast B-mode recordings were acquired at 31 lines, spaced at 0.9 mm and covering 29 mm, yielding a frame rate of approximately 300 Hz. The RF signals were sampled at 50 MHz corresponding to a sample distance of approximately 15 µm (assumed c=1540 m/s) and recorded on hard disk for off-line evaluation.

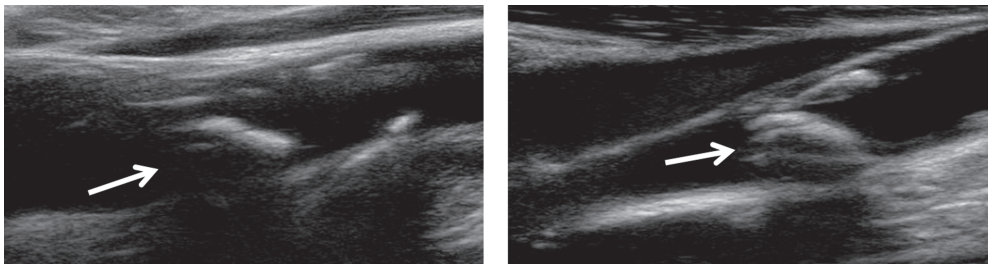

Figure 6

To get a quasi 3D impression of 2D recordings, B-mode recordings of a severe stenosis (indicated by the white arrow) in the internal carotid artery were acquired in the longitudinal plane at anterolateral (left) and posterolateral (right) angles perpendicularly to each other.

Arterial wall echo tracking

The phase of the RF signal is commonly used to track the displacement of the media-adventitia transitions over time. The difference of the displacement waveforms of the anterior and posterior walls yields the diameter, and hence the distension waveform with high accuracy and precision (Meinders et al. 2001). Several different algorithms for phase tracking have been developed which are not interchangeable as observed distensions are significantly different (Segers et al. 2004; Palombo et al. 2012). An efficient and commonly used algorithm for wall tracking employs a complex cross-correlation model (Brands et al. 1997). However, the complex cross-correlation model may exhibit a minor velocity dependent bias (Brands et al. 1997). A periodic reset, e.g. at end-diastole, is necessary to remove the associated accumulative drift. In addition, phase tracking requires a dedicated ultrasound and RF acquisition system.

Alternatively, diameter and distension waveforms may be obtained from B-mode video sequences by so-called edge tracking which uses an amplitude threshold to determine the location of the media-adventitia transition. Algorithms for vessel wall tracking of B-mode video sequences rely, e.g. on grey-level gradient analysis (Bianchini et al. 2010) or on the first absolute central moment (Stadler et al. 1997). Since in the clinic standard B-mode images are recorded and the PARISK project aims at an easy to use method to follow plaque development, this thesis proposes and explores an echo edge tracking method for standard B-mode images to extract diameter, distension and intima-media thickness, and their inhomogeneities.

References

Baumgartner RW. Handbook on neurovascular ultrasound. Karger, Basel ; New York, 2006.

Bianchini E, Bozec E, Gemignani V, Faita F, Giannarelli C, Ghiadoni L, Demi M, Boutouyrie P, Laurent S. Assessment of carotid stiffness and intima-media thickness from ultrasound data: comparison between two methods. J Ultrasound Med 2010;29:1169-1175.

Brands PJ, Hoeks AP, Ledoux LA, Reneman RS. A radio frequency domain complex cross-correlation model to estimate blood flow velocity and tissue motion by means of ultrasound. Ultrasound Med Biol 1997;23:911-920.

Cobbold RSC. Foundations of biomedical ultrasound. Oxford University Press, Oxford ; New York, 2007.

Entrekin RR, Porter BA, Sillesen HH, Wong AD, Cooperberg PL, Fix CH. Real-time spatial compound imaging: application to breast, vascular, and musculoskeletal ultrasound. Semin Ultrasound CT MR 2001;22:50-64.

Evans DH, McDicken WN, Skidmore R, Woodcock JP. Doppler ultrasound : physics, instrumentation, and clinical applications. Wiley, 1989.

Gabor D. Theory of communication. Part 1: The analysis of information. Electrical Engineers - Part III: Radio and Communication Engineering, Journal of the Institution of 1946;93:429-441.

Hoeks APG, Reneman RS. Do Doppler Systems Color Arteries Red? In: Kowalewski TA, ed. Blood Flow Modelling and Diagnostics. Warschau: 2005. pp.

Kremkau FW. Diagnostic ultrasound : principles and instruments. 5th. W.B. Saunders, Philadelphia, Pa., 1998.

Meinders JM, Brands PJ, Willigers JM, Kornet L, Hoeks AP. Assessment of the spatial homogeneity of artery dimension parameters with high frame rate 2-D B-mode. Ultrasound Med Biol 2001;27:785-794.

Nichols WW, O'Rourke MF, Vlachopoulos C. McDonald's blood flow in arteries : theoretic, experimental, and clinical principles. 6th. Hodder Arnold, London, 2011.

Palombo C, Kozakova M, Guraschi N, Bini G, Cesana F, Castoldi G, Stella A, Morizzo C, Giannattasio C. Radiofrequency-based carotid wall tracking: a comparison between two different systems. J Hypertens 2012;30:1614-1619.

Reneman RS, Spencer MP. Local Doppler audio spectra in normal and stenosed carotid arteries in man. Ultrasound Med Biol 1979;5:1-11.

Segers P, Rabben SI, De Backer J, De Sutter J, Gillebert TC, Van Bortel L, Verdonck P. Functional analysis of the common carotid artery: relative distension differences over the vessel wall measured in vivo. J Hypertens 2004;22:973-981.

Stadler RW, Taylor JA, Lees RS. Comparison of B-mode, M-mode and echo-tracking methods for measurement of the arterial distension waveform. Ultrasound Med Biol 1997;23:879-887.

Appendix

PARISK WP4 Ultrasound protocol

Objectives

- ambulant emboli detection
- inhomogeneity distension and IMT common carotid artery
- plaque morphology and composition (grey scale analysis)
- deformation pattern along plaque
- strain distribution within plaque (platform 1, partly platform 2)

Ambulant emboli detection

- Aaslid will prepare a transcranial Doppler system with integrated probe repositioning and emboli detection.
- Present system is unilateral (single transducer) but can probably be extended to bilateral
- Recording time 4 hours
- Local read-out of distribution of emboli per hour and Doppler spectra
- Central (Maastricht) post-processing of Doppler waveforms (cerebral regulation) ensures common detection criterion

Preparation ultrasound B-mode recording

- high resolution ultrasound probe (10 MHz)
- linear array
- high frame rate (>40 Hz)
- on system with
  - logging of cine view recording (5 seconds)
  - includes display of ECG (for timing purposes)
  - and display of amplitude calibration bar (for image analysis)
- All participating centers have access to the Philips iU22 scanner
- Always use moderate gain settings (avoid saturation, relevant for grey level analysis)!
- To get feedback, a dedicated program will be made available to test on-site gain settings (requires transfer of data to PC) or alternatively the user can employ the Dicom viewer that comes with the system.
- The iU22 supports high-frame rate cine-view output via “Set up -> Print/Network ->Export Frame rate” to set export rate at “Acquisition rate” which can be 60 Hz depending on depth setting. This option replaces the standard Dicom output rate of 15 or 30 Hz.

Measurement protocol

- Allow 5-10 minutes rest in supine position (stabilization hemodynamic condition)
- Use this time to
  - complete forms
  - attach ECG if available/standard in hospital
- Perform arm-cuff blood pressure measurements on both sides (to exclude subclavia stenosis)
- Execute left-right ultrasound measurements in random error (to avoid measurement bias)

- Screen common carotid artery (CCA), carotid bulb, internal carotid artery (ICA) and external carotid artery for plaques
- Note kinky/twisted morphology of arteries
- Note position of plaques with bulb bifurcation as reference
- Make ultrasound recording of CCA in plane of bulb bifurcation (upper tip probe 1 cm proximal to flow divider); longitudinal view; frame rate >40 Hz.
- Store 5 seconds
- Repeat measurement at orientation shift of 90 degrees, longitudinal view
- Repeat measurement in bulb (plane of bifurcation), longitudinal view
- If plaque, then it should be centered in image plane
- Repeat B-mode measurement in cross-sectional view while sliding transducer within 5 seconds from (normal part of) CCA to ICA over a distance of 8 cm (note distance)
- Make pulsed Doppler recordings CCA and carotid bulb (sample volume 1 mm).
- Store 5 seconds
- Repeat in color Doppler mode (store 5 seconds)
- Repeat sequence for other side
- Repeat everything (intrasubject variation).

Off-line analysis (Maastricht)

- Select images in end-diastole (R-top)
- Identify region of interest
- Measure lumen diameter and wall thickness
- Perform grey-scale analysis
- For image sequences, wall-lumen transitions will be identified on a frame-to-frame base providing spatial distribution of wall displacement and changes in lumen diameter over time (cooperation with Pie Medical Imaging)
- Inhomogeneity in IMT and wall displacement (healthy) common carotid artery (serves also as reference for bulb)
- Inhomogeneity in wall displacement along plaque is indicative of site-dependent pressure or deformation (link to WP 3)
- Maastricht will add to the above analysis off-line processing of radio frequency signals (see Appendix) to obtain wall strain distributions (perpendicular observation), according to same acquisition protocol, but with another type of system.

Werner Mess, Department of Clinical Neurophysiology, azM, T: 043-3875273, Werner.Mess@mumc.nl; Arnold Hoeks, Department of Biomedical Engineering, Maastricht University, T: 043-3881668, A.Hoeks@bme.unimaas.nl

Maastricht, February 2010

RF signal acquisition protocol

- Allow 5-10 minutes rest in supine position (stabilization hemodynamic condition)
- Use this time to
    - complete forms
    - attach ECG
    - attach Nexfin finger cuffs
- Perform regularly arm-cuff blood pressure measurements at least twice before and after the RF measurements (also to validate finger pressures)
- Execute intermittently fingercuff blood pressure calibration
- Make B-mode clip of the plaque
- During the RF measurements: keep the light of the probe to the head
- Make RF ultrasound recording of CCA in plane of bulb bifurcation using 31 lines (upper tip probe 1 cm proximal to flow divider); longitudinal view
- Repeat measurement at orientation shift of 90 degrees, longitudinal view
- Repeat measurement in bulb (plane of bifurcation) using 31 lines, longitudinal view
- If plaque, then it should be centered in image plane
- Repeat measurement in bulb (plane of bifurcation) using 19 lines, longitudinal view
- Repeat sequence in bulb at orientation shift of 90 degrees
- Repeat sequence for other side
- Repeat everything (intrasubject variation).

Maastricht, May 2012

3

Standard B-mode ultrasound measures local carotid artery characteristics as reliably as radiofrequency phase tracking in symptomatic carotid artery patients

Steinbuch J, Hoeks AP, Hermeling E, Truijman MT, Schreuder FH, Mess WH. Standard B-mode ultrasound measures local carotid artery characteristics as reliably as radiofrequency phase tracking in symptomatic carotid artery patients. Ultrasound Med Biol 2016;42:586-595.

Abstract

Local arterial stiffness can be assessed with high accuracy and precision by measuring arterial distension based on phase tracking of radiofrequency ultrasound signals acquired at a high frame rate. However, in clinical practice B-mode ultrasound registrations are made at a low frame rate (20-50 Hz). We compared in symptomatic carotid artery patients the accuracy and intra-subject precision of edge tracking and phase tracking distension. B-mode US-recordings (40 mm, 37 fps) and radiofrequency recordings (31 lines covering 29 mm, 300 fps) were acquired from the left common carotid artery of 30 patients (age 45-88 yrs.) with recent cerebrovascular events. To extract the distension, semi-automatic echo edge and phase tracking algorithms were applied to B-mode and RF recordings, respectively. Both methods exhibited a similar intra-subject precision for distension (SD=44 μm and SD=47 μm, p=0.66) and mean distension (difference:-6±69 μm, p=0.67). Intra-subject distension inhomogeneity tends to be larger for edge tracking (difference: 15±35 μm, p=0.04). Standard B-mode scanners are suitable to measure local artery characteristics in symptomatic carotid artery patients with good precision and accuracy.

Introduction

Arterial stiffness, quantified with carotid-femoral pulse wave velocity (cfPWV), is associated with risk of coronary heart disease, cerebrovascular events and all-cause mortality (Laurent et al. 2001; Mattace-Raso et al. 2006; Karras et al. 2012). Alternatively, arterial stiffness can be assessed locally by means of the distensibility coefficient, the relative change in diameter with respect to the local change in pressure over the cardiac cycle. Although arterial stiffness, quantified with the distensibility coefficient, is also associated with coronary heart disease (Leone et al. 2008) and vascular disease (van Sloten et al. 2014), it has not been validated as extensively as cfPWV (Boutouyrie et al. 2014). One important reason is that it requires an accurate and precise assessment of the distension, i.e., the diameter change over the cardiac cycle, in combination with the measurement of local pulse pressure, and is therefore technically challenging (Laurent et al. 2006; Boutouyrie et al. 2014), requiring dedicated hardware and analysis software.

Atherosclerosis, an important contributor to cardiovascular disease, affects arteries locally. A major advantage of arterial stiffness assessment using the distensibility coefficient is that this method allows assessment of local features of an artery whereas cfPWV provides average stiffness over a long trajectory, masking local information. The distension measurement, needed for distensibility assessment, reveals also intra-subject spatial distension inhomogeneity, i.e., variation of distension along a short arterial wall segment. Spatial distension inhomogeneity of the common carotid artery (CCA) is associated with focal atherosclerotic plaques in the carotid bulb (Graf et al. 2010) and can therefore be a clinically important marker of advanced atherosclerosis.

To assess arterial distension, the phase of the radiofrequency (RF) signal is used to track the displacement curves, of both the anterior and posterior media-adventitia transitions over time, and take the difference. An efficient and frequently used algorithm for phase tracking employs a complex cross-correlation model for signals with a Gaussian shaped spectral distribution (Brands et al. 1997) , providing high accuracy and precision (Meinders et al. 2001). It is applied to unprocessed RF ultrasound signals sampled at a moderate frequency (typically 4 times the carrier frequency) at a high repetition rate (>200 Hz). Consequently, this method requires a dedicated ultrasound and RF acquisition system, limiting its use to a small number of specialized hospitals.

The instantaneous diameter can also be extracted directly by processing the acquired videosequence with B-mode edge tracking. In clinical practice, B-mode ultrasound registrations are made at a low frame repetition rate (20-50 Hz), and are subjected to various video smoothing, compounding and compression techniques which vary across ultrasound systems. Consequently, these techniques may alter the apparent lumen diameter and wall thickness as demonstrated in phantoms (Potter et al. 2008) as well as in humans in the CCA (Rossi et al. 2009). These studies only considered the diastolic diameter; the effect of video processing on arterial distension measurements is unknown.

It remains unclear whether distension obtained with B-mode edge tracking is as accurate and precise as obtained with RF phase tracking in a clinical population having tortuous, motile or irregular arteries, e.g., elderly people suffering from cerebrovascular events with atherosclerotic plaques. To plan clinical studies, it is essential to know the accuracy and precision of the tracking methods, especially for technically and clinically challenging patients. Therefore, the aim of this study is to compare the accuracy and precision of the distension determined using B-mode edge tracking and RF phase tracking within a clinically relevant population with carotid atherosclerotic plaques. More specifically, we will 1) evaluate the intra-subject precision of edge and phase tracking distension, 2) compare B-mode edge tracking distension and RF phase tracking distension, and 3) compare the beat-to-beat variation and the intra-subject spatial inhomogeneity of both methods.

Methods

Study subjects

30 patients with a recent ischemic stroke or transient ischemic attack and a 30-69% stenosis of the ipsilateral internal carotid artery were randomly selected from the Plaque At RISK (PARISK) study (clinical trials.gov NCT01208025) (Truijman et al. 2014). The study was approved by the Medical Ethics Committee of Maastricht University Medical Center (MUMC). All patients gave written informed consent after explanation of the study.

Data acquisition

Ultrasound examinations of the left CCA were performed in duplicate on all patients, irrespective of side of symptoms, with two different ultrasound scanners. Recordings were acquired in a longitudinal plane at an anterolateral angle for at least 5 seconds, covering 3-6 complete heart cycles. During all ultrasound examinations, the patients were in supine position with their head slightly tilted towards the opposite side. The standard B-mode ultrasound examinations were performed with a Philips iU22 scanner (Philips Medical Systems, Bothell, USA) using a 17-5 MHz linear probe (width 40 mm) using compound imaging and post-processing techniques, i.e., smoothing, at a frame rate of 37 Hz. The image sequence with a pixel size of 66*66 µm was stored in DICOM format (Digital Imaging and Communications in Medicine). The RF examinations were performed on a Mylab70 scanner (Esaote Europe, Maastricht, The Netherlands) using a 13-4 MHz linear array transducer (width 40 mm), operating in fast B-mode, i.e., B-mode with a high frame rate of approximately 300 Hz but consequently a reduced number of recording positions (31 lines, spaced at 0.9 mm, covering 29 mm). The RF signals were sampled at 50 MHz, enabling a sample distance in depth of approximately 15 µm, and recorded on hard disk for off-line evaluation. A summary of all recording settings is shown in Table 1.

Table 1

Specifications of recording settings of B-mode and RF recordings.

	B-mode recordings (IU22)	**RF recordings (Mylab)**
Transducer [Mhz]	17-5	13-4
Frame rate [Hz]	37	300
Image width [mm]	40	29
Lines per image [-]	Unspecified (>100)	31
Sample width [µm]	66	900
Sample depth [µm]	66	15
ECG [-]	No	Yes
Recording time [s]	>5	>5

Vessel wall tracking

The distension of the artery was extracted with either edge tracking for the B-mode recordings or phase tracking for the RF recordings (Figure 1). Both tracking methods require initialization to determine the initial positions of the media-adventitia transition. After the explanation of wall tracking initialization, both tracking methods will be explained in detail.

Wall tracking initialization

For the initialization for B-mode edge tracking, the video movie (pixel size 66 by 66 μm) was reviewed to select a video-sequence without recording artifacts. A region of interest (ROI) was selected with at least 2.4 mm of tissue above and below the CCA and a width of 29 mm. On the first frame, 4 media-adventitia transitions were manually identified on the anterior (left, right) and posterior (left, right) walls (Figure 2). Linear extrapolation yielded a first guess for the media-adventitia transition of both the anterior and posterior wall. To reduce speckle artifacts (Welch 1967) a local spatial average over multiple echo lines was considered for actual edge detection rather than individual lines. For that purpose, the ROI was divided into approximately 25 segments with an 80% overlap and with a width of 4.5 mm, which is on the order of three times the lateral resolution of the ultrasound systems used. To improve precision of edge detection, the image was interpolated in depth with a factor 4, resulting eventually in a sample distance of 16.5 μm. The media-adventitia transitions of the anterior and posterior walls were automatically determined for each segment using a 1.6 mm search window symmetrically around the initial media-adventitia transition. A threshold of 65% of the trailing maximal grey value was used within the search window, likely the echo of the local adventitia wall. Subsequently, the detected media-adventitia transitions across the image were presented on screen, allowing manual adjustment if needed (Figure 3, left).

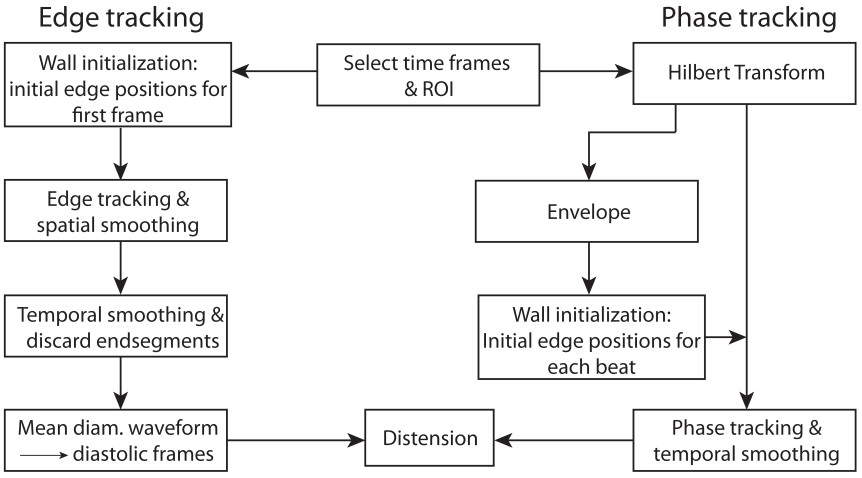

Figure 1

Flow chart for edge tracking (left) and phase tracking (right).

For phase tracking initialization, the RF signal was transformed into a complex signal using the Hilbert transformation. Its envelope, the absolute value of the complex signal, is used to obtain gray scale images of the RF recordings. A sequence of gray scale images without recording artifacts was selected for further analysis. A ROI was selected (width 29 mm) and the initial wall positions across the image were identified and manually adjusted if needed, similarly as for edge tracking (Figure 3, right).

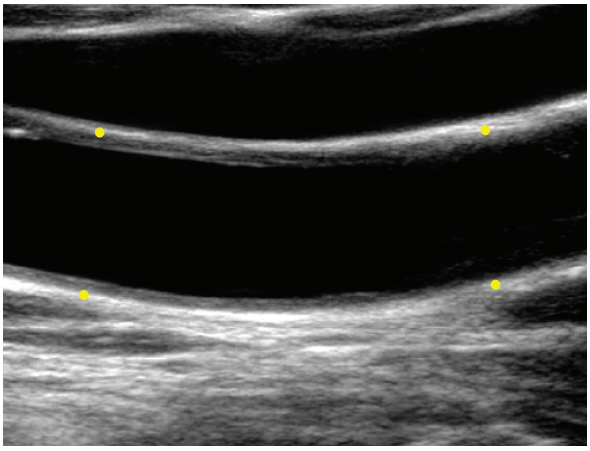

Figure 2

Media-adventitia transition markers on the anterior and posterior walls for wall initialization.

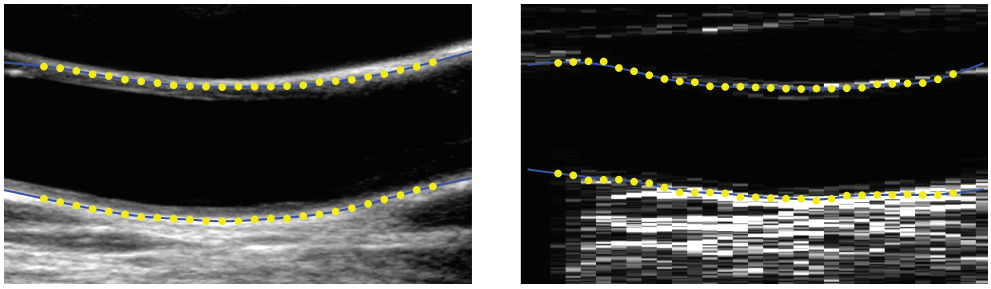

Figure 3

Example of wall initialization of B-mode recording (left) and RF recording (right) of CCA. Blue line and yellow dots indicate initial wall positions of the media-adventitia transition. The B-mode image has a high line density and is generated and post-processed by advanced image processing algorithms. Envelope of the RF signal provides a coarse gray scale image with a large interline distance (0.9 mm) where individual lines are clearly discernibly.

B-mode edge tracking

Edge wall tracking of the B-mode recordings was done with dedicated software developed by Maastricht University Medical Centre (MUMC, Maastricht, The Netherlands) based on previously published algorithms (Rossi et al. 2009). To track the media-adventitia transitions, for each segment a window was symmetrically placed around the media-adventitia transition of that particular segment as obtained in the previous frame. As a result, the total image region for wall initialization was reshaped into a rectangular form (Figure 4 left), with the wall transitions, as produced by the edge detection algorithm (Figure 4 right), distributed along a straight line. Incidental large deviations from the lumen center line were limited to the mean ± standard deviation of the observed deviations. The observed deviations were added to the input position, generating an updated wall edge distribution. In a final step the wall positions were smoothed across the image with a 2nd order Savitsky-Golay filter with a 7 mm window.

The detection process was independently executed for the anterior and posterior wall and repeated for the subsequent frames. The local difference between anterior and posterior media-adventitia transition provides an estimate for the instantaneous local lumen diameter within each segment.

After wall tracking, the distension waveforms of the edge segments were discarded to suppress possible errors from spatial filtering. The remaining distension waveforms were smoothed over time with a 2nd order Savitsky-Golay low pass filter, using a filter span of 0.2 s, which corresponds effectively to a 10 Hz cut-off frequency. The mean distension waveform over all segments was calculated to identify end-diastolic frames.

RF-based phase tracking

After wall initialization, the complex cross-correlation model (Brands et al. 1997), applied to a sliding window starting at the identified media-adventitia transitions, was used to track the wall motion over the cardiac heart cycle. The sliding correlation window had a size of 0.4 mm * 4.5 mm * 10 ms, corresponding to 26 sample points in depth, 5 lateral positions and 3 time points. The local difference between anterior and posterior media-adventitia displacement waveforms provides an estimate for the instantaneous local diameter. All distension waveforms were smoothed over time with a 2nd order low pass Butterworth filter (cut-off frequency 40 Hz). Phase tracking, using the complex cross-correlation model (Brands et al. 1997), may exhibit a slight velocity dependent drift over the cardiac cycle, necessitating wall initialization at each end-diastolic frame. For that purpose one may use a simultaneously recorded ECG as time reference. In the current study we used the end-diastolic frames extracted similarly as for edge tracking from the mean distension waveform, to prevent discrepancy between methods. At those end-diastolic frames, the initial wall positions were adjusted interactively (see wall initialization) when necessary and distension waveforms were corrected accordingly.

Statistical analyses

After wall tracking, the distension was extracted from each distension waveform by taking its peak-to-peak difference, i.e., the difference between systolic and diastolic diameter. The end-diastolic diameter and distension for a recording were defined as the median over all image segments and subsequently all available heart beats. To calculate the intra-subject precision, the difference between both individual recordings and their average is considered, the average being the gold standard. Intra-subject precision is then calculated as the standard deviation (SD) of differences over all recordings and all patients and evaluated with an F-test. The temporal beat-to-beat variation is defined as the standard deviation over all available heart beats. For both edge and phase tracking, the average diameter and distension over two repeated recordings of a subject were calculated and subjected to a paired t-test. Coefficient of variation is defined as intra-subject precision (standard deviation) divided by the mean.

Intra-subject inhomogeneity, i.e., spatial variation, of end-diastolic diameter and of distension were calculated as the standard deviation over the segments, averaged over heart beats and evaluated with a paired t-test. The average distension and its intra-subject inhomogeneity were also evaluated by Bland-Altman plots, illustrating the differences between edge and phase tracking with respect to each other. Values are quantified as mean ± standard deviation (SD) and the significance level is set at $p<0.05$.

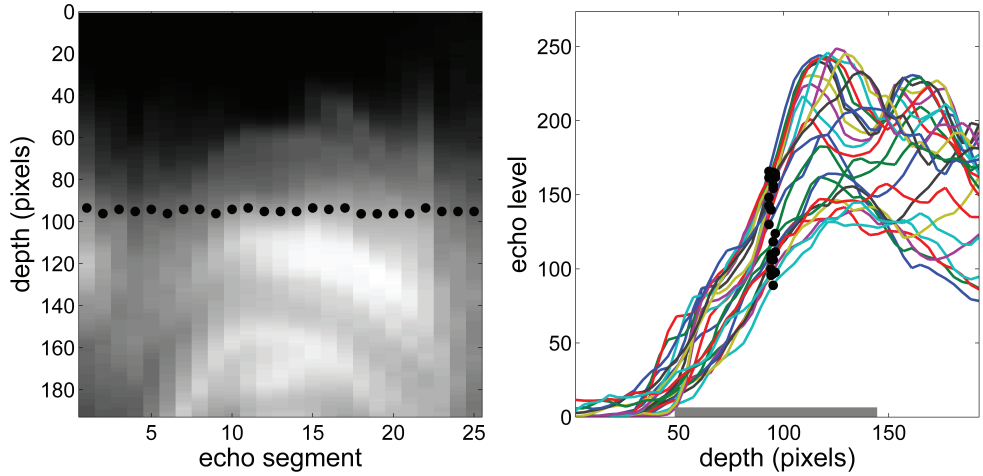

Figure 4

Example of detected media-adventitia transitions of the posterior wall for all segments. The selected image region, reshaped into a rectangular form, is displayed in the left panel. The identified media-adventitia transitions, indicated by black dots, are distributed along a straight line. A-mode signals of the posterior artery wall for all segments are shown in the right panel, with the dots marking the detected media-adventitia within the search region (thick bottom line).

Results

Of the 30 patients included in the study, three patients were excluded from image analysis due to either substantial out of plane motion, poor image quality or missing data. Therefore, 27 patients (mean age 68±10 yrs.) were used for final analysis. 13 patients had a stroke and 14 had a TIA. Further clinical characteristics are listed in Table 2.

Table 2

Patient characteristics of symptomatic carotid artery patients. Data are presented as mean ± standard deviation.

N	27
Age [years]	68±10
Male/female [-]	17/10
BMI [kg/m^2]	26±4
Diastolic blood pressure [mmHg]	85±10
Systolic blood pressure [mmHg]	156±17
Heart rate [beats/min]	65±19
Stroke / TIA [-]	13/14
Side of symptoms [left/right]	13/14
Range of bulb stenosis [%]	30-69

Diastolic diameter

The intra-subject precision of end-diastolic diameter, defined as the standard deviation over all recordings and all patients, is significantly lower (i.e., better) for edge tracking than for phase tracking (SD=120 μm and SD=170 μm, respectively, F-test: p-value=0.01), shown in Table 3. Also, the temporal beat-to-beat variation is significantly smaller for edge tracking (difference -76±55 μm, paired t-test: p-value<0.001). The B-mode edge tracking yields significantly smaller end-diastolic diameters than the RF-based phase tracking (difference -269±339 μm, paired t-test: p-value<0.001). Despite the differences in intra-subject precision and mean end-diastolic diameter, both tracking methods exhibit a similar, very low, coefficient of variation for the end-diastolic diameter (CV≈2%).

End-diastolic diameter inhomogeneity, defined as the standard deviation of end-diastolic diameter over the segments, is also shown in Table 3. Intra-subject precision of diameter inhomogeneity is similar for both tracking methods (SD=56 μm and SD=57 μm, respectively, F-test: p-value=0.84). However, temporal beat-to-beat variation is smaller for edge tracking (difference -29±24 μm, paired t-test: p-value<0.001), similarly as the beat-to-beat variation of end-diastolic diameter. The average end-diastolic diameter inhomogeneity over all patients is similar for both tracking methods (difference -8±184 μm, paired t-test: p-value=0.83).

Distension

An example of distension waveforms over two heart beats of the same patient obtained with edge and phase tracking is shown in Figure 5. The raw distension waveforms obtained with edge tracking exhibit speckle noise (Figure 5 left), which is removed by the low pass filter (Figure 5, middle). The distension waveforms obtained with phase tracking (Figure 5, right),

lowpass filtered with a cut-off frequency of 40 Hz, retain more temporal detail than those obtained with edge tracking. The tracking waveforms obtained with edge tracking seem to be more dispersed than those obtained with phase tracking.

Despite the differences in distension waveforms, phase tracking as well as edge tracking exhibit similar intra-subject precision (SD=44 μm and SD=47 μm, F-test: p-value=0.66) and coefficient of variation (CV=12%) for distension, as shown in Table 4. However, temporal beat-to-beat variation is significantly larger for edge tracking (difference 10±19 μm, paired t-test: p-value=0.014).

Table 3

End-diastolic diameter and its inhomogeneity of the CCA determined by edge and phase tracking. Values are presented as mean ± standard deviation. Intra-subject precision is defined as standard deviation of differences over all recordings and all patients. Temporal beat-to-beat variation is defined as the standard deviation over the heart beats.

	(N=27)	Edge tracking	Phase tracking	P-value
End-diastolic diameter	Intra-subject precision [μm]	120	170	0.01
	Beat-to-beat variation [μm]	46±22	121±52	<0.001
	Diameter [μm]	7909±614	8178±684	<0.001
	CV [%]	1.5	2.1	
End-diastolic diameter inhomogeneity	Intra-subject precision [μm]	56	57	0.84
	Beat-to-beat variation [μm]	24±14	53±25	<0.001
	Inhomogeneity [μm]	269±182	277±103	0.83

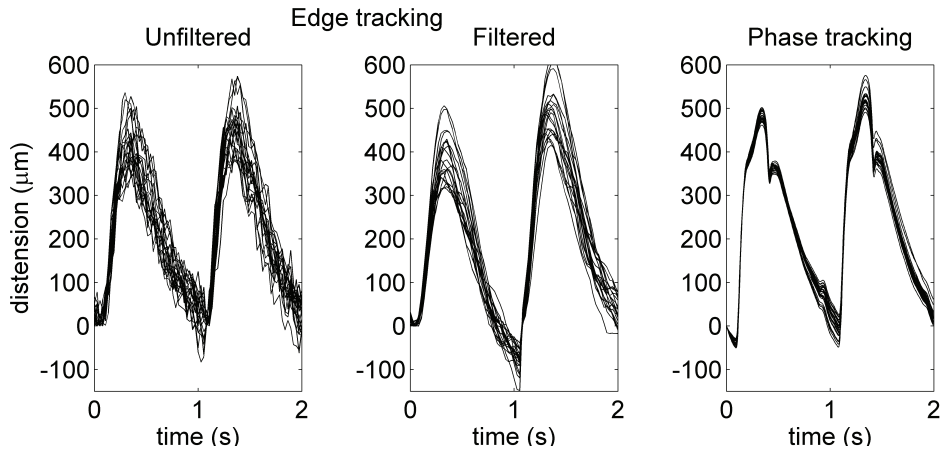

Figure 5

Example of distension waveforms over two heart beats of unfiltered edge tracking (left), filtered edge tracking (middle) and phase tracking (right) of the same patient. Edge tracking distension waveforms exhibit more noise; phase tracking distension waveforms retain more temporal detail.

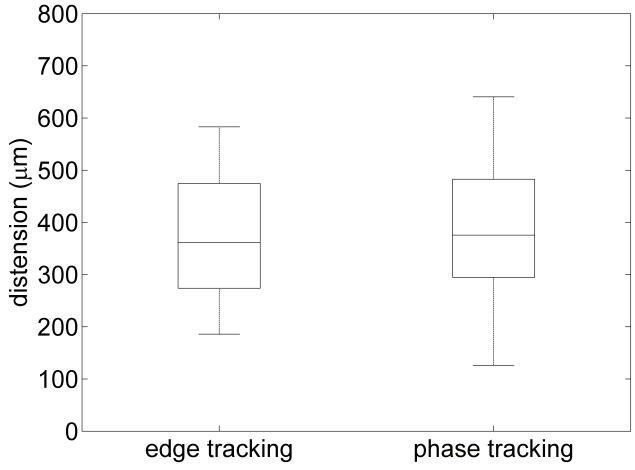

Figure 6

Boxplot of median distension obtained with edge- and phase tracking. Whiskers represent the minimum and maximum distension. Mean distension obtained with B-mode edge tracking and with RF phase tracking is similar.

For both methods, the distribution of the median distension, averaged over image segments and heart beats, is shown in Figure 6. Despite the differences in distension waveforms, edge and phase tracking have a similar average distension (difference is -6±69 μm, paired t-test: p-value=0.67). The Bland-Altman plot (Figure 7) shows good concordance between edge tracking and phase tracking distension.

The spatial distension inhomogeneity, defined as the standard deviation of distension over the segments, is shown in Table 4. Intra-subject precision of distension inhomogeneity is similar for edge and phase tracking (SD=19 and SD=17 μm, respectively, F-test: p-value=0.46). Despite similar intra-subject precision, the average distension inhomogeneity (Figure 8) tends to be larger for edge tracking (inter-method difference 15±35 μm, p-value=0.042) and at higher mean inhomogeneity (SD=25 μm upper 50% and SD=10 μm lower 50%), implying relative rather than absolute errors. A similar trend is seen for intra-subject precision of distension inhomogeneity for both methods (edge tracking: SD=25 μm upper 50% and phase tracking: SD=22 μm upper 50%). The temporal beat-to-beat variation of distension inhomogeneity is significantly larger for edge tracking (difference is 8±10 μm, paired t-test: p-value<0.001), similarly as for the beat-to-beat variation of distension.

Table 4

Distension and its inhomogeneity of the CCA determined by edge and phase tracking. Values are presented as mean ± standard deviation. Intra-subject precision is defined as standard deviation of differences over all recordings and all patients. Temporal beat-to-beat variation is defined as the standard deviation over the heart beats.

	(N=27)	Edge tracking	Phase tracking	P-value
End-diastolic diameter	Intra-subject precision [μm]	44	47	0.66
	Beat-to-beat variation [μm]	37±16	27±18	0.01
	Diameter [μm]	377±122	383±128	0.67
	CV [%]	12	12	
End-diastolic diameter inhomogeneity	Intra-subject precision [μm]	19	17	0.46
	Beat-to-beat variation [μm]	21±12	13±8	<0.001
	Inhomogeneity [μm]	78±33	64±28	0.04

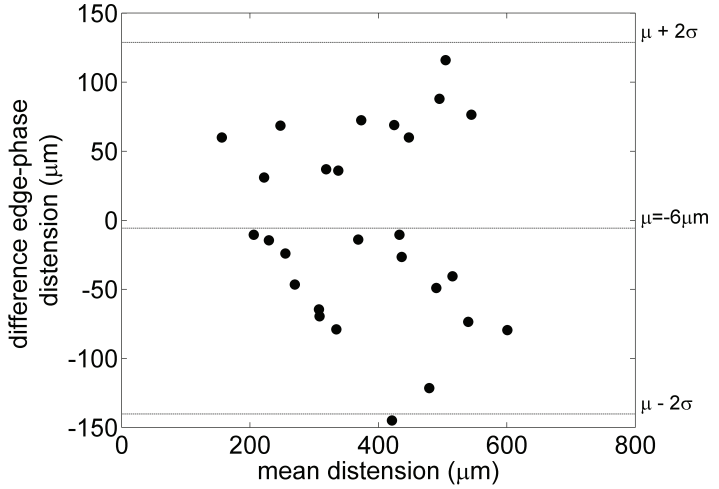

Figure 7

Bland-Altman plot of edge- and phase tracking distension shows good concordance (difference is -6±69 μm).

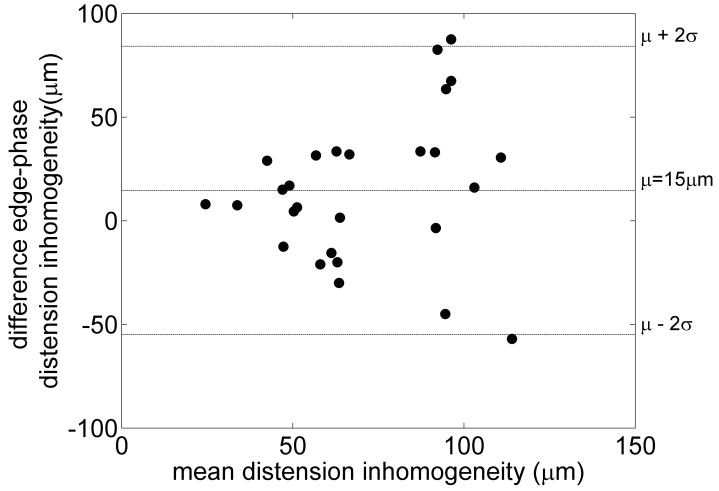

Figure 8

Bland-Altman plot of distension inhomogeneity obtained with edge- and phase tracking shows a minor bias (bias 15±35 μm). The increasing spread at higher values originates from variations in positioning and orientation of the scan plane.

Discussion

We evaluated the performance of two ultrasonography methods, namely edge tracking using standard B-mode data and phase tracking using high frame rate B-mode and dedicated hardware. Both methods extracted end-diastolic diameter, distension and their spatial inhomogeneity in an elderly population with carotid artery disease who recently suffered from cerebrovascular symptoms. Despite differences in distension waveforms, the intra-subject precision of distension (SD=44 μm and SD=47 μm) as well as the mean artery distension are similar (accuracy: difference -6±69 μm). Although distension inhomogeneity tends to be larger for edge tracking (difference 15±35 μm), the intra-subject precision is similar (SD=19 μm and SD=17 μm). Therefore, in clinical practice scanners operating in B-mode provide a good alternative to measure local artery characteristics.

The distension obtained with RF phase tracking has been compared to B-mode tracking previously, using either first absolute central moment (Bianchini et al. 2010) or grey-level gradient analysis (Stadler et al. 1997). In both studies, the distension reproducibility of RF phase tracking and B-mode tracking were similar. However, Bianchini et al. found similar mean distension whereas Stadler et al. found significantly lower distension with RF tracking than with B-mode tracking (447 and 509 μm; respectively). Both studies did not consider spatial distension inhomogeneity and in both studies a mixed group of subjects, i.e., healthy subjects and patients with different pathologies, were enrolled.

In the current study elderly symptomatic carotid artery patients are considered. Compared to younger individuals, elderly often have curved arteries that generally exhibit high spatial inhomogeneity, i.e., more irregularities in the vessel wall. In addition, arteries of elderly frequently exhibit motion artifacts. Due to high spatial inhomogeneity and artery motility in elderly, reproducibility or intra-subject precision might be poorer than in young healthy individuals. However, it is important to focus on an elderly population with a recent TIA or stroke since these individuals will typically require a workup of their vascular status. If ultrasound systems are capable of evaluating the aforementioned vascular parameters properly in this technically most challenging patient group, it is likely that they will also work properly in younger patients or those without overt atherosclerotic disease. To make our tracking robust for challenging patients, we preferred to use a semi-automatic tracking method with wall initialization, above a fully automatic method or semi-automatic method with manual correction afterwards.

For both systems and repeated acquisitions, focus, emission frequency and bandwidth were kept constant, hence the ultrasound depth resolution and lateral resolution were also similar (estimated value 300 μm and 1.3 mm, respectively, for both systems). To prevent discrepancies between methods, processing steps were similar, i.e., wall initialization, ROI width, segment length and segment overlap. In literature, diastolic-time points for phase tracking are usually referenced to the R-wave in the ECG signal, recorded simultaneously with the ultrasound registration. In contrast, we choose to use the mean distension waveform obtained with edge tracking to identify the diastolic time-points for both methods. This approach circumvents simultaneous ECG-registration, simplifying the acquisition protocol.

One of the major differences between edge and phase tracking is the end-diastolic reset of phase tracking. Phase tracking considers multiple frames to calculate the phase shift and, hence, wall displacement, whereas edge tracking determines the position of the wall edge for each frame separately. Therefore, during phase tracking drift may occur due to a velocity dependent bias in the estimation algorithm (Brands et al. 1997), necessitating wall initialization at every end-diastolic frame. Because of intermittent manual repositioning, phase tracking will be more labor-intensive and probably more observer dependent than edge tracking, especially for end-diastolic diameter. Another major difference is the tracking window used to identify the movement of the media-adventitia transition. Phase tracking uses the average displacement from the tracking window (size=0.4 mm * 4.5 mm * 10 ms) whereas edge tracking considers a single point within a search window, i.e., where the amplitude threshold value is crossed. Diameter and distension obtained with edge tracking are therefore dependent on a single threshold value. Due to speckle pattern perturbations, the echo amplitude may fluctuate substantially between segments (see, e.g., Figure 4) but also over time, which may result in noisier signals. To avoid aliasing, phase tracking requires a substantially higher frame update rate (~300 fps) than edge tracking. The latter method will function properly at lower frame rates because the algorithm requires that the echo edge remains within a relatively wide search window of 1.6 mm.

A high frame rate is preferred to properly capture the frequency content of distension waveforms. In the present study, the ultrasound system supported in B-mode a frame rate of 37 fps, which, in combination with the lowpass filtering, explains the difference in temporal details in Figure 5. Processing video sequences with lower frame rates (25/30 Hz) will further degrade temporal detail. Therefore, waveform details, e.g., the dicrotic notch, may be masked at lower frame-rates with B-mode edge tracking compared to RF phase tracking. Since reliable identification of time points, other than diastolic or systolic diameter, might be difficult for edge tracking, it is recommended to use RF phase tracking when more advanced waveform analysis is needed, i.e., wave intensity analysis, augmentation index etc.

Mean end-diastolic diameter of edge tracking (7.9 mm) is significant lower than of phase tracking (8.2 mm). The smoothing and compression techniques applied to the video images will broaden the adventitia complex and, hence, reduce the diastolic diameter. We examined the compression of the B-mode images with a special algorithm and it appeared that no or very little compression was applied (results not shown here). Phase tracking depends on manually adjusted wall positions at each heartbeat introducing manual errors. This may explain the larger intra-subject precision (170 µm, Table 3) and temporal beat-to-beat variation (121±52 µm) in end-diastolic diameter for phase tracking compared to edge tracking.

Phase tracking results in a higher end-diastolic diameter and a slightly higher intra-subject precision and temporal beat-to-beat variation than previously reported by others (7.6 mm and 7.8 mm, precision: 150 µm and beat-to-beat variation: 110 µm) (Meinders et al. 2003; Graf et al. 2010; Rossi et al. 2010). The coefficient of variation (2.1%) is similar as determined with cross-correlation (2.6%) (Yli-Ollila et al. 2013). In contrast to a higher end-diastolic diameter,

the average distension of our population (phase tracking 383±128 μm) is lower than values found in literature (450±120 μm) (Graf et al. 2010) and substantially lower than for a healthy young population. The average distension was 802 μm in a healthy young population with a mean age of 25 years (Kornet et al. 2002) and 500 μm for a healthy male population with a mean age of 37 years (Meinders et al. 2003). This clearly indicates that arteries stiffen with ageing. The observed differences in distension and diameter are probably due to the fact that our population was relatively old and had symptomatic carotid artery disease.

The observed intra-subject precision of distension (44 and 47 μm) is similar to the subgroups of Graf et. al. (Graf et al. 2010) with plaques in the ipsilateral or contralateral common or internal carotid artery. Similar intra-subject precision is expected since all stroke patients in our study have at least a plaque in one or both carotid bifurcations. It should be noted that we calculated the intra-subject precision with the average as reference (see section on statistical analysis) while Graf et. al. used one measurement as reference, yielding a value which is two times higher than in our approach. The coefficient of variation (12%) is similar as determined with B-mode cross-correlation (11%) (Yli-Ollila et al. 2013), but substantially higher than determined with RF phase tracking (6%) (Bianchini et al. 2010). However, both studies considered young healthy subjects.

Intra-subject beat-to-beat variation of distension is significantly larger for edge tracking (37±16 μm) compared to phase tracking (27±18 μm), which is probably caused by noise in the edge tracking signals. Beat-to-beat variation is mainly determined by physiological variations in pulse pressure (10% variation), which will not differ for both video and RF recordings. Beat-to-beat variation of distension obtained with phase tracking is similar as observed by Meinders et. al. (males 40 μm and females 30 μm) (Meinders et al. 2003).

The spatial distension inhomogeneity (Figure 8) tends to be larger for edge tracking (78±33 μm) than for phase tracking (64±28 μm). One of the reasons could be an echogenic intima-media complex where a threshold of 65% might cause an intermittent detection of the lumen-intima rather than the media-adventitia transition. Therefore, the edge tracking algorithm might be improved by incorporating an extra check that prevents switching. The differences between edge and phase tracking inhomogeneity are larger for higher mean inhomogeneity, implying relative rather than absolute errors. The concordance between inter-method and intra-subject precision corroborates the notion that the inhomogeneity highly depends on the incidental location of a wall irregularity. Apparently distention inhomogeneity, probably caused by wall irregularities, is more susceptible for location and scan plane variations.

The spatial inhomogeneity of our elderly stroke population (64±28 μm for phase tracking) is higher than values reported for an elderly healthy population (50 μm male; 40 μm female) (Meinders et al. 2003). Moreover, the difference between spatial inhomogeneity in our study and observed by Meinders et.al. suggests that inhomogeneity is correlated with the presence of carotid atherosclerotic disease. This corroborates the findings of Graf et al., where distension inhomogeneity of the CCA is associated with focal atherosclerotic lesions within

the carotid bulb. Despite the limitation of a single threshold for edge tracking algorithm, the intra-subject precision of inhomogeneity is similar to that of the phase tracking algorithm. Moreover, both methods have an intra-subject precision and beat-to-beat variation of average diameter, distension and its inhomogeneity that is substantial smaller than the inter-subject variation, which is essential to discriminate patients.

The observed difference in distension between edge and phase tracking is smaller than its intra-subject precision. A better estimate can be obtained by increasing the number N of repeated measurements, resulting in a reduction of the inter-registration variation by a factor of square-root of N. However, even for five repeated measurements, the observed difference between methods (distension difference 6 μm, Table 4) remains smaller than the inter-registration variation (about 20 μm) and is, therefore, insignificant. A larger number of repeated measurements is unrealistic for clinical studies considering time issues.

A great advantage of using a standard B-mode scanner is the superior image quality due to the utilization of advanced image processing techniques, e.g., spatial compounding, edge enhancement and smoothing. These techniques facilitate acquisition of high quality images and may thereby reduce the operator dependency. In addition, the high image quality may facilitate easier identification of the media-adventitia transition for wall initialization, which positively influences end-diastolic diameter determination. Moreover, a wider exploration width of 40 mm has the advantage of easier identification of recording location and also improves detection of the spatial inhomogeneity. Furthermore, standard B-mode scanners are widely available in contrast to RF scanners which are limited to a small number of specialized hospitals.

Limitations of our study include the absence of a fixed recording site as well as a fixed angle of observation, causing differences in parameters between the RF and B-mode recordings. Some patients exhibited indeed large differences in diameter, distension and spatial distension inhomogeneity between the duplicate recordings. However, slightly different recordings sites resemble the real situation in clinical practice. Another limitation of this study is the use of a single B-mode scanner. It is not known whether other scanners provide the same results since recording settings, i.e., compound imaging, and post-processing techniques, i.e., compression and smoothing techniques, can be different. It is known that compression may substantially alter the end-diastolic diameter in the CCA (Rossi et al. 2009). Since distension of both methods was similar, video processing techniques used in our study did not alter the distension whereas it seems to have altered the end-diastolic diameter. During recording, compound imaging was used, a technique where three frames recorded under slightly different angles are averaged. The main advantage of compounding is reduction of speckle and clutter artefacts which improves image quality, especially for arteries which are not parallel to the ultrasound probe, e.g., curved vessel walls (Entrekin et al. 2001). Since the specific effect of compression and compound imaging is not considered in our study, its effect on distension remains open for future investigation.

Because a similar distension and a 3% smaller end-diastolic diameter were found for edge tracking (Table 3), the relative distension will be on average 3% higher. This is substantially smaller than the observed intra-subject coefficient of variation (12%, Table 4). Hence, B-mode scanners can be used to extract relative distension.

In conclusion, scanners operating in standard B-mode are suitable to measure local morphological and physiological artery characteristics with good precision and accuracy in symptomatic carotid artery patients. However, waveform details may be masked at lower frame-rates, impeding the use of B-mode for more advanced waveform analysis.

References

Bianchini E, Bozec E, Gemignani V, Faita F, Giannarelli C, Ghiadoni L, Demi M, Boutouyrie P, Laurent S. Assessment of carotid stiffness and intima-media thickness from ultrasound data: comparison between two methods. J Ultrasound Med 2010;29:1169-1175.

Boutouyrie P, Fliser D, Goldsmith D, Covic A, Wiecek A, Ortiz A, Martinez-Castelao A, Lindholm B, Massy ZA, Suleymanlar G, Sicari R, Gargani L, Parati G, Mallamaci F, Zoccali C, London GM. Assessment of arterial stiffness for clinical and epidemiological studies: methodological considerations for validation and entry into the European Renal and Cardiovascular Medicine registry. Nephrol Dial Transplant 2014;29:232-239.

Brands PJ, Hoeks AP, Ledoux LA, Reneman RS. A radio frequency domain complex cross-correlation model to estimate blood flow velocity and tissue motion by means of ultrasound. Ultrasound Med Biol 1997;23:911-920.

Entrekin RR, Porter BA, Sillesen HH, Wong AD, Cooperberg PL, Fix CH. Real-time spatial compound imaging: application to breast, vascular, and musculoskeletal ultrasound. Semin Ultrasound CT MR 2001;22:50-64.

Graf IM, Schreuder FH, Mess WH, Reneman RS, Hoeks AP. Spatial distension variations are associated with focal atherosclerotic plaques. Cerebrovasc Dis 2010;29:199-205.

Karras A, Haymann JP, Bozec E, Metzger M, Jacquot C, Maruani G, Houillier P, Froissart M, Stengel B, Guardiola P, Laurent S, Boutouyrie P, Briet M, Nephro Test Study G. Large artery stiffening and remodeling are independently associated with all-cause mortality and cardiovascular events in chronic kidney disease. Hypertension 2012;60:1451-1457.

Kornet L, Hoeks AP, Janssen BJ, Willigers JM, Reneman RS. Carotid diameter variations as a non-invasive tool to examine cardiac baroreceptor sensitivity. J Hypertens 2002;20:1165-1173.

Laurent S, Boutouyrie P, Asmar R, Gautier I, Laloux B, Guize L, Ducimetiere P, Benetos A. Aortic stiffness is an independent predictor of all-cause and cardiovascular mortality in hypertensive patients. Hypertension 2001;37:1236-1241.

Laurent S, Cockcroft J, Van Bortel L, Boutouyrie P, Giannattasio C, Hayoz D, Pannier B, Vlachopoulos C, Wilkinson I, Struijker-Boudier H, European Network for Non-invasive Investigation of Large A. Expert consensus document on arterial stiffness: methodological issues and clinical applications. Eur Heart J 2006;27:2588-2605.

Leone N, Ducimetiere P, Gariepy J, Courbon D, Tzourio C, Dartigues JF, Ritchie K, Alperovitch A, Amouyel P, Safar ME, Zureik M. Distension of the carotid artery and risk of coronary events: the three-city study. Arterioscler Thromb Vasc Biol 2008;28:1392-1397.

Mattace-Raso FU, van der Cammen TJ, Hofman A, van Popele NM, Bos ML, Schalekamp MA, Asmar R, Reneman RS, Hoeks AP, Breteler MM, Witteman JC. Arterial stiffness and risk of coronary heart disease and stroke: the Rotterdam Study. Circulation 2006;113:657-663.

Meinders JM, Brands PJ, Willigers JM, Kornet L, Hoeks AP. Assessment of the spatial homogeneity of artery dimension parameters with high frame rate 2-D B-mode. Ultrasound Med Biol 2001;27:785-794.

Meinders JM, Kornet L, Hoeks AP. Assessment of spatial inhomogeneities in intima media thickness along an arterial segment using its dynamic behavior. Am J Physiol Heart Circ Physiol 2003;285:H384-391.

Potter K, Reed CJ, Green DJ, Hankey GJ, Arnolda LF. Ultrasound settings significantly alter arterial lumen and wall thickness measurements. Cardiovasc Ultrasound 2008;6:6.

Rossi AC, Brands PJ, Hoeks AP. Nonlinear processing in B-mode ultrasound affects carotid diameter assessment. Ultrasound Med Biol 2009;35:736-747.

Rossi AC, Brands PJ, Hoeks AP. Automatic localization of intimal and adventitial carotid artery layers with noninvasive ultrasound: a novel algorithm providing scan quality control. Ultrasound Med Biol 2010;36:467-479.

Stadler RW, Taylor JA, Lees RS. Comparison of B-mode, M-mode and echo-tracking methods for measurement of the arterial distension waveform. Ultrasound Med Biol 1997;23:879-887.

Truijman MT, Kooi ME, van Dijk AC, de Rotte AA, van der Kolk AG, Liem MI, Schreuder FH, Boersma E, Mess WH, van Oostenbrugge RJ, Koudstaal PJ, Kappelle LJ, Nederkoorn PJ, Nederveen AJ, Hendrikse J, van der Steen AF, Daemen MJ, van der Lugt A. Plaque At RISK (PARISK): prospective multicenter study to improve diagnosis of high-risk carotid plaques. Int J Stroke 2014;9:747-754.

van Sloten TT, Schram MT, van den Hurk K, Dekker JM, Nijpels G, Henry RM, Stehouwer CD. Local stiffness of the carotid and femoral artery is associated with incident cardiovascular events and all-cause mortality: the Hoorn study. J Am Coll Cardiol 2014;63:1739-1747.

Welch PD. The use of fast Fourier transform for the estimation of power spectra: A method based on time averaging over short, modified periodograms. IEEE Trans Audio Electroacoust 1967;15:70-73.

Yli-Ollila H, Laitinen T, Weckstrom M, Laitinen TM. Axial and radia waveforms in common carotid artery: an advanced method for studying arterial elastic properties in ultrasound imaging. Ultrasound Med Biol 2013;39:1168-1177.

4

High spatial inhomogeneity in the intima-media thickness of the common carotid artery is associated with a larger degree of stenosis in the internal carotid artery: The PARISK study

Steinbuch J, Van Dijk AC, Schreuder FHBM, Truijman MTB, De Rotte AAJ, Nederkoorn PJ, Van der Lugt A, Hermeling E, Hoeks APG, Mess WH. High spatial inhomogeneity in the intima-media thickness of the common carotid artery is associated with a larger degree of stenosis in the internal carotid artery: The PARISK study. Ultraschall Med 2016

Abstract

Purpose

Inhomogeneity of arterial wall thickness may be indicative for distal plaques. This study investigates the intra-subject association between relative spatial intima-media thickness (IMT) inhomogeneity of the common carotid artery (CCA) and degree of stenosis of plaques in the internal carotid artery (ICA).

Materials and Methods

We included 240 patients with a recent ischemic stroke or transient ischemic attack and a mild-to-moderate stenosis in the ipsilateral ICA. IMT inhomogeneity was extracted from B-mode ultrasound recordings. The degree of ICA stenosis was assessed on CT angiography according to the European Carotid Surgery Trial method. Patients were divided into groups with a low (≤2%) and a high (>2%) IMT inhomogeneity scaled with respect to the local end-diastolic diameter.

Results

182 patients had both suitable CT and ultrasound registrations. Relative CCA-IMT inhomogeneity was similar for the symptomatic and asymptomatic side (difference: 0.02%, $p=0.85$). High relative IMT inhomogeneity was associated with a larger IMT (difference: 235μm, $p<0.001$) and larger degree of ICA stenosis (difference: 5%, $p=0.023$) which remained significant ($p=0.016$) after adjustment for common risk factors.

Conclusion

High relative CCA-IMT inhomogeneity is, independently of common risk factors, associated with a larger degree of ICA stenosis and, hence, indicative for atherosclerotic disease. The predictive value of CCA-IMT inhomogeneity for plaque progression and recurrence of cerebrovascular symptoms will be determined in the follow-up phase of PARISK.

Introduction

Atherosclerosis involves changes in structural and mechanical properties of an artery, specifically of the intima. Increased mean and maximal intima-media thickness (IMT) of the common carotid artery (CCA) are associated with the presence of an atherosclerotic plaque in the internal carotid artery (ICA) (Persson et al. 1994; Bonithon-Kopp et al. 1996; Rundek et al. 2015). In addition, after adjustment for cardiovascular risk factors such as age, smoking and diabetes mellitus, enlarged maximal CCA-IMT is associated with increased risk on myocardial infarction and stroke in a large population without stroke at enrollment (O'Leary et al. 1999; Silvestrini et al. 2010). In a stroke population, enlarged mean and maximal IMT is a predictor of recurrent stroke (Tsivgoulis et al. 2006; Roquer et al. 2011). In addition, in stroke patients mean CCA-IMT may also be used to discriminate brain or lacunar infarction from intracerebral hemorrhage (Vemmos et al. 2004; Tsivgoulis et al. 2005). Although mean IMT is a significant predictor of prevalent cardiovascular disease on a population base (Polak et al. 2010), including mean IMT does not improve the traditional cardiovascular risk prediction models on an individual base (Lorenz et al. 2010; den Ruijter et al. 2013; van den Oord et al. 2013; Bots et al. 2014). Although IMT progression is more pronounced in patients with cardiovascular events (Uthoff et al. 2008), drug therapies inducing regression or slower progression of IMT do not improve clinical outcome, i.e., reduction in cardiovascular events (Costanzo et al. 2010).

As an alternative, one may consider the CCA-IMT irregularity. It increases with age and is significantly larger in patients with coronary artery disease (CAD) compared to patients without CAD (Schmidt-Trucksass et al. 2003). Similarly, dialysis patients with cardiovascular disease (CVD) exhibit larger IMT irregularity than dialysis patients without CVD (Hermans et al. 2007). Furthermore, abnormal IMT irregularity is more often observed in subjects who recently had a stroke or transient ischemic attack (TIA) than in asymptomatic subjects (Saba et al. 2012).

The association between IMT and cardiovascular disease is only present in studies involving large patient groups. Moreover, IMT exhibits a wide distribution across gender, age and within the same age category (Engelen et al. 2013). IMT can therefore not be used to predict the risk of (future) cardiovascular events for an individual patient. As an alternative, the intra-subject spatial IMT inhomogeneity, defined as the wall thickness irregularity along the vessel within a B-mode ultrasound image, might be a promising tool. In a mixed population of cerebro- and cardiovascular diseased patients, wall irregularity as deduced from duplicate B-mode recordings is associated with nearby atherosclerosis (Graf et al. 2009). Alternatively, one may consider within a single ultrasound measurement the spatial IMT inhomogeneity (Meinders et al. 2001), either in absolute terms or relative to the artery diameter. An irregular vessel wall, i.e., high inhomogeneity, may affect the wall stress distribution and local hemodynamics. IMT inhomogeneity might provide, therefore, additional information on top of IMT as extracted from the same recording.

The aim of the present study is to investigate whether spatial CCA-IMT inhomogeneity is related to plaque burden of the carotid bifurcation or ICA in patients with recent ischemic stroke or TIA. More specifically, we will 1) compare the relative CCA-IMT inhomogeneity between ipsilateral and contralateral arteries and 2) investigate the association between relative CCA-IMT inhomogeneity and degree of ICA stenosis. This study pertains to the baseline measurements of a 2-year follow-up study which will relate wall inhomogeneity and future/recurrent cerebrovascular events.

Methods

Study subjects

A total of 240 patients with a recent ischemic stroke, TIA or amaurosis fugax were recruited for the Plaque At RISK (PARISK) study (clinical trials.gov NCT01208025) (Truijman et al. 2014). This is an ongoing, prospective multicenter (MUMC, EMC, UMCU, AMC) observational cohort study which investigates (a combination of) non-invasive imaging techniques to improve identification of patients at increased risk of recurrent stroke during a 2-year follow-up. Patients who had an ipsilateral mild-to-moderate carotid artery stenosis were included within three months after the clinical event. Details of the study protocol, including cardiovascular risk factors considered, have been previously described (Truijman et al. 2014). The study was approved by the Medical Ethics Committees of all four participating centers. All patients gave written informed consent.

Data acquisition

Ultrasound examinations of the CCA were performed bilaterally on 233 patients with a Philips iU22 scanner (Philips Medical Systems, Bothell, USA) operating in B-mode at a frame rate of approximately 40 Hz using a 17-5 MHz, 12-5 MHz or 9-3 MHz probe, depending on the depth of the CCA. Two-dimensional recordings were acquired in duplicate from anterolateral and posterolateral angles (i.e. four CCA recordings per patient) for about five seconds, covering on average 5 heartbeats. In addition, blood pressure was measured from the brachial artery using a semi-automatic oscillometric device (Omron 705IT, OMRON Healthcare Europe B.V., Hoofddorp, Netherlands). Due to CT contra-indications only 201 patients had a multidetector CT angiogram (MDCTA) for further analysis of the degree of stenosis in the carotid bifurcation or ICA. Maximum degree of stenosis perpendicular to the central lumen line was manually scored according to the European Carotid Surgery Trial (ECST) criteria (European Carotid Surgery Trialists' Collaborative 1998) by a trained observer using a Siemens workstation with dedicated 3D analysis software.

Edge tracking

To extract wall thickness and diameter statistics, edge detection and tracking of B-mode images of the CCA (image width 4 cm), was performed by a trained observer blinded to the MDCTA results using dedicated software developed by Maastricht University Medical Centre (MUMC, Maastricht, The Netherlands) (Steinbuch et al. 2016). A clear section of the artery of the B-mode image was selected and divided into approximately 15 half-overlapping seg-

ments (width 3.7 mm, 7-23 segments depending on section length). Media-adventitia edge detection was performed within a short window of 1.6 mm in depth following the same procedure as previously described (Steinbuch et al. 2016). Edge threshold was set at 65% of the maximal grey value of the local adventitia at the anterior and posterior. To prevent erratic switching towards the lumen-intima transition in case of an echogenic intima boundary, wall detection was repeated with a threshold of 83%. If a large difference (>0.23 mm) between the threshold positions of 65% and 83% was observed, the edge position for the highest threshold (adventitia transition) was used. The local difference between anterior and posterior media-adventitia transition provides an estimate for the instantaneous adventitia- adventitia local diameter. The above procedure was repeated for all subsequent frames. The resulting distribution of diameter waveforms was smoothed over time with a 2nd order Savitsky-Golay filter (filter span 0.2 s). The end-diastolic frames were identified from the mean diameter waveform after spatial averaging of the waveform distribution.At those end-diastolic phases, the lumen-intima transition across the artery section was identified. Starting from the observed media-adventitia position (Figure 1), the first local minimum of the first derivative was found for each segment within a 0.68 mm depth window. Starting from this minimum position, the local maxima of the first derivative were found using a sliding window with a width of 0.45 mm, which is approximately 2 times the depth resolution. A local maximum is identified if the same peak is observed twice within consecutive window positions (spaced at one depth resolution). The last maximum found is considered the lumen-intima transition provided its value is not lower than 60% of the first maximum after the minimum. The distribution of the lumen-intima transitions along the artery section was corrected interactively if necessary (Figure 1).

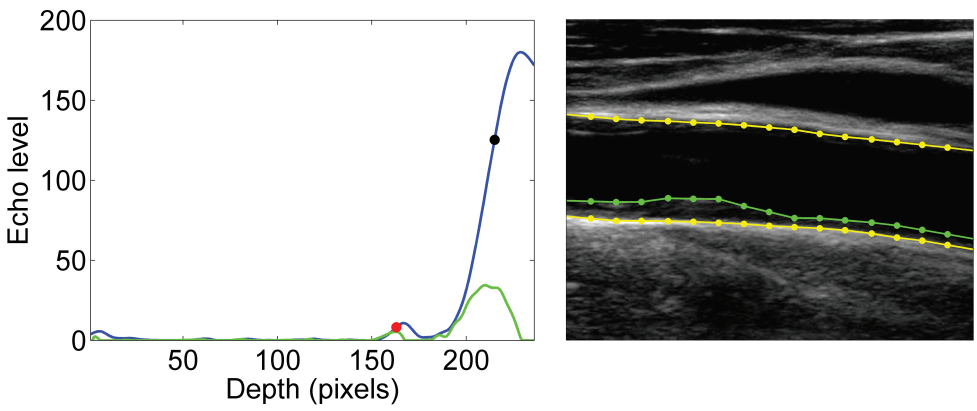

Figure 1

Example of edge detection of the lumen-intima transition for one segment (left) and of a CCA with irregular IMT (right). In the left image, the blue line indicates the echo signal for the posterior wall and the green line indicates its first derivative, scaled by a factor 5 for visibility. Starting from the media-adventitia edge position (black dot), the first minimum of the derivative is found which is followed by an iterative search for a local maximum. In the right image, the yellow line indicates the media-adventitia transition and the green line indicates the lumen-intima transition, which can be manually modified if necessary.

Statistical processing

The IMT was defined as the end-diastolic difference between the lumen-intima and media-adventitia transitions at the posterior wall. The median of end-diastolic diameter, distension (i.e. diameter change over the cardiac cycle), and IMT over all segments were calculated. To correct for diameter related variations (Liang et al. 2001; Nichols et al. 2011), IMT was scaled relative to the local end-diastolic adventitia-adventitia diameter. The spatial standard deviation of the distension and relative IMT over all segments is considered as a measure for distension inhomogeneity and relative IMT inhomogeneity (intra-recording variation), e.g., a zero IMT inhomogeneity implies that the IMT has everywhere the same value. Intra-subject precision of all parameters was calculated by the standard deviation of differences, i.e., between duplicate recordings and their average, over all recordings and patients. All other parameters were averaged over all available beats and recordings. Degree of stenosis was averaged over the left and right ICA for each patient to obtain a global measure of atherosclerosis.

A paired t-test was used to compare the relative IMT inhomogeneity between ipsilateral and contralateral arteries, before data was averaged over both common carotid arteries (CCAs) for each patient. The intra-subject precision and inter-subject values of wall characteristics of the four centers were compared with an F-test and ANOVA. Small random variations in IMT are expected due to the limitations imposed by the depth resolution of the ultrasound system used (300 μm), which converts to a maximum variation in IMT of 150 μm, i.e., a relative IMT inhomogeneity of 2% for an 8 mm end-diastolic diameter. A Student t-test was used to assess the difference in CCA wall characteristics and degree of ICA stenosis between patients with low and high relative IMT inhomogeneity, using the noise cut-off level of 2%. Additionally, Pearson correlation and stepwise linear regression were used to further investigate the association between relative IMT inhomogeneity and degree of ICA stenosis. To adjust for the effect of traditional risk factors, i.e., age, BMI, smoking, diabetes mellitus and hypertension on the association, those risk factors were included as confounders in the linear regression model. Values are quantified as mean ± standard variation (SD). Significance level was set at $p<0.05$.

Results

In total, 194 patients received both MDCTA and US examination of both carotid arteries. 7 US examinations and 2 MDCTA registrations were unsuitable for further analyses due to technical recording failure (N=5) or quality (N=4). In addition, degree of ICA stenosis could not be determined in 3 patients due to an occluded ICA or stent on the contralateral side. So, 182 patients (mean age 68±9 years) were available for a complete data analysis. Patient baseline characteristics are shown in Table 1. Because the relative IMT inhomogeneity of the ipsilateral CCA was similar of that of the contralateral CCA (difference 0.02%, paired t-test: p-value=0.85), data were averaged over both CCAs of each patient.

Wall characteristics across participating centers

Intra-subject precision of all wall characteristics (Table 2), except IMT, was larger for one center (EMC, F-test, p-value<=0.03 compared to MUMC). Inter-subject values (Table 2) were not significantly different across the four centers (ANOVA: p-value=>0.1, respectively), allowing pooling of data.

Table 1

Patient characteristics. Data are presented as mean ± standard deviation.

N [-]	182
Age [years]	68±9
Male [%]	73
BMI [kg/m^2]	27±4
Diastolic blood pressure (during US) [mmHg]	79±10
Systolic blood pressure (during US) [mmHg]	140±19
Classification event [%]	
Stroke	46
TIA	43
Amaurosis fugax	11
Current smoking [%]	23
Diabetes mellitus[1] [%]	20
Hypercholesterolemia[1] [%]	56
Hypertension[1] [%]	57

[1]*Definitions of diabetes mellitus, hypercholesterolemia or hypertension as previously described (Truijman et al. 2014)*

IMT inhomogeneity

Figure 2 shows the relative CCA-IMT inhomogeneity as function of the degree of ICA stenosis. Patients with high relative IMT inhomogeneity (>2%) are more often seen with a larger degree of stenosis, whereas patients with low relative inhomogeneity have a wide range of plaque sizes.

Table 3 shows the wall characteristics for low and high relative IMT inhomogeneity with a 2% cut-off. Mean end-diastolic diameter and distension were similar for both groups (difference 54 μm and 12 μm, respectively, Student t-test: p-value>0.6). The 40 patients (28%) with a high relative IMT inhomogeneity exhibited a higher mean IMT (difference 235 μm, Student t-test: p-value<0.001) and distension inhomogeneity (difference 16 μm, Student t-test: p-value=0.01) compared to patients with low relative IMT inhomogeneity. Moreover, a high relative IMT inhomogeneity in the CCA was associated with a larger degree of ICA stenosis (difference 5%, Student t-test: p-value=0.023). Furthermore, relative IMT inhomogeneity was significantly correlated with the degree of ICA stenosis (Pearson correlation: ρ=0.21, p=0.004). After adjustment for risk factors, i.e., age, BMI, smoking, diabetes mellitus and hypertension, only hypertension and relative IMT inhomogeneity remained independently associated with the degree of ICA stenosis (standardized β=0.27, p<0.001 and standardized β=0.18, p=0.016, respectively).

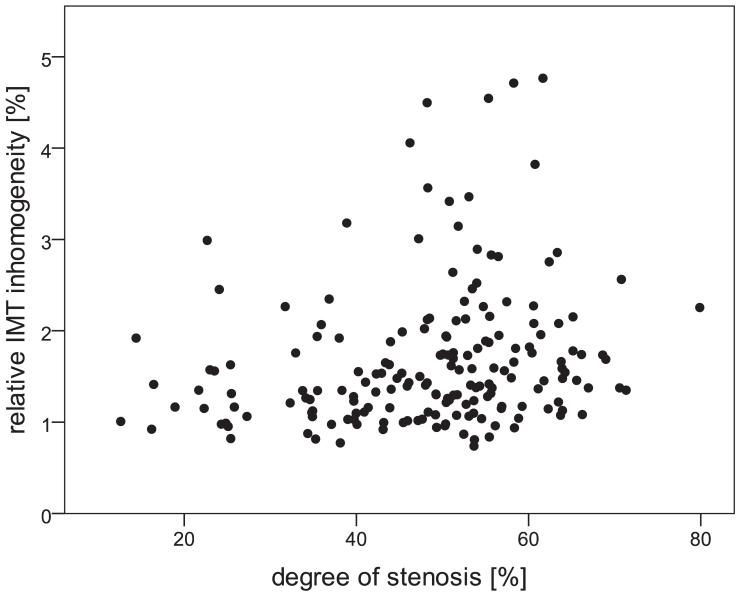

Figure 2

Relative CCA-IMT inhomogeneity as function of degree of ICA stenosis. Patients with high relative inhomogeneity (>2%) have a larger degree of stenosis, whereas patients with low relative inhomogeneity have a wide range of plaque sizes.

Table 2

Wall characteristics for the four centers. Values are presented as mean ± standard deviation. Intra-subject precision is defined as the standard deviation of differences between all recordings and arteries. IMT, intima-media thickness; MUMC, Maastricht University Medical Center; EMC, Erasmus Medical Center; UMCU, University Medical Center Utrecht; AMC, Academic Medical Center

		All	MUMC	EMC	UMCU	AMC	P-value
	N	182	98	45	28	11	-
end-diastolic Diameter	Intra-subject precision	194	176	260	154	115	-
	Diameter	8012±960	8063±927	7860±876	8145±1038	7834±1362	0.51
Distension	Intra-subject precision	59	47	86	39	52	-
	Distension	440±153	431±154	481±181	433±97	369±92	0.11
Distension inhomogeneity	Intra-subject precision	27	25	32	23	26	-
	inhomogeneity	98±36	94±37	104±34	106±36	83±23	0.12
IMT	Intra-subject precision	99	97	99	106	91	-
	IMT	1007±202	1002±228	1003±164	1007±168	1070±171	0.77
IMT inhomogeneity	Intra-subject precision	54	47	70	45	57	-
	Inhomogeneity	136±68	137±74	136±59	137±75	126±34	0.96

Table 3

Wall characteristics of the CCA and degree of ICA stenosis determined for patients with low and high relative IMT inhomogeneity (cut-off 2%).

	IMT inhomogeneity / diastolic diameter		**P-value**
	≤2%	>2%	
N	142	40	-
Age	67±9	69±8	0.18
Diastolic diameter [µm]	8000±1004	8054±797	0.75
IMT [µm]	956±132	1190±285	<0.001
IMT/diastolic diameter [%]	12±2	15±3	<0.001
Max. IMT [µm]	1335±329	2028±456	<0.001
Distension [µm]	437±146	449±176	0.66
Distension/diastolic diameter [%]	5.5±1.8	5.6±2.0	0.79
Distension inhomogeneity [µm]	94±34	111±38	0.01
Distension inhomogeneity/diastolic diameter [%]	1.2±0.4	1.4±0.5	0.008
Degree of distal stenosis [%]	47±13	52±11	0.023

Discussion

We evaluated the characteristics of the CCA wall in patients who recently experienced an ischemic stroke or TIA and had a mild-to-moderate plaque in the carotid artery bifurcation or ICA. Ipsilateral and contralateral arteries had a similar relative IMT inhomogeneity. A high (>0.2%) relative CCA-IMT inhomogeneity is associated with a larger mean IMT, higher distension inhomogeneity and a larger degree of ICA stenosis. The association between relative CCA-IMT inhomogeneity and degree of ICA stenosis remained significant after adjustment for common risk factors, i.e., age, BMI, smoking, diabetes mellitus and hypertension.

The intra-subject precision of all wall characteristics, except IMT, was larger for one participating center, i.e., the wall characteristics were less precisely determined. Due to a diverging CCA near the bifurcation and slightly different locations of the CCA scanning plane for duplicate recordings, spatial changes in wall characteristics can be expected. Despite differences in precision, inter-subject values were not significantly different across centers, so data can be pooled. Multiple centers are necessary to provide a large sample size to ensure sufficient power for the follow-up phase. Similar values across centers imply that this method can be easily implemented in clinical practice.

The degree of stenosis was defined according to ECST criterion, i.e., lumen diameter divided by vessel diameter at the same location. In clinical practice, the degree of stenosis according to the North American Symptomatic Carotid Endarterectomy Trial (NASCET) criterion (North American Symptomatic Carotid Endarterectomy Trial 1991) is commonly used for selecting patients with severe plaques for carotid endarterectomy. In the latter case the lumen diameter at the site of the plaque is divided by the vessel diameter of the ICA just distally. Since the degree of stenosis according the NASCET criterion underestimates the actual burden of atherosclerosis (Staikov et al. 2000), we decided to use the ECST criterion.

The mean IMT of our population (1007±202 μm) is substantially larger compared to the IMT reference value (677 μm) of a 68 year old healthy male (Engelen et al. 2013). Additionally, it was also larger than values reported for patients with cardiovascular disease (779±196 μm) (Schreuder et al. 2009) and with plaques in the bifurcation (760±180 μm) (Graf et al. 2009). Moreover, the spatial IMT inhomogeneity (136±68 μm) is also substantially higher than values reported for an elderly healthy population (50 μm male; 40 μm female) (Meinders et al. 2003) and reported for an elderly patient population (59±49 μm) obtained with duplicate recordings (Graf et al. 2009). All our patients suffered from a recent cerebrovascular event associated with atherosclerosis, which explains the higher IMT and its inhomogeneity.

Since wall thickness is related to end-diastolic diameter (Liang et al. 2001; Nichols et al. 2011), we looked at relative IMT inhomogeneity. Patients with a mean end-diastolic diameter in the first quartile (25%, <7287 µm, N=47) indeed had a significantly lower IMT and IMT inhomogeneity (mean difference IMT 193 µm and IMT inhomogeneity 47 µm, Student t-test, p-value<=0.005) than patients with a mean end-diastolic diameter in the fourth quartile (75%, >8646 µm, N=38). Nonetheless, absolute IMT inhomogeneity showed a similar trend as relative IMT inhomogeneity, i.e., a higher IMT inhomogeneity is associated with a larger degree of distal stenosis.

In this study, a cut-off of 2% is chosen for relative IMT inhomogeneity to account for the baseline random fluctuations due to US resolution. Low relative IMT inhomogeneity is therefore considered a normal stochastic variation. Further studies are needed to determine whether the selected cut-off is the most optimal value.

Patients with a low relative IMT inhomogeneity exhibit a wide range of plaque sizes, as shown in Figure 2, without a direct relationship between relative IMT inhomogeneity and degree of ICA stenosis. On the other hand, a high relative inhomogeneity is associated with a larger degree of ICA stenosis and, hence, indicative for atherosclerotic burden. However, most plaques with a high degree of ICA stenosis do not necessarily have a larger IMT inhomogeneity, which might be possibly explained by a different plaque composition.

Relative IMT inhomogeneity reflects an irregular vessel wall and will increase for a higher maximal IMT. Therefore, it remains unclear whether irregularity itself is a valuable parameter on top of maximal CCA-IMT values , as already noted by Bots (Bots and den Ruijter 2012). Nonetheless, the observed association between IMT inhomogeneity and degree of stenosis, which remained significant after adjustment for common risk factors, may indicate the clinical value of IMT inhomogeneity. Whether this is mainly driven by maximal IMT or irregularity itself is not important as long as its effect is stronger than the individual values. The follow-up phase of the PARISK study will consider the value of IMT inhomogeneity independent of maximal IMT values in relation to recurrent cerebrovascular events.

One of the limitations of the current study is that patients were included after a recent ischemic stroke or TIA, which may be years after the initial development of atherosclerotic plaques. The current cross-sectional study can only demonstrate an association between high relative IMT inhomogeneity and larger plaque size when plaques have already developed. Whether IMT inhomogeneity is also present prior to plaque development and whether IMT inhomogeneity can predict new plaque development is subject for future longitudinal studies.

In conclusion, a high relative CCA-IMT inhomogeneity is associated with a larger degree of ICA stenosis, independent of common risk factors, and hence indicative for atherosclerotic burden. In the follow-up of the PARISK study, we will analyse if IMT inhomogeneity can predict plaque progression and/or the occurrence of recurrence of cerebrovascular symptoms.

References

Bonithon-Kopp C, Touboul PJ, Berr C, Leroux C, Mainard F, Courbon D, Ducimetiere P. Relation of intima-media thickness to atherosclerotic plaques in carotid arteries. The Vascular Aging (EVA) Study. Arterioscler Thromb Vasc Biol 1996;16:310-316.

Bots ML, den Ruijter HM. Variability in the intima-media thickness measurement as marker for cardiovascular risk? Not quite settled yet. Cardiovasc Diagn Ther 2012;2:3-5.

Bots ML, Groenewegen KA, Anderson TJ, Britton AR, Dekker JM, Engstrom G, Evans GW, de Graaf J, Grobbee DE, Hedblad B, Hofman A, Holewijn S, Ikeda A, Kavousi M, Kitagawa K, Kitamura A, Ikram MA, Lonn EM, Lorenz MW, Mathiesen EB, Nijpels G, Okazaki S, O'Leary DH, Polak JF, Price JF, Robertson C, Rembold CM, Rosvall M, Rundek T, Salonen JT, Sitzer M, Stehouwer CD, Franco OH, Peters SA, den Ruijter HM. Common carotid intima-media thickness measurements do not improve cardiovascular risk prediction in individuals with elevated blood pressure: the USE-IMT collaboration. Hypertension 2014;63:1173-1181.

Costanzo P, Perrone-Filardi P, Vassallo E, Paolillo S, Cesarano P, Brevetti G, Chiariello M. Does carotid intima-media thickness regression predict reduction of cardiovascular events? A meta-analysis of 41 randomized trials. J Am Coll Cardiol 2010;56:2006-2020.

den Ruijter HM, Peters SA, Groenewegen KA, Anderson TJ, Britton AR, Dekker JM, Engstrom G, Eijkemans MJ, Evans GW, de Graaf J, Grobbee DE, Hedblad B, Hofman A, Holewijn S, Ikeda A, Kavousi M, Kitagawa K, Kitamura A, Koffijberg H, Ikram MA, Lonn EM, Lorenz MW, Mathiesen EB, Nijpels G, Okazaki S, O'Leary DH, Polak JF, Price JF, Robertson C, Rembold CM, Rosvall M, Rundek T, Salonen JT, Sitzer M, Stehouwer CD, Witteman JC, Moons KG, Bots ML. Common carotid intima-media thickness does not add to Framingham risk score in individuals with diabetes mellitus: the USE-IMT initiative. Diabetologia 2013;56:1494-1502.

Engelen L, Ferreira I, Stehouwer CD, Boutouyrie P, Laurent S, Reference Values for Arterial Measurements C. Reference intervals for common carotid intima-media thickness measured with echotracking: relation with risk factors. Eur Heart J 2013;34:2368-2380.

European Carotid Surgery Trialists' Collaborative G. Randomised trial of endarterectomy for recently symptomatic carotid stenosis: final results of the MRC European Carotid Surgery Trial (ECST). The Lancet 1998;351:1379-1387.

Graf IM, Schreuder FH, Hameleers JM, Mess WH, Reneman RS, Hoeks AP. Wall irregularity rather than intima-media thickness is associated with nearby atherosclerosis. Ultrasound Med Biol 2009;35:955-961.

Hermans MM, Kooman JP, Brandenburg V, Ketteler M, Damoiseaux JG, Tervaert JW, Ferreira I, Rensma PL, Gladziwa U, Kroon AA, Hoeks AP, Stehouwer CD, Leunissen KM. Spatial inhomogeneity of common carotid artery intima-media is increased in dialysis patients. Nephrol Dial Transplant 2007;22:1205-1212.

Liang YL, Shiel LM, Teede H, Kotsopoulos D, McNeil J, Cameron JD, McGrath BP. Effects of Blood Pressure, Smoking, and Their Interaction on Carotid Artery Structure and Function. Hypertension 2001;37:6-11.

Lorenz MW, Schaefer C, Steinmetz H, Sitzer M. Is carotid intima media thickness useful for individual prediction of cardiovascular risk? Ten-year results from the Carotid Atherosclerosis Progression Study (CAPS). Eur Heart J 2010;31:2041-2048.

Meinders JM, Brands PJ, Willigers JM, Kornet L, Hoeks AP. Assessment of the spatial homogeneity of artery dimension parameters with high frame rate 2-D B-mode. Ultrasound Med Biol 2001;27:785-794.

Meinders JM, Kornet L, Hoeks AP. Assessment of spatial inhomogeneities in intima media thickness along an arterial segment using its dynamic behavior. Am J Physiol Heart Circ Physiol 2003;285:H384-391.

Nichols WW, O'Rourke MF, Vlachopoulos C. McDonald's blood flow in arteries : theoretic, experimental, and clinical principles. 6th. Hodder Arnold, London, 2011.

North American Symptomatic Carotid Endarterectomy Trial C. Beneficial effect of carotid endarterectomy in symptomatic patients with high-grade carotid stenosis. N Engl J Med 1991;325:445-453.

O'Leary DH, Polak JF, Kronmal RA, Manolio TA, Burke GL, Wolfson SK, Jr. Carotid-artery intima and media thickness as a risk factor for myocardial infarction and stroke in older adults. Cardiovascular Health Study Collaborative Research Group. N Engl J Med 1999;340:14-22.

Persson J, Formgren J, Israelsson B, Berglund G. Ultrasound-determined intima-media thickness and atherosclerosis. Direct and indirect validation. Arterioscler Thromb 1994;14:261-264.

Polak JF, Pencina MJ, Meisner A, Pencina KM, Brown LS, Wolf PA, D'Agostino RB, Sr. Associations of carotid artery intima-media thickness (IMT) with risk factors and prevalent cardiovascular disease: comparison of mean common carotid artery IMT with maximum internal carotid artery IMT. J Ultrasound Med 2010;29:1759-1768.

Roquer J, Segura T, Serena J, Cuadrado-Godia E, Blanco M, Garcia-Garcia J, Castillo J, Study A. Value of carotid intima-media thickness and significant carotid stenosis as markers of stroke recurrence. Stroke 2011;42:3099-3104.

Rundek T, Gardener H, Della-Morte D, Dong C, Cabral D, Tiozzo E, Roberts E, Crisby M, Cheung K, Demmer R, Elkind MS, Sacco RL, Desvarieux M. The relationship between carotid intima-media thickness and carotid plaque in the Northern Manhattan Study. Atherosclerosis 2015;241:364-370.

Saba L, Meiburger KM, Molinari F, Ledda G, Anzidei M, Acharya UR, Zeng G, Shafique S, Nicolaides A, Suri JS. Carotid IMT variability (IMTV) and its validation in symptomatic versus asymptomatic Italian population: can this be a useful index for studying symptomaticity? Echocardiography 2012;29:1111-1119.

Schmidt-Trucksass A, Sandrock M, Cheng DC, Muller HM, Baumstark MW, Rauramaa R, Berg A, Huonker M. Quantitative measurement of carotid intima-media roughness--effect of age and manifest coronary artery disease. Atherosclerosis 2003;166:57-65.

Schreuder FH, Graf M, Hameleers JM, Mess WH, Hoeks AP. Measurement of common carotid artery intima-media thickness in clinical practice: comparison of B-mode and RF-based technique. Ultraschall Med 2009;30:459-465.

Silvestrini M, Cagnetti C, Pasqualetti P, Albanesi C, Altamura C, Lanciotti C, Bartolini M, Mattei F, Provinciali L, Vernieri F. Carotid wall thickness and stroke risk in patients with asymptomatic internal carotid stenosis. Atherosclerosis 2010;210:452-457.

Staikov IN, Arnold M, Mattle HP, Remonda L, Sturzenegger M, Baumgartner RW, Schroth G. Comparison of the ECST, CC, and NASCET grading methods and ultrasound for assessing carotid stenosis. European Carotid Surgery Trial. North American Symptomatic Carotid Endarterectomy Trial. J Neurol 2000;247:681-686.

Steinbuch J, Hoeks AP, Hermeling E, Truijman MT, Schreuder FH, Mess WH. Standard B-Mode Ultrasound Measures Local Carotid Artery Characteristics as Reliably as Radiofrequency Phase Tracking in Symptomatic Carotid Artery Patients. Ultrasound Med Biol 2016;42:586-595.

Truijman MT, Kooi ME, van Dijk AC, de Rotte AA, van der Kolk AG, Liem MI, Schreuder FH, Boersma E, Mess WH, van Oostenbrugge RJ, Koudstaal PJ, Kappelle LJ, Nederkoorn PJ, Nederveen AJ, Hendrikse J, van der Steen AF, Daemen MJ, van der Lugt A. Plaque At RISK (PARISK): prospective multicenter study to improve diagnosis of high-risk carotid plaques. Int J Stroke 2014;9:747-754.

Tsivgoulis G, Vemmos K, Papamichael C, Spengos K, Manios E, Stamatelopoulos K, Vassilopoulos D, Zakopoulos N. Common carotid artery intima-media thickness and the risk of stroke recurrence. Stroke 2006;37:1913-1916.

Tsivgoulis G, Vemmos KN, Spengos K, Papamichael CM, Cimboneriu A, Zis V, Zakopoulos N, Mavrikakis M. Common carotid artery intima-media thickness for the risk assessment of lacunar infarction versus intracerebral haemorrhage. J Neurol 2005;252:1093-1100.

Uthoff H, Staub D, Meyerhans A, Hochuli M, Bundi B, Schmid HP, Frauchiger B. Intima-media thickness and carotid resistive index: progression over 6 years and predictive value for cardiovascular events. Ultraschall Med 2008;29:604-610.

van den Oord SC, Sijbrands EJ, ten Kate GL, van Klaveren D, van Domburg RT, van der Steen AF, Schinkel AF. Carotid intima-media thickness for cardiovascular risk assessment: systematic review and meta-analysis. Atherosclerosis 2013;228:1-11.

Vemmos KN, Tsivgoulis G, Spengos K, Papamichael CM, Zakopoulos N, Daffertshofer M, Lekakis JP, Mavrikakis M. Common carotid artery intima-media thickness in patients with brain infarction and intracerebral haemorrhage. Cerebrovasc Dis 2004;17:280-286.

5

Definition of common carotid wall thickness affects risk classification in relation to degree of internal carotid artery stenosis: The Plaque At RISK (PARISK) study

Steinbuch J, Van Dijk AC, Schreuder FHBM, Truijman MTB, Hendrikse J, Nederkoorn PJ, Van der Lugt A, Hermeling E, Hoeks APG, Mess WH. Definition of common carotid wall thickness affects risk classification in relation to degree of internal carotid artery stenosis: The Plaque At RISK (PARISK) study. Cardiovasc Ultrasound 2017;15:9.

Abstract

Background

Mean or maximal intima-media thickness (IMT) is commonly used as surrogate endpoint in intervention studies. However, the effect of normalization by surrounding or median IMT or by diameter is unknown. In addition, it is unclear whether IMT inhomogeneity is a useful predictor beyond common wall parameters like maximal wall thickness, either absolute or normalized to IMT or lumen size. We investigated the interrelationship of common carotid artery (CCA) thickness parameters and their association with the ipsilateral internal carotid artery (ICA) stenosis degree.

Methods

CCA thickness parameters were extracted by edge detection applied to ultrasound B-mode recordings of 240 patients. Degree of ICA stenosis was determined from CT angiography.

Results

Normalization of maximal CCA wall thickness to median IMT leads to large variations. Higher CCA thickness parameter values are associated with a higher degree of ipsilateral ICA stenosis ($p<0.001$), though IMT inhomogeneity does not provide extra information. When the ratio of wall thickness and diameter instead of absolute maximal wall thickness is used as risk marker for having moderate ipsilateral ICA stenosis (>50%), 55 arteries (15%) are reclassified to another risk category.

Conclusion

It is more reasonable to normalize maximal wall thickness to end-diastolic diameter rather than to IMT, affecting risk classification and suggesting modification of the Mannheim criteria.

Introduction

An irregular intima-media thickness (IMT) of the common carotid artery (CCA) is indicative for atherosclerotic burden (Graf et al. 2009; Steinbuch et al. 2016b) and hence, might be a useful predictor in risk assessment. In a vascular diseased patient population CCA-IMT irregularity is associated with nearby atherosclerosis (Graf et al. 2009). Furthermore, in symptomatic patients high CCA-IMT irregularity is associated with a higher degree of stenosis of distal plaques (Steinbuch et al. 2016b) and is more prominent in symptomatic than in asymptomatic subjects (Saba et al. 2012). However, as previously discussed by Bots et al. (Bots and den Ruijter 2012), it remains unclear whether IMT irregularity itself is a useful predictor in addition to maximal IMT. It has been shown that after adjustment for coronary risk factors the combined IMT irregularity of CCA, bulb and internal carotid artery (ICA) is a more accurate predictor for coronary artery disease than mean and maximum IMT (Ishizu et al. 2002). But, for patients with cerebrovascular disease and ICA stenosis it is still unknown.

CCA-IMT progression is commonly used as surrogate endpoint for cardiovascular risk for evaluating drug therapy in interventional studies (Huang et al. 2013; Davidson et al. 2014; Ishigaki et al. 2014; Oyama et al. 2016). However, CCA-IMT is affected by the dynamic range and frequency bandwidth of the ultrasound system employed (Gaarder and Seierstad 2015), while for an elderly subject population image quality is generally poorer than for young healthy subjects. As a consequence the observed IMT distribution is subject to large relative errors. Moreover, CCA-IMT measures vary across studies (Qu and Qu 2015), e.g., mean or maximal CCA-IMT with or without CCA plaque. According to the Mannheim consensus (Touboul et al. 2012), plaques are defined as having a wall thickness 1) extending more than 500 μm into the lumen, 2) and higher than 50% of surrounding IMT and/or 3) higher than 1500 μm. Therefore, the Mannheim criteria use absolute maximal wall thickness (criterion 3) or wall thickness normalized to surrounding IMT (criterion 2) or a combination of both (criterion 1). Because IMT values are slightly higher than the ultrasound resolution (about 0.3 mm for commonly used ultrasound systems), normalization of maximum wall thickness with respect to the surrounding IMT (criterion 2) will introduce wide variations. Considering the interrelationship between wall thickness and artery diameter according to the Lamé's equation (Liang et al. 2001; Nichols et al. 2011) and the wider range in CCA diameter (6-9 mm) in a healthy population (Engelen et al. 2015), it seems physiologically more reasonable to normalize absolute maximal wall thickness by diameter. Using local wall thickness normalized to either IMT (i.e., thickness-to-IMT ratio) or diameter (i.e., thickness-to-diameter ratio) instead of the CCA-IMT as surrogate endpoint may affect the interpretation of drug therapy results. In addition, normalized wall thickness may lead to reclassification of CCAs towards another risk category, e.g. risk of having more than 50% degree of ICA stenosis. This study analyses the baseline results of a 2-year follow-up PARISK study in which the association between CCA wall parameters and risk of plaque rupture will be investigated (Truijman et al. 2014). As a first step, we will investigate the interrelationship of CCA-IMT parameters and their association with the degree of ipsilateral ICA stenosis. More specifically, we will investigate in a large group of symptomatic subjects 1) the relevance of absolute and normalized maximal wall thickness with or without CCA plaques, 2) their relation with CCA-IMT inhomogeneity and 3) the association between absolute wall thickness, thickness-to-diameter ratio, thickness-to-IMT ratio, CCA plaques and CCA-IMT inhomogeneity with the degree of ipsilateral ICA stenosis.

Methods

Study subjects

240 patients with mild-to-moderate ICA stenosis (<70% according to the NASCET criteria) and recent ischemic stroke, transient ischemic attack or amaurosis fugax, were included in the Plaque At RISK (PARISK) study (clinical trials.gov NCT01208025), an ongoing multicenter cohort study with 2-year follow-up. Details of the study were previously described (Truijman et al. 2014). The study was approved by the Medical Ethics Committees of the participating centers and all patients gave written informed consent. Currently, only baseline observations are available.

Data acquisition

Longitudinal ultrasound B-mode recordings (40 mm width, 5 seconds, 37 fps) of both CCAs were acquired in duplicate of 233 patients at anterolateral and posterolateral angles with a Philips iU22 scanner (Philips Medical Systems, Bothell, USA) using different probes (17-5, 12-5 or 9-3 MHz) depending on the CCA depth. The distal end of the recorded CCA segment was located 1-2 cm proximal to the flow divider. During ultrasound recordings, patients lay in supine position with their head slightly tilted to the opposite side. Due to contra-indications (low renal clearance (<60 ml/minute) or allergy to CT contrast media), only 201 patients were subjected to multidetector computed tomography angiography (MDCTA).

Echo edge detection

Wall thickness was extracted at end-diastole by edge detection of B-mode images with dedicated software developed by Maastricht University Medical Center (MUMC, Maastricht, The Netherlands) (Steinbuch et al. 2016a) by a trained observer blinded to the MDCTA results. The intra-subject precision of the adopted software for absolute IMT of an artery segment, i.e. the standard deviation of differences between duplicate recordings and their average, is on average 99 μm (Steinbuch et al. 2016b). The maximum variation of IMT expected due to the ultrasound depth resolution is 150 μm (Steinbuch et al. 2016b). For each B-mode frame, automatic wall detection of the media-adventitia transition at the anterior and posterior wall was performed for half-overlapping segments (width 3.7 mm) using a threshold of 65% (or half of the difference between this threshold and the maximum, i.e., 83%, in case of an echogenic lumen-intima boundary) of the maximal grey value of the adventitia segment (Steinbuch et al. 2016b). The local diameter was defined as the local difference along the ultrasound beam between anterior and posterior media-adventitia transitions.

The diameter waveforms, as extracted by edge detection, were smoothed over time (0.2 s filter span) with a 2nd order zero-phase Savitsky-Golay filter. After discarding the end-segments, the mean diameter waveform was calculated and the end-diastolic frames identified. At those frames, the lumen-intima transition along the posterior wall was identified, based on the maximum of the first derivative of the echo amplitude, and corrected manually when necessary (Steinbuch et al. 2016b). The spatial IMT distribution was obtained as the differences along the ultrasound beam between the posterior lumen-intima and media-adventitia transitions over the artery segment.

Absolute and normalized maximal wall thickness

For each end-diastolic image, the diameter and IMT were obtained as the spatial median while the maximal wall thickness as spatial maximum, and averaged (median) over all available heart beats (on average 5). Absolute maximal wall thickness was normalized to the median end-diastolic diameter, defined as thickness-to-diameter ratio, and to the median IMT, defined as thickness-to-IMT ratio. All parameters were averaged (median) over all ipsilateral recordings.

IMT inhomogeneity

Absolute IMT inhomogeneity was defined as the standard deviation of the IMT over the artery segment and averaged (median) over available heart beats and all ipsilateral recordings (anterolateral, posterolateral, duplicate). IMT inhomogeneity was also normalized to the local end-diastolic diameter, i.e., relative IMT inhomogeneity.

Degree of ICA stenosis

MDCTA images were analyzed with dedicated 3D analysis software (Leonardo and syngo. via; Siemens, Erlangen, Germany). Degree of stenosis in both carotid arteries (bifurcation or ICA), based on the European Carotid Surgery Trial criteria (European Carotid Surgery Trialists' Collaborative 1998), was manually assessed perpendicularly to the central lumen line by a trained observer.

Statistical analysis

To compare the maximal wall thickness parameters, the parameters were transformed to a normal z-score distribution using the expression (value-mean)/SD. The mean and standard deviation (SD), used as reference in this equation, were derived for CCA arteries without plaques according to the Mannheim criteria. To compare maximal wall thickness parameters with IMT inhomogeneity, correlation coefficients were calculated.

Optimal cut-offs for absolute maximal wall thickness, thickness-to-diameter ratio and thickness-to-IMT ratio for the presence of a >50% ipsilateral stenosis were derived from ROC curves. The optimal cut-off follows from the shortest distance towards the upper left corner of the ROC curve. In addition, a Student t-test was used to assess the difference in degree of ICA stenosis for ipsilateral CCA arteries with low and high wall thickness parameters. To establish the risk for having more than 50% degree of ipsilateral ICA stenosis, the CCAs were divided into low and high absolute maximal wall thickness, thickness-to-diameter ratio and thickness-to-IMT ratio according to the ROC defined cut-offs. Since the variation in IMT due to the ultrasound depth resolution (conservatively estimated at 300 μm) is about 150 μm, i.e. 2% for an end-diastolic diameter of 7.5 mm, the cut-off level for relative IMT inhomogeneity was tentatively set at 2% (Steinbuch et al. 2016b). To investigate the effect of wall thickness parameters as risk markers on the defined risk categories, reclassification of arteries was defined as the number of CCAs that switched to another risk category, using either the maximal wall thickness parameters instead of the Mannheim criteria or thickness-to-diameter ratio instead of absolute maximal wall thickness. Values are quantified as mean±SD. Significance level was set at $p<0.05$.

Results

In total, 197 patients received an MDCTA as well as an ultrasound examination. Five patients were excluded due to insufficient quality of MDCTA (N=2) or due to failure to have an ultrasound registration of both CCAs (N=3). In addition, patients with an ICA occlusion or stent (N=3) were excluded, leading to 189 included patients (371 CCAs; mean age 68±9 yrs). Patient characteristics are shown in Table 1. Prior to the study we estimated the B-mode depth resolution both from the spatial speckle frequency (ensemble average power spectral density across image) and from the width at half-maximum of distinct lumen-intima echoes (average of 10 independent observations) at 264 and 267 μm, respectively.

Table 1

Patient characteristics. Data are presented as mean ± SD (range or number of patients).

N	189
Age [years]	68±9 (39-88)
Male [%]	73 (N=138)
BMI [kg/m^2]	27±4 (17-43)
Systolic blood pressure [mmHg]	140±19 (97-210)
Diastolic blood pressure [mmHg]	79±9 (54-105)
Pulse pressure [mmHg]	61±16 (27-117)
Stroke / TIA/ amaurosis fugax [%]	46/42/12 (N=87/80/22)
Current smoking [%]	23 (N=43)
Diabetes Mellitus [%]	21 (N=41)
Hypercholesterolemia [%]	57 (N=107)
Hypertension [%]	59 (N=111)

Absolute and normalized maximal wall thickness

Figure 1 contains a boxplot of absolute and normalized maximal wall thickness, expressed as normal z-scores. CCA arteries with plaques (N=140) according to the Mannheim criteria clearly have a higher absolute maximal wall thickness, thickness-to-diameter ratio and thickness-to-IMT ratio than CCAs without plaques (N=231; mean difference 5, 5 and 4, respectively, Student t-test p-value<0.001). The values of the thickness-to-IMT ratio of CCAs with plaques are spread over a wider range than the other wall thickness parameters (Figure 1) due to resolution related variations. Therefore, thickness-to-IMT ratio is not considered for correlation with IMT inhomogeneity.

Maximal wall thickness and IMT inhomogeneity

Absolute maximal wall thickness is strongly correlated with absolute IMT inhomogeneity (R=0.76, Figure 2). In addition, maximal thickness-to-diameter ratio is also strongly associated with relative IMT inhomogeneity (R=0.73, Figure 2).

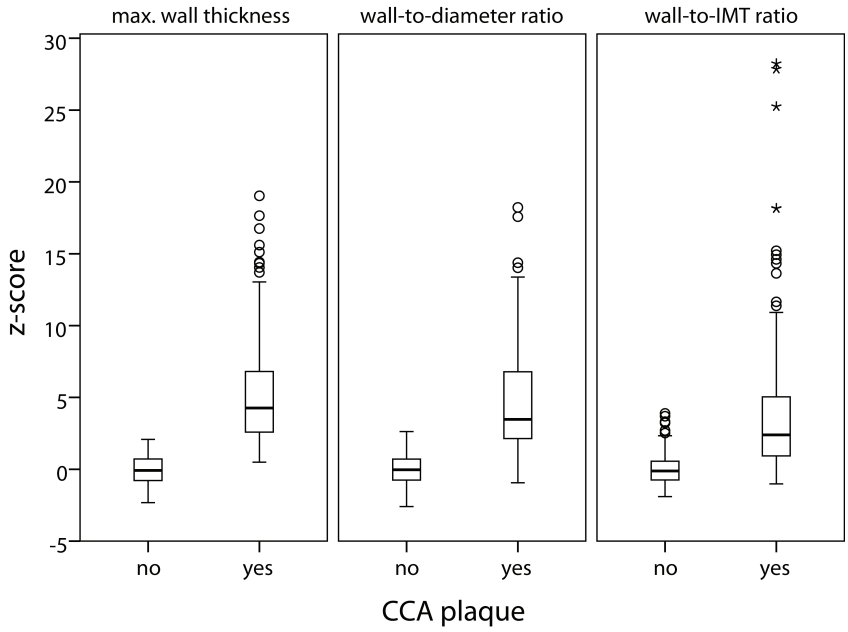

Figure 1

Absolute maximal wall thickness, thickness-to-diameter ratio and thickness-to-IMT ratio of the CCA as function of the presence of CCA plaque. Values are presented as normal z-scores, based on the mean and SD of the thickness parameters for arteries without CCA plaques. Arteries with CCA plaques clearly have a significantly larger wall thickness. Normalized thickness-to-IMT has a wider distribution than maximal wall thickness and thickness-to-diameter ratio.

Maximal wall thickness and degree of ipsilateral ICA stenosis

ROC curves of absolute and normalized maximal wall thickness for detecting an ipsilateral ICA stenosis greater than 50% are shown in Figure 3. Optimal cut-offs for absolute maximal wall thickness, thickness-to-diameter ratio and thickness-to-IMT ratio are 1277 μm, 17% and 129%, respectively. When only the side with the highest ICA plaque is considered, optimal cut-offs are 1191 μm, 16% and 124%, respectively.

Risk Stratification

Arteries were divided into two risk categories according to the ROC defined cut-offs for an ICA stenosis (see above). When thickness-to-IMT ratio instead of Mannheim criteria is used as risk marker, a large number of arteries (Table 2, N=95, 26%) are reclassified to another risk category. Moreover, thickness-to-diameter ratio reclassifies 53 arteries (14%), whereas absolute maximal wall thickness reclassifies 56 arteries (15%). Since thickness-to-IMT ratio is more prone to resolution related variations (Figure 1), only absolute maximal wall thickness and thickness-to-diameter ratio are considered for further analyses.

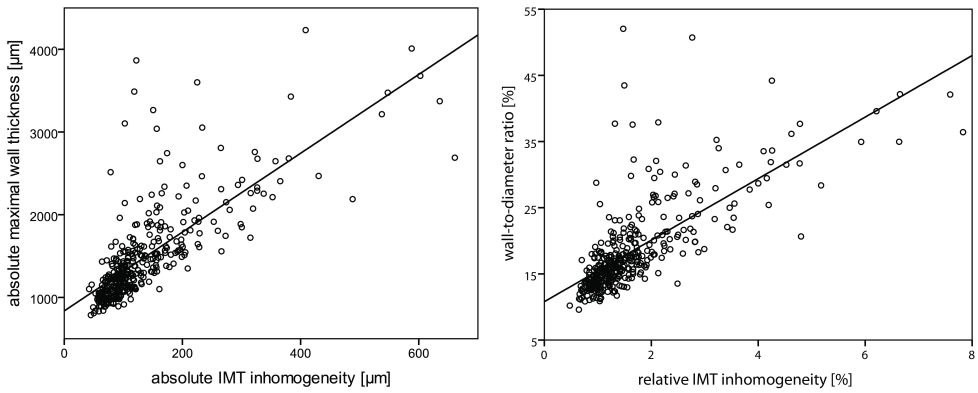

Figure 2

Absolute maximal wall thickness as function of absolute IMT inhomogeneity (left) and thickness-to-diameter ratio as function of relative IMT inhomogeneity (right). A strong correlation exists between absolute maximal wall thickness and absolute IMT inhomogeneity (R=0.76) and between thickness-to-diameter ratio and relative IMT inhomogeneity (R=0.73).

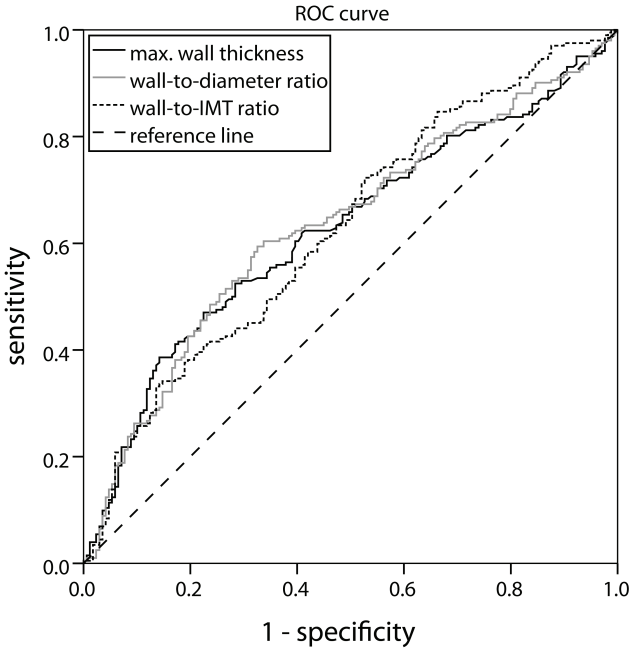

Figure 3

ROC curve for absolute maximal wall thickness (black line), thickness-to-diameter ratio (grey line) and thickness-to-IMT ratio (dotted line) for determination of a >50% ipsilateral ICA stenosis. Optimal cut-off values with the shortest distance (0.60, 0.61 and 0.64, respectively) towards the left upper corner are 1277 µm for absolute maximal wall thickness, 17% for thickness-to-diameter ratio and 129% for thickness-to-IMT ratio.

Table 2

Number of arteries with low or high maximal wall thickness parameters, stratified according to CCA plaque presence (Mannheim criteria). Using maximal wall thickness parameters as risk markers instead of Mannheim criteria results in reclassification of subjects towards another risk category. For example, the thickness-to-IMT ratio (right columns) reclassifies 70 and 25 subjects towards a higher and lower risk category, respectively, in total 26%.

CCA plaque	Absolute maximal wall thickness		Thickness-to-diameter ratio		Thickness-to-IMT ratio	
	<1277 µm	>1277 µm	<17%	>17%	<129%	>129%
No	176	55	185	46	161	70
Yes	1	139	7	133	25	115
Total	177	194	192	179	186	185

Patients with absolute maximal wall thickness below 1277 µm have a wide range of degree of ipsilateral ICA stenosis (N=174), whereas patients with absolute wall thickness above 1277 µm (N=197) exhibit a higher degree of ICA stenosis (Figure 4). Both absolute maximal wall thickness and thickness-to-diameter ratio above cut-off values are associated with a higher ipsilateral stenosis degree (Table 3 and 4, 52±15% and 52±16%, respectively) than below the cut-off values (mean difference 8% and 7%, Student t-test p-value<0.001). This association remains borderline significant after excluding patients with CCA plaques (Table 3 and 4, mean difference 7% and 5%, Student t-test p-value 0.02 and 0.15, respectively). Moreover, similar trends are seen when only the side with the highest ICA plaque is considered (Table 3 and 4). In addition, CCAs with a plaque (N=140) exhibit a stronger association with a higher distal stenosis degree than arteries without a plaque (N=231; 52±15% and 46±19%, respectively, mean difference 7%, Student t-test p-value<0.001). When thickness-to-diameter ratio instead of absolute maximal wall thickness is used as risk marker for having more than ipsilateral 50% degree of ICA stenosis, 55 CCAs (15%) are reclassified towards the other risk category (of which N=20 towards a higher category).

IMT inhomogeneity and degree of ipsilateral ICA stenosis

Arteries with a relative IMT inhomogeneity above 2% (N=81) are associated with a higher degree of ipsilateral ICA stenosis (53±11%) than arteries (N=290) with a relative IMT inhomogeneity below 2% (mean difference 6%, Student t-test p-value<0.001).

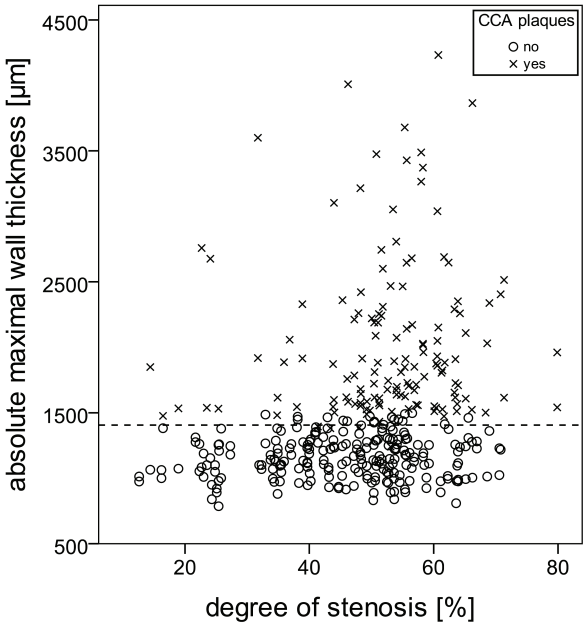

Figure 4

Absolute maximal wall thickness of the CCA as function of degree of ipsilateral ICA stenosis. Patients with absolute maximal wall thickness below the ROC defined cut-off (dashed line) have a wide range of plaque sizes whereas patients with absolute maximal wall thickness above the ROC defined cut-off have larger degree of ICA stenosis.

Table 3

ICA stenosis degree according to the ipsilateral absolute maximal wall thickness cut-off for ICA stenosis at either side or for the largest ICA stenosis. Data are presented as mean ± SD. A high absolute maximal wall thickness is indicative for a higher degree of ipsilateral ICA stenosis.

ICA Plaque	N ICAs	CCA plaque	Cut-off	ICA stenosis	p-value
Either side	174	yes/no	<1277 µm	44±20%	<0.001
	197		>1277 µm	52±15%	
	173	no	<1277 µm	44±20%	0.02
	58		>1277 µm	51±16%	
Largest	64	yes/no	<1191 µm	55±14%	0.006
	121		>1191 µm	60±11%	
	64	no	<1191 µm	55±14%	0.04
	54		>1191 µm	60±12%	

Table 4

ICA stenosis degree according to the ipsilateral thickness-to-diameter ratio cut-off for ICA stenosis at either side or for the largest ICA stenosis. Data are presented as mean ± SD. A high thickness-to-diameter ratio is indicative for a higher degree of ipsilateral ICA stenosis.

ICA plaque	N ICAs	CCA plaque	Cut-off	ICA stenosis	p-value
Either side	192	yes/no	<17%	45±19%	<0.001
	179		>17%	52±16%	
	185	no	<17%	45±19%	0.15
	46		>17%	50±18%	
Largest	91	yes/no	<16%	56±13%	0.03
	94		>16%	61±12%	
	90	no	<16%	56±13%	0.3
	23		>16%	58±12%	

Discussion

We evaluated the absolute and normalized maximal wall thickness and CCA-IMT inhomogeneity in patients with a recent cerebrovascular accident and mild-to-moderate ICA stenosis. Normalization by median IMT leads to large variations. Absolute maximal wall thickness and thickness-to-diameter ratio are strongly correlated with absolute and relative IMT inhomogeneity, respectively. IMT inhomogeneity does not provide extra information on top of absolute maximal wall thickness or thickness-to-diameter ratio in relation to the degree of ipsilateral ICA stenosis. Mainly CCA plaques are strongly associated with a higher degree of ipsilateral ICA stenosis. Although a similar trend is seen for both absolute maximal wall thickness and thickness-to-diameter ratio, 15% of CCAs are reclassified when thickness-to-diameter ratio instead of absolute maximal wall thickness is used as risk marker for a >50% ipsilateral ICA stenosis.

Maximal wall thickness is normalized by the median end-diastolic diameter as well as the median IMT. As expected, patients with CCA plaques have a significantly higher absolute and normalized maximal wall thickness ($p<0.001$). Normalization by the median IMT leads to similar values for arteries without CCA plaques, whereas a large variation is found for CCA arteries with large plaques (Figure 1).

Risk stratification

Optimal cut-offs for absolute and normalized maximal wall thickness are derived from ROC curves for a >50% ipsilateral ICA stenosis (Figure 3). We have chosen those plaques since the smaller plaques in the curved carotid bulb hardly induce hemodynamic changes (Ahmed and Giddens 1983; Gijsen et al. 1996). 96 CCAs (Table 2; 26%) are reclassified towards another risk category when thickness-to-IMT ratio rather than the Mannheim criteria are used as a risk marker for a >50% ipsilateral ICA stenosis. Since observed IMT values are generally noisy because they are slightly higher than the ultrasound depth resolution, normalization of maximum wall thickness with respect to median IMT will introduce wide variations. Therefore, it is questionable whether the Mannheim criterion (Touboul et al. 2012), defining a plaque if the maximum thickness is 50% greater than the surrounding IMT, is consistent. Moreover, "surrounding IMT" is quite arbitrary (where does a plaque begin or end); that is why we decided to normalize the maximum thickness by the median IMT.

For the risk stratification of individual patients an optimal cut-off is needed. Although maximal wall thickness and thickness-to-diameter ratio show similar associations with the degree of ipsilateral ICA stenosis (Table 3 and 4), 55 arteries (15%) are reclassified when thickness-to-diameter ratio instead of absolute maximal wall thickness is used as risk marker for a >50% ipsilateral ICA stenosis.. Alternately, an age dependent cut-off for absolute maximal wall thickness may be considered to correct for differences in CCA diameter (Engelen et al. 2013; Engelen et al. 2015). However, our population has a wide diameter distribution (8083±1048 μm; range 5769-11702 μm), which cannot be explained by age differences only (68±9 yrs; range 39-88 yrs). Since the vessel diameter depends on subject size, and diameter and wall thickness are interrelated via the Lamé's equation (Liang et al. 2001; Nichols et al. 2011), it seems more reasonable to use normalized rather than absolute maximal wall thickness values.

Wall thickness parameters and ipsilateral stenosis degree

High relative IMT inhomogeneity and high thickness-to-diameter ratio are both associated with a higher degree of ICA stenosis (mean difference 6% and 7%, respectively, Student t-test p-value<0.001). Since we look at local CCA features, the current p-value is lower than observed when the average relative IMT inhomogeneity of both CCAs is considered (Steinbuch et al. 2016b). Because maximal wall thickness and thickness-to-diameter ratio are highly correlated with absolute and relative IMT inhomogeneity (Figure 2) and similar trends are observed in relation to degree of stenosis, absolute or relative IMT inhomogeneity does not provide extra information on top of maximal wall thickness or thickness-to-diameter ratio. Mainly the presence of a CCA plaque dominates the association with a higher degree of ICA stenosis (mean difference 7%, Student t-test p-value<0.001).

Plaques and wall thickness

Almost all CCAs with plaques according to the Mannheim consensus have a high maximal wall thickness and thickness-to-diameter ratio according to the cut-off derived with the ROC. Our population has a high incidence of CCA plaques (140 of 371 arteries; 38%). The presence of CCA plaques is rare in a healthy population, male 6% and female 3% (Johnsen et al. 2007), and is more prevalent (22%) in older subjects (>65 yrs) (Scuteri et al. 2009). The relatively high incidence of CCA plaques in our population is attributable to the fact that subjects exhibited cerebrovascular symptoms and, therefore, belong to a diseased population.

It is questionable whether IMT and plaque formation are driven by the same process. IMT is strongly associated with hypertension and age (Al-Shali et al. 2005) and is inheritable (Fox et al. 2003; Juo et al. 2004; Moskau et al. 2005). However, the heritability of plaque is less strong (Moskau et al. 2005) and attributed to various genes (Al-Shali et al. 2004; Moskau et al. 2005; Pollex and Hegele 2006). Furthermore, since the intima thickness is approximately only 0.02 mm (Salonen and Salonen 1993), IMT is mainly affected by hypertensive medial hypertrophy (Spence 2006) whereas atherosclerosis is an inflammatory process where plaque formation starts with pathological intimal thickening and lesions containing lipid pools (Finn et al. 2010). Therefore, IMT and plaque formation are likely different phenotypes (Spence and Hegele 2004; Hegele et al. 2005; Spence 2008). Our study shows that the association between ICA stenosis and ipsilateral CCA plaques is highly significant (Table 3), which is in line with the concept of atherosclerosis as a more widespread instead of a focal disease, prompting a global rather than a focused vascular examination. Whether elevated CCA wall parameters are present before development of an ICA stenosis cannot be established in our study.

Conclusion

In conclusion, to evaluate wall thickness it is more reasonable to normalize maximal wall thickness by end-diastolic diameter rather than by IMT, suggesting a modification of the Mannheim criteria. Absolute or relative IMT inhomogeneity does not provide extra information on top of maximal wall thickness or thickness-to-diameter ratio. Mainly CCA plaques are strongly associated with a higher degree of ipsilateral ICA stenosis. Although a similar trend is seen for both absolute maximal wall thickness and thickness-to-diameter ratio, 55 arteries (15%) are reclassified when thickness-to-diameter ratio instead of absolute maximal wall thickness is used as risk marker for a >50% ICA stenosis. Whether this reclassification is clinically important and relative IMT inhomogeneity and thickness-to-diameter ratio have predictive value for plaque progression and cerebrovascular events will be evaluated in the follow-up phase of the PARISK study.

References

Ahmed SA, Giddens DP. Flow disturbance measurements through a constricted tube at moderate Reynolds numbers. J Biomech 1983;16:955-963.

Al-Shali K, House AA, Hanley AJ, Khan HM, Harris SB, Mamakeesick M, Zinman B, Fenster A, Spence JD, Hegele RA. Differences between carotid wall morphological phenotypes measured by ultrasound in one, two and three dimensions. Atherosclerosis 2005;178:319-325.

Al-Shali KZ, House AA, Hanley AJ, Khan HM, Harris SB, Zinman B, Mamakeesick M, Fenster A, Spence JD, Hegele RA. Genetic variation in PPARG encoding peroxisome proliferator-activated receptor gamma associated with carotid atherosclerosis. Stroke 2004;35:2036-2040.

Bots ML, den Ruijter HM. Variability in the intima-media thickness measurement as marker for cardiovascular risk? Not quite settled yet. Cardiovasc Diagn Ther 2012;2:3-5.

Davidson MH, Rosenson RS, Maki KC, Nicholls SJ, Ballantyne CM, Mazzone T, Carlson DM, Williams LA, Kelly MT, Camp HS, Lele A, Stolzenbach JC. Effects of fenofibric acid on carotid intima-media thickness in patients with mixed dyslipidemia on atorvastatin therapy: randomized, placebo-controlled study (FIRST). Arterioscler Thromb Vasc Biol 2014;34:1298-1306.

Engelen L, Bossuyt J, Ferreira I, van Bortel LM, Reesink KD, Segers P, Stehouwer CD, Laurent S, Boutouyrie P. Reference values for local arterial stiffness. Part A. Journal of Hypertension 2015;33:1981-1996.

Engelen L, Ferreira I, Stehouwer CD, Boutouyrie P, Laurent S, Reference Values for Arterial Measurements C. Reference intervals for common carotid intima-media thickness measured with echotracking: relation with risk factors. Eur Heart J 2013;34:2368-2380.

European Carotid Surgery Trialists' Collaborative G. Randomised trial of endarterectomy for recently symptomatic carotid stenosis: final results of the MRC European Carotid Surgery Trial (ECST). The Lancet 1998;351:1379-1387.

Finn AV, Kolodgie FD, Virmani R. Correlation between carotid intimal/medial thickness and atherosclerosis: a point of view from pathology. Arterioscler Thromb Vasc Biol 2010;30:177-181.

Fox CS, Polak JF, Chazaro I, Cupples A, Wolf PA, D'Agostino RA, O'Donnell CJ. Genetic and Environmental Contributions to Atherosclerosis Phenotypes in Men and Women: Heritability of Carotid Intima-Media Thickness in the Framingham Heart Study. Stroke 2003;34:397-401.

Gaarder M, Seierstad T. Measurements of carotid intima media thickness in non-invasive high-frequency ultrasound images: the effect of dynamic range setting. Cardiovasc Ultrasound 2015;13:5.

Gijsen FJ, Palmen DE, van der Beek MH, van de Vosse FN, van Dongen ME, Janssen JD. Analysis of the axial flow field in stenosed carotid artery bifurcation models--LDA experiments. J Biomech 1996;29:1483-1489.

Graf IM, Schreuder FH, Hameleers JM, Mess WH, Reneman RS, Hoeks AP. Wall irregularity rather than intima-media thickness is associated with nearby atherosclerosis. Ultrasound Med Biol 2009;35:955-961.

Hegele RA, Al-Shali K, Khan HMR, Hanley AJG, Harris SB, Mamakeesick M, Zinman B, Fenster A, Spence JD, House AA. Carotid Ultrasound in One, Two and Three Dimensions. Vasc Dis Prev 2005;2:87-91.

Huang Y, Li W, Dong L, Li R, Wu Y. Effect of statin therapy on the progression of common carotid artery intima-media thickness: an updated systematic review and meta-analysis of randomized controlled trials. J Atheroscler Thromb 2013;20:108-121.

Ishigaki Y, Kono S, Katagiri H, Oka Y, Oikawa S, investigators N. Elevation of HDL-C in response to statin treatment is involved in the regression of carotid atherosclerosis. J Atheroscler Thromb 2014;21:1055-1065.

Ishizu T, Ishimitsu T, Kamiya H, Seo Y, Moriyama N, Obara K, Watanabe S, Yamaguchi I. The correlation of irregularities in carotid arterial intima-media thickness with coronary artery disease. Heart Vessels 2002;17:1-6.

Johnsen SH, Mathiesen EB, Joakimsen O, Stensland E, Wilsgaard T, Lochen ML, Njolstad I, Arnesen E. Carotid atherosclerosis is a stronger predictor of myocardial infarction in women than in men: a 6-year follow-up study of 6226 persons: the Tromso Study. Stroke 2007;38:2873-2880.

Juo SH, Lin HF, Rundek T, Sabala EA, Boden-Albala B, Park N, Lan MY, Sacco RL. Genetic and environmental contributions to carotid intima-media thickness and obesity phenotypes in the Northern Manhattan Family Study. Stroke 2004;35:2243-2247.

Liang YL, Shiel LM, Teede H, Kotsopoulos D, McNeil J, Cameron JD, McGrath BP. Effects of Blood Pressure, Smoking, and Their Interaction on Carotid Artery Structure and Function. Hypertension 2001;37:6-11.

Moskau S, Golla A, Grothe C, Boes M, Pohl C, Klockgether T. Heritability of carotid artery atherosclerotic lesions: an ultrasound study in 154 families. Stroke 2005;36:5-8.

Nichols WW, O'Rourke MF, Vlachopoulos C. McDonald's blood flow in arteries : theoretic, experimental, and clinical principles. 6th. Hodder Arnold, London, 2011.

Oyama J, Murohara T, Kitakaze M, Ishizu T, Sato Y, Kitagawa K, Kamiya H, Ajioka M, Ishihara M, Dai K, Nanasato M, Sata M, Maemura K, Tomiyama H, Higashi Y, Kaku K, Yamada H, Matsuhisa M, Yamashita K, Bando YK, Kashihara N, Ueda S, Inoue T, Tanaka A, Node K, Investigators PS. The Effect of Sitagliptin on Carotid Artery Atherosclerosis in Type 2 Diabetes: The PROLOGUE Randomized Controlled Trial. PLoS Med 2016;13:e1002051.

Pollex RL, Hegele R. Genetic determinants of carotid ultrasound traits. Curr Atheroscler Rep 2006;8:206-215.

Qu B, Qu T. Causes of changes in carotid intima-media thickness: a literature review. Cardiovasc Ultrasound 2015;13:46.

Saba L, Meiburger KM, Molinari F, Ledda G, Anzidei M, Acharya UR, Zeng G, Shafique S, Nicolaides A, Suri JS. Carotid IMT variability (IMTV) and its validation in symptomatic versus asymptomatic Italian population: can this be a useful index for studying symptomaticity? Echocardiography 2012;29:1111-1119.

Salonen JT, Salonen R. Ultrasound B-mode imaging in observational studies of atherosclerotic progression. Circulation 1993;87:II56-65.

Scuteri A, Najjar SS, Orru M, Albai G, Strait J, Tarasov KV, Piras MG, Cao A, Schlessinger D, Uda M, Lakatta EG. Age- and gender-specific awareness, treatment, and control of cardiovascular risk factors and subclinical vascular lesions in a founder population: the SardiNIA Study. Nutr Metab Cardiovasc Dis 2009;19:532-541.

Spence JD. Technology Insight: ultrasound measurement of carotid plaque--patient management, genetic research, and therapy evaluation. Nat Clin Pract Neurol 2006;2:611-619.

Spence JD. The importance of distinguishing between diffuse carotid intima-media thickening and focal plaque. Can J Cardiol 2008;24:61C-64C.

Spence JD, Hegele RA. Noninvasive phenotypes of atherosclerosis: similar windows but different views. Stroke 2004;35:649-653.

Steinbuch J, Hoeks AP, Hermeling E, Truijman MT, Schreuder FH, Mess WH. Standard B-Mode Ultrasound Measures Local Carotid Artery Characteristics as Reliably as Radiofrequency Phase Tracking in

Symptomatic Carotid Artery Patients. Ultrasound Med Biol 2016a;42:586-595.

Steinbuch J, van Dijk AC, Schreuder FH, Truijman MT, de Rotte AA, Nederkoorn PJ, van der Lugt A, Hermeling E, Hoeks AP, Mess WH. High Spatial Inhomogeneity in the Intima-Media Thickness of the Common Carotid Artery is Associated with a Larger Degree of Stenosis in the Internal Carotid Artery: The PARISK Study. Ultraschall Med 2016b;

Touboul PJ, Hennerici MG, Meairs S, Adams H, Amarenco P, Bornstein N, Csiba L, Desvarieux M, Ebrahim S, Hernandez Hernandez R, Jaff M, Kownator S, Naqvi T, Prati P, Rundek T, Sitzer M, Schminke U, Tardif JC, Taylor A, Vicaut E, Woo KS. Mannheim carotid intima-media thickness and plaque consensus (2004-2006-2011). An update on behalf of the advisory board of the 3rd, 4th and 5th watching the risk symposia, at the 13th, 15th and 20th European Stroke Conferences, Mannheim, Germany, 2004, Brussels, Belgium, 2006, and Hamburg, Germany, 2011. Cerebrovasc Dis 2012;34:290-296.

Truijman MT, Kooi ME, van Dijk AC, de Rotte AA, van der Kolk AG, Liem MI, Schreuder FH, Boersma E, Mess WH, van Oostenbrugge RJ, Koudstaal PJ, Kappelle LJ, Nederkoorn PJ, Nederveen AJ, Hendrikse J, van der Steen AF, Daemen MJ, van der Lugt A. Plaque At RISK (PARISK): prospective multicenter study to improve diagnosis of high-risk carotid plaques. Int J Stroke 2014;9:747-754.

6

Spatial inhomogeneity of diastolic-systolic risetime of the distension waveform in the common carotid artery is associated with lipid-rich necrotic core in distal plaques: The Plaque At RISK (PARISK) study

Steinbuch J, Schreuder FHBM, Truijman MTB, Hendrikse J, Nederkoorn PJ, Van der Lugt A, Kooi ME, Hoeks APG, Mess WH. Spatial inhomogeneity of diastolic-systolic risetime of the distension waveform in the common carotid artery is associated with lipid-rich necrotic core in distal plaques: The Plaque At RISK (PARISK) study (submitted).

Abstract

Purpose

Diastolic-systolic risetime characteristics of the distension waveform distribution might be modified by pressure wave reflections from distal plaques. We investigated the association between risetime characteristics of the common carotid artery (CCA) and the internal carotid artery (ICA) plaque properties.

Materials and Methods

The distension waveform distribution, derived from B-mode ultrasound CCA recordings of patients with symptomatic mild-to-moderate ICA stenosis, provided the risetime inhomogeneity. 3T-MRI was used to determine plaque composition: lipid-rich necrotic core (LRNC), intraplaque hemorrhage (IPH), and thin/ruptured fibrous cap (TRFC). Degree of stenosis was determined by CT-angiography.

Results

211 patients were included. CCA risetime inhomogeneity did not vary with stenosis degree nor with IPH ($p=0.99$ and 0.3, respectively). Compared to stable plaques, risetime inhomogeneity was significantly lower for plaques with a TRFC or LRNC ($p=0.012$ and 0.045, respectively). Furthermore, risetime inhomogeneity was significantly lower for patients with a LRNC (>10%) in the proximal part of the plaque than for patients without LRNC ($p=0.002$) and equal for contralateral sides without substantial stenosis (<30%; $p=0.36$).

Conclusion

CCA risetime inhomogeneity is significantly lower for vulnerable ICA plaques (LRNC>10% and TRFC) as compared with stable plaques, indicating a cushioning effect on wave reflection. This might offer a non-invasive and inexpensive method to characterize the nature of distal plaques.

Introduction

In Europe, around 1.1 million people die annually of stroke, the second most common cause of death (Nichols 2012). Rupture of atherosclerotic plaques in the supplying internal carotid artery (ICA), and subsequently embolism to the brain, plays an important role in the pathogenesis of ischemic strokes. Vulnerable plaques are characterized by a lipid-rich necrotic core (LRNC), intraplaque hemorrhage (IPH) and/or a thin or ruptured fibrous cap (TRFC) (Naghavi et al. 2003) and are associated with an increased risk of future ischemic events (Gupta et al. 2013). Therefore, identifying vulnerable plaques might contribute to treatment optimization for individual patients.

Despite the fact that vulnerable plaques have a higher risk for rupture, it remains unclear why. Mechanical plaque characteristics in combination with mechanical load exerted by blood pressure play important roles in plaque rupture. Due to pressure wave reflections the pulse pressure proximal to and across the stenosis will increase. In addition, due to the Venturi effect, an increase of local blood velocity caused by a smaller lumen area at the stenosis is accompanied with a decrease in local blood pressure (Holen et al. 1987; Xu et al. 2016); the transmural blood pressure gradient is reduced or even reversed (Hoeks et al. 2008; Xu et al. 2016). The pressure wave reflections in combination with the inwards directed transmural blood pressure gradient and plaque composition may lead to plaque deformation, subsequent plaque fissuring, intraplaque hemorrhage, and eventually plaque rupture (Hoeks et al. 2008; Xu et al. 2016). Since pressure wave reflections play a role in plaque rupture and may be modulated by degree of luminal obstruction and plaque composition, wave reflection parameters might identify plaque vulnerability.

We hypothesize that pressure wave reflections, originating from an ICA plaque, affect the distension waveform distribution as observed at a more proximal location, e.g., the ipsilateral common carotid artery (CCA). Particularly, the distension amplitude and the diastolic-systolic risetime mean and inhomogeneity across the distension waveform distribution might be affected.

The aim is to investigate the association between the characteristics of the distension waveform distribution observed in the CCA and degree of stenosis and plaque composition (presence of LRNC, IPH and/or TRFC) of plaques located distally. More specifically, we will evaluate 1) median distension, 2) median diastolic-systolic risetime and 3) spatial inhomogeneity of diastolic-systolic risetime.

Methods

Study subjects

In total, 240 patients who recently (<3 months) had an ischemic stroke, transient ischemic attack (TIA) or amaurosis fugax and an ipsilateral mild-to-moderate carotid artery stenosis (<70% according to NASCET criteria (North American Symptomatic Carotid Endarterectomy Trial 1991)) were included in the multicenter Plaque At RISK (PARISK) study (clinical trials.gov NCT01208025) (Truijman et al. 2014). The study is composed of a baseline and a 2-year follow-up assessment and was approved by the Medical Ethics Committees of all centers involved. All patients gave written informed consent. The present evaluation pertains only to the baseline characteristics.

Ultrasound data acquisition

Both the ipsilateral (i.e. symptomatic) and contralateral CCAs of 233 patients were recorded in duplicate with standard ultrasound B-mode (40 mm, 5 s, approximately 37 fps) at antero- and posterolateral angles with a Philips iU22 scanner (Philips Medical Systems, Bothell, USA) using different probes (17-5 MHz, 12-5 MHz or 9-3 MHz) depending on the depth of the scanned artery. All patients lay in supine position with their head slightly turned away from the examined side.

Edge detection

Distension waveforms were extracted by edge detection with dedicated software developed by MUMC (Maastricht University Medical Centre, Maastricht, The Netherlands) (Steinbuch et al. 2016a). For arterial wall detection, an artery region of sufficient quality was divided into approximately 15 half-overlapping segments (width 3.7 mm). Wall detection of the anterior and posterior media-adventitia transition was performed using a threshold of 65% of the maximal adventitia grey value (or 83% in case of an echogenic intima boundary) (Steinbuch et al. 2016b). For each segment, the local diameter was defined as the difference between the media-adventitia transition of the anterior and posterior walls. Wall detection was repeated for each frame providing a diameter and distension waveform distribution along the artery over a few cardiac cycles.

Distension waveforms of all segments were smoothed in time with a zero phase 4th order Butterworth lowpass filter with a 6 Hz cut-off (response time 54 ms). All distension waveforms were interpolated in time with a factor 25, resulting in a sample point distance of approximately 1 ms. The spatial average of the distribution allowed identification of the end-diastolic and systolic frames, and, hence, the distension defined as the change from end-diastolic to systolic diameter. The distension was averaged over all segments and heart beats (median). Since a distension below 2% relative to the diameter is rare according to reference values (Engelen et al. 2015), segments with a value lower than 2% were excluded for further analyses. The diastolic-systolic risetime was defined as the time difference between the 20% and 80% of the diastolic-systolic upstroke in the distension waveforms (Figure 1) with linear interpolation between sample values. The risetime for each segment was averaged over heart beats (median). The median and spatial standard deviation of the risetime over all segments provided the median risetime and its inhomogeneity. Precision was calculated as the standard deviation of differences between the values obtained in duplicate recordings and their average.

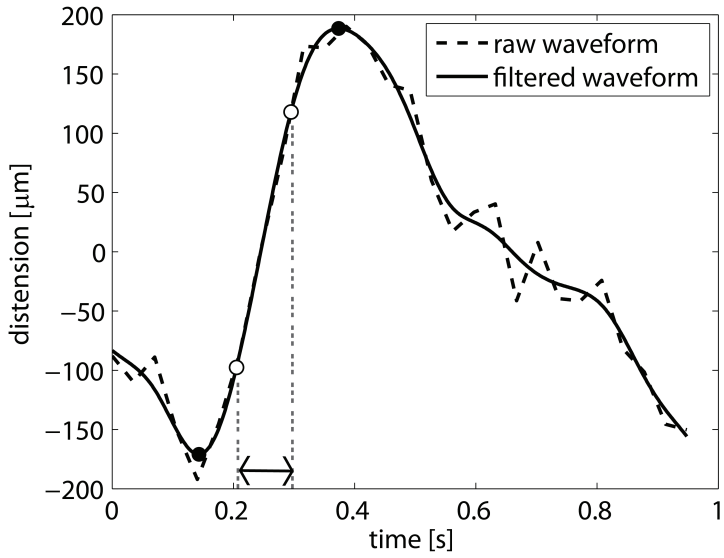

Figure 1

Raw and zero-phase filtered distension waveform (one heartbeat of one segment) as function of time. Black dots indicate minimum and maximum distension and white dots indicate 20 and 80% levels of the distension upstroke. Risetime is defined as the time difference between 20 and 80% of the distension upstroke, as indicated by the arrows.

MRI analysis of plaque composition

To determine plaque composition, 229 of the 240 patients (limited due to contra-indications) got a 3T magnetic resonance imaging (3T-MRI) scan of the ipsilateral ICA (Achieva or Ingenia; Philips Healthcare, Best, The Netherlands, or Discovery MR750 system; GE Healthcare, Milwaukee, WI) using a dedicated phased-array carotid coil (Shanghai Chenguang Medical Technologies Co, Shanghai China or Machnet B.V., Roden, The Netherlands). A standardized protocol for carotid plaque MRI was used (Truijman et al. 2014) to determine plaque components (LRNC, IPH and TRFC) according to previously described criteria (Cai et al. 2005; Cappendijk et al. 2008; Kwee et al. 2009). Multiple trained observers scored plaque components on a per-slice basis using vessel wall analysis software (VesselMASS; Leiden University Medical Center, Leiden, the Netherlands), blinded for the ultrasound results. LRNC and IPH were classified as either "present" or "not present". FC status was classified as "thick and intact" or "thin and/or ruptured". In addition, by dividing the plaque defined by the slices with a vessel wall thickness larger than 2 mm into three equal parts in a longitudinal direction, the proximal LRNC area was determined by the sum of LRNC areas across all MRI slices of the proximal part of the plaque. The relative LRNC size (%) was defined as the LRNC area divided by the cumulative area.

MDCTA analysis of degree of ICA stenosis

To determine the degree of ICA stenosis, 201 of the 240 patients (limited due to contra-indications) got a multidetector computed tomography angiogram (MDCTA). The ipsilateral (i.e. symptomatic) and contralateral degree of ICA stenosis was determined using the European Carotid Surgery Trial (ECST) criteria (European Carotid Surgery Trialists' Collaborative 1998) on a Siemens workstation by a trained observer blinded to the MRI and ultrasound results.

Statistical analysis

The risetime inhomogeneity of the contralateral CCA in patients with less than 30% degree of contralateral ICA stenosis was considered as baseline reference level. A Student t-test was used to assess the relations between median distension, risetime and its inhomogeneity, degree of ICA stenosis (50% ECST as threshold since <50% hardly induce hemodynamic changes) and plaque composition (LRNC, IPH and TRFC). Furthermore, a Student t-test and ANOVA were used to assess the relationship between the spatial risetime inhomogeneity and the proximal LRNC size using either a threshold (10% LRNC size)or LRNC percentage. Values are quantified as mean ± standard variation (SD). Significance level is set at $p<0.05$.

Results

In total, 224 patients underwent both an ultrasound and MRI examination of the ipsilateral (symptomatic) carotid artery. After exclusion due to insufficient quality (US: N=4; MRI: N=4) or technical recording failure (US: N=4; MRI: N=1), US and MRI recordings of 211 patients were available for further analysis. The degree of stenosis was available in a subset of patients (N=178). Baseline patient characteristics are shown in Table 1. Intra-subject precision and mean of distension waveform characteristics are given in Table 2. Median diameter and distension were similar across centers (ANOVA p-value 0.9 and 0.2, respectively). For one center the median risetime and inhomogeneity was significantly lower (largest mean difference 10 ms and 5 ms, ANOVA Bonferroni corrected p-value<0.001 and 0.006, respectively).

64% of the plaques (N=134) in the ipsilateral ICA had an LRNC of which 63% (N=84) had a TRFC and 62% (N=83) included IPH. TRFC could not be determined in 7 patients. An LRNC was found in the proximal part of the plaque in 48% of the patients (N=101). 36% of the patients (N=76) also had an ipsilateral CCA plaque. Median CCA distension and median diastolic-systolic risetime did not vary with ICA plaque composition (Table 3; p-value>=0.2) nor with the degree of ICA stenosis (Table 4; p-value>0.7).

33 patients (16%) had a small or no plaque (<30% ECST) at the contralateral ICA. For those patients, risetime inhomogeneity of the contralateral CCA was approximately 15±6 ms (Table 3), providing a baseline reference level for risetime inhomogeneity. Plaques without LRNC induced a significantly higher risetime inhomogeneity than plaques with LRNC: mean difference 2.7 ms; p=0.045 (Table 3). Moreover, patients with a thick fibrous cap had a significantly higher risetime inhomogeneity than patients with a TRFC: mean difference 3.4 ms; p=0.012. On the other hand, CCA risetime inhomogeneity was similar for ICA plaques with or without IPH (mean difference 1.4 ms; p=0.3) and similar for patients with or without CCA plaques (mean difference 1.5 ms; p=0.28).

Table 1

Patient characteristics. Values are presented as mean ± standard deviation (range or N).

N	211
Age [years]	69±9 (39-89)
Male [%]	69 (N=146)
BMI [kg/m²]	27±4 (17-42)
Systolic blood pressure (during US) [mmHg]	142±19 (97-210)
Diastolic blood pressure (during US) [mmHg]	79±10 (54-105)
Pulse pressure (during US) [mmHg]	63±16 (27-117)
Type of cerebrovascular event Stroke/TIA/amaurosis fugax [%]	45/44/11 (N=94/93/24)
Current smoking [%]	23 (N=48)
Diabetes Mellitus [%]	21 (N=44)
Hypercholesterolemia [%]	53 (N=112)
Hypertension [%]	62 (N=130)

Table 2

Wall characteristics for the ipsilateral CCA of all patients. Intra-subject precision is defined as the standard deviation of differences between the mean and all recordings. Values are presented as mean ± standard deviation (range).

	N	211
End-diastolic Diameter [μm]	Intra-subject precision	185
	Diameter	8150±1007 (5847-11567)
Relative distension [%]	Intra-subject precision	0.7
	Distension	5±1.6 (2-11)
Risetime [ms]	Intra-subject precision	7
	Risetime	96±14 (63-158)
Risetime inhomogeneity [ms]	Intra-subject precision	6
	Inhomogeneity	17±9 (4-73)

Table 3

Waveform characteristics in relation to composition of the whole plaque. Values are presented as mean ± standard deviation.

	Cont. side	Lipid-rich necrotic core (LRNC)			Intraplaque hemorage (IPH)			Fibrous cap (FC)		
	<30% degree	LRNC	No LRNC	p-value	IPH	No IPH	p-value	Thin FC	Thick FC	p-value
N	33	134	77		83	128		84	120	
Relative median distension [μm]	5.3±1.3	5.2±1.6	5.1±1.7	0.98	5.1±1.6	5.2±1.6	0.81	5.1±1.6	5.2±1.6	0.89
Median Risetime [ms]	93±15	95±15	97±12	0.42	96±16	96±13	0.84	94±15	96±13	0.29
Risetime inhomogeneity [ms]	15±6	16±8	18±11	0.045	16±8	17±10	0.29	14±8	18±10	0.012

Table 4

Waveform characteristics in relation to degree of stenosis. Values are presented as mean ± standard deviation.

	Cont. side	Ipsilateral side		
	<30% degree	**<50% degree**	**>50% degree**	**p-value**
N	33	63	115	
Relative median distension [μm]	5.3±1.3	5.2±1.4	5.2±1.8	0.72
Median Risetime [ms]	93±15	96±12	95±15	0.79
Risetime inhomogeneity [ms]	15±6	16±8	16±9	0.99

Patients with a large proximal LRNC (>10%, N=50) had a significantly lower risetime inhomogeneity than patients without or with a small LRNC (<=10% LRNC, N=161): mean difference 3.7 ms; p=0.002 (Figure 2). This association remained significant when only patients with more than 50% ICA stenosis were selected (mean difference 3.9 ms; p=0.008). Compared to the reference group, i.e., patients with less than 30% stenosis at the contralateral ICA, the CCA risetime inhomogeneity of patients with or without proximal LRNC was similar (mean difference 1.3 ms; p=0.36), respectively borderline (mean difference 2.4 ms; p=0.085). Combining a TRFC and proximal LRNC (>10%) results in the largest difference in risetime inhomogeneity compared to a stable ICA plaque (without proximal LRNC and thick fibrous cap): 14±6 ms and 18±11 ms, respectively, mean difference 4.4 ms; p=0.001. The relation between a decline in risetime inhomogeneity and the area percentage of proximal LRNC, as may be apparent from Figure 3, was not significant (Table 5; ANOVA p-value=0.06), indicating the inhomogeneity reached its baseline level for contents exceeding 10%.

Table 5

Risetime inhomogeneity in relation to the size of proximal LRNC (%) in distal plaque. Values are presented as mean ± standard deviation.

Proximal LRNC	**0%**	**0-10%**	**10-30%**	**>30%**	**p-value**
N	108	53	35	15	ANOVA
Risetime inhomogeneity [ms]	18±11	16±9	13±6	15±6	0.06

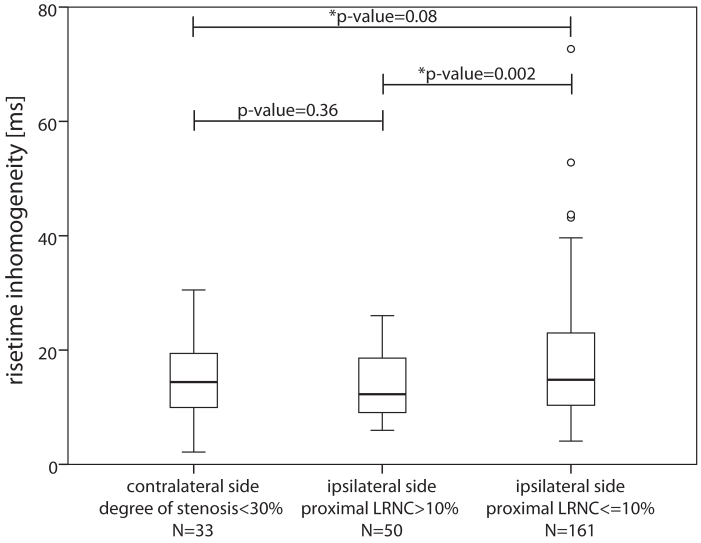

Figure 2

Boxplot of the risetime inhomogeneity for contralateral CCA arteries (left) with less than 30% ICA stenosis (reference artery), and for ipsilateral arteries with more (center) or less (right) than 10% proximal LRNC in the ICA plaque. The risetime inhomogeneity of the CCA distension waveform distribution is significantly lower for patients with LRNC than for patients with no or small LRNC size in the proximal part of the ICA plaque. No significant difference was found between arteries with proximal LRNC at ipsilateral side and the reference artery.

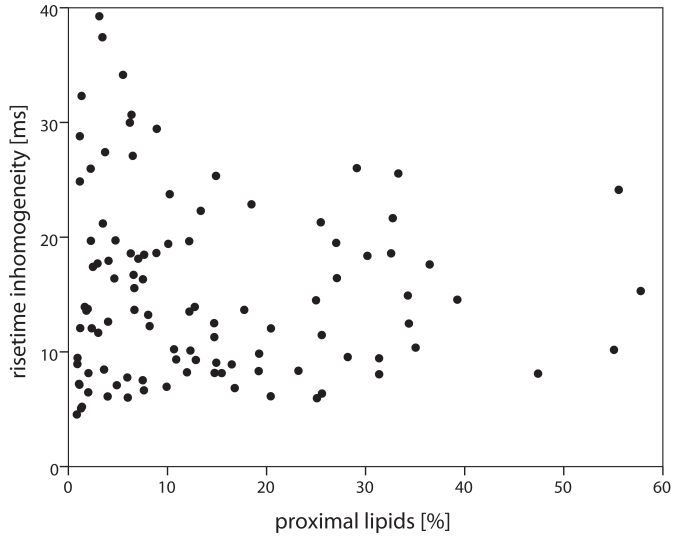

Figure 3

Risetime inhomogeneity in the common carotid artery in relation to the size of LRNC in the proximal part of the ICA plaque. It should be noted that only plaques with proximal LRNC were taken into account. Risetime inhomogeneity seems to decline with proximal LRNC, but this relationship is not significant for content exceeding 10%.

Discussion

Median CCA distension and median risetime are not associated with stenosis degree nor the composition of ipsilateral ICA plaques. However, the current study demonstrates that CCA risetime inhomogeneity is significantly lower for ICA plaques with an LRNC or with a TRFC. Moreover, the association is even stronger if specifically plaques with a large proximal LRNC (>10%) or a combination of vulnerable plaque features (plaques with a proximal LRNC and TRFC) are considered. However, there is no trend between the proximal LRNC size and risetime inhomogeneity, indicating the latter is at its baseline reference if the LRNC size exceeds 10%. Only stable plaques without LRNC induce risetime inhomogeneity while LRNC within the ICA plaque, especially in its proximal part, has a cushioning effect on wave reflection.

Median risetime and its inhomogeneity were significantly lower for one center (ANOVA p-value Bonferroni corrected: <0.001 and 0.006, respectively). Only 20% of the patients in this center had a stable plaque (no LRNC), which could explain differences with other centers.

Because the intra-subject reference is composed of contralateral arteries with less than 30% stenosis, wave reflections will be limited. The CCA risetime inhomogeneity of the reference artery is of the same order as for ipsilateral plaques with a large proximal LRNC (Figure 2). ICA plaques with small LRNC induce a significantly higher CCA risetime inhomogeneity than plaques with large proximal LRNC (Figure 2). Proximal LRNC appears to be more important for the risetime inhomogeneity than LRNC of the whole plaque, possibly because the former is the impact site of the pressure wave.

However, for the group with a large LRNC size (>10%) in the proximal part of an ICA plaque risetime inhomogeneity does not vary with the LRNC size (Table 5). This can be explained by the low number of patients with a large proximal LRNC in combination with a few outliers (Figure 3) dominating the standard deviation. More likely, the moderating effect of plaque LRNC size on the reflection wave and, hence, on CCA risetime inhomogeneity is quickly maximal as is corroborated by the similar inhomogeneity for the ipsilateral and the reference artery (Table 5, Figure 2 and 3).

An inhomogeneous distribution of distension waveforms, as observed in the CCA, may be caused by inhomogeneous local artery wall characteristics. Indeed we previously have shown that CCA wall thickness inhomogeneity is directly related to the presence of CCA plaques (Steinbuch et al. 2017). The present study demonstrates that CCA distension, risetime and risetime inhomogeneity are not associated with the CCA plaques. One would expect that the degree of ICA stenosis affects pressure wave reflection and, hence, the characteristics of the CCA distension distribution. However, we could not establish such an association, which may result from our population who only had a mild-to-moderate ICA stenosis (<70% according to NASCET criteria).

Risetime inhomogeneity is slightly lowered by an LRNC or TRFC (Table 3). However, we could not demonstrate an effect of IPH, which is another strong predictor of stroke recurrence (Altaf et al. 2007; Altaf et al. 2008; Gupta et al. 2013; Kwee et al. 2013; Saam et al. 2013). We believe that the absence of an association between risetime characteristics and IPH might be caused by the more diffuse distribution of IPH over the plaque instead of pooling in the proximal part (Saam et al. 2005; Cappendijk et al. 2008).

As an alternative to determine plaque composition and thereby plaque vulnerability with ultrasound, grey scale values of the plaque can be used. Echolucent plaques are associated with hemorrhage and LRNC (Gronholdt et al. 1997; Schulte-Altedorneburg et al. 2000). However, the grey scale median of a plaque on ultrasound is predominantly determined by the elastin and calcium content of the plaque (Goncalves et al. 2004) rather than LRNC or fibrous cap status. Since plaques with an LRNC and a TRFC are associated with an increased risk of future ischemic events (Gupta et al. 2013), risetime inhomogeneity might have more potential than grey scale values to identify non-invasively the plaque nature and thereby plaque vulnerability.

Our study has several possible limitations. First, risetime is often defined as the time difference between 10 and 90% of the diastolic upstroke in the distension waveform recorded at a high frame rate (>300 fps) (Hoeks et al. 1990). Since our ultrasound recordings are made at a lower frame rate (around 37 fps), the blurring effect of filter response time on transients in the distension derivative will be more pronounced. To exclude this filter effect, we decided to define the risetime as the time difference between 20 and 80% of the systolic upstroke.

Another limitation of this study is the absence of reference values for risetime inhomogeneity for an elderly healthy population. To compensate for this limitation, we considered as reference level the risetime inhomogeneity in the contralateral CCA in a subset of patients (<30% ICA stenosis). Disadvantages of this approach are a relatively small reference group suffering from atherosclerosis although the contralateral ICA stenosis is less than 30%.

In conclusion, CCA risetime inhomogeneity is significantly lower for vulnerable plaques (proximal LRNC>10% and/or TRFC) than for a stable plaque (proximal LRNC<10% and thick fibrous cap). This may indicate a cushioning effect of LRNC at the proximal part of a plaque on wave reflection and might offer a non-invasive and inexpensive additional diagnostic test to characterize the nature of a distally located plaque in patients with symptomatic carotid stenosis.

References

Altaf N, Daniels L, Morgan PS, Auer D, MacSweeney ST, Moody AR, Gladman JR. Detection of intraplaque hemorrhage by magnetic resonance imaging in symptomatic patients with mild to moderate carotid stenosis predicts recurrent neurological events. J Vasc Surg 2008;47:337-342.

Altaf N, MacSweeney ST, Gladman J, Auer DP. Carotid intraplaque hemorrhage predicts recurrent symptoms in patients with high-grade carotid stenosis. Stroke 2007;38:1633-1635.

Cai J, Hatsukami TS, Ferguson MS, Kerwin WS, Saam T, Chu B, Takaya N, Polissar NL, Yuan C. In vivo quantitative measurement of intact fibrous cap and lipid-rich necrotic core size in atherosclerotic carotid plaque: comparison of high-resolution, contrast-enhanced magnetic resonance imaging and histology. Circulation 2005;112:3437-3444.

Cappendijk VC, Heeneman S, Kessels AG, Cleutjens KB, Schurink GW, Welten RJ, Mess WH, van Suylen RJ, Leiner T, Daemen MJ, van Engelshoven JM, Kooi ME. Comparison of single-sequence T1w TFE MRI with multisequence MRI for the quantification of lipid-rich necrotic core in atherosclerotic plaque. J Magn Reson Imaging 2008;27:1347-1355.

Engelen L, Bossuyt J, Ferreira I, van Bortel LM, Reesink KD, Segers P, Stehouwer CD, Laurent S, Boutouyrie P. Reference values for local arterial stiffness. Part A. Journal of Hypertension 2015;33:1981-1996.

European Carotid Surgery Trialists' Collaborative G. Randomised trial of endarterectomy for recently symptomatic carotid stenosis: final results of the MRC European Carotid Surgery Trial (ECST). The Lancet 1998;351:1379-1387.

Goncalves I, Lindholm MW, Pedro LM, Dias N, Fernandes e Fernandes J, Fredrikson GN, Nilsson J, Moses J, Ares MP. Elastin and calcium rather than collagen or lipid content are associated with echogenicity of human carotid plaques. Stroke 2004;35:2795-2800.

Gronholdt ML, Wiebe BM, Laursen H, Nielsen TG, Schroeder TV, Sillesen H. Lipid-rich carotid artery plaques appear echolucent on ultrasound B-mode images and may be associated with intraplaque haemorrhage. Eur J Vasc Endovasc Surg 1997;14:439-445.

Gupta A, Baradaran H, Schweitzer AD, Kamel H, Pandya A, Delgado D, Dunning A, Mushlin AI, Sanelli PC. Carotid plaque MRI and stroke risk: a systematic review and meta-analysis. Stroke 2013;44:3071-3077.

Hoeks AP, Reesink KD, Hermeling E, Reneman RS. Local blood pressure rather than shear stress should be blamed for plaque rupture. J Am Coll Cardiol 2008;52:1107-1108; author reply 1108-1109.

Hoeks APG, Brands PJ, Smeets FAM, Reneman RS. Assessment of the Distensibility of Superficial Arteries. Ultrasound Med Biol 1990;16:121-128.

Holen J, Waag RC, Gramiak R. Doppler ultrasound in aortic stenosis: in vitro studies of pressure gradient determination. Ultrasound Med Biol 1987;13:321-328.

Kwee RM, van Engelshoven JM, Mess WH, ter Berg JW, Schreuder FH, Franke CL, Korten AG, Meems BJ, van Oostenbrugge RJ, Wildberger JE, Kooi ME. Reproducibility of fibrous cap status assessment of carotid artery plaques by contrast-enhanced MRI. Stroke 2009;40:3017-3021.

Kwee RM, van Oostenbrugge RJ, Mess WH, Prins MH, van der Geest RJ, ter Berg JW, Franke CL, Korten AG, Meems BJ, van Engelshoven JM, Wildberger JE, Kooi ME. MRI of carotid atherosclerosis to identify TIA and stroke patients who are at risk of a recurrence. J Magn Reson Imaging 2013;37:1189-1194.

Naghavi M, Libby P, Falk E, Casscells SW, Litovsky S, Rumberger J, Badimon JJ, Stefanadis C, Moreno P, Pasterkamp G, Fayad Z, Stone PH, Waxman S, Raggi P, Madjid M, Zarrabi A, Burke A, Yuan C, Fitzgerald PJ, Siscovick DS, de Korte CL, Aikawa M, Juhani Airaksinen KE, Assmann G, Becker CR, Chesebro JH, Farb A, Galis ZS, Jackson C, Jang IK, Koenig W, Lodder RA, March K, Demirovic J, Navab M, Priori SG, Rekhter MD, Bahr R, Grundy SM, Mehran R, Colombo A, Boerwinkle E, Ballantyne C, Insull W, Jr., Schwartz RS, Vogel R, Serruys PW, Hansson GK, Faxon DP, Kaul S, Drexler H, Greenland P, Muller JE,

Virmani R, Ridker PM, Zipes DP, Shah PK, Willerson JT. From vulnerable plaque to vulnerable patient: a call for new definitions and risk assessment strategies: Part I. Circulation 2003;108:1664-1672.

Nichols M, Townsend N, Luengo-Fernandez R, Leal J, Gray A, Scarborough P, Rayner M. European cardiovascular disease statistics 2012. European Heart Network, Brussels, European Society of Cardiology, Sophia Antipolis 2012;

North American Symptomatic Carotid Endarterectomy Trial C. Beneficial effect of carotid endarterectomy in symptomatic patients with high-grade carotid stenosis. N Engl J Med 1991;325:445-453.

Saam T, Ferguson MS, Yarnykh VL, Takaya N, Xu D, Polissar NL, Hatsukami TS, Yuan C. Quantitative evaluation of carotid plaque composition by in vivo MRI. Arterioscler Thromb Vasc Biol 2005;25:234-239.

Saam T, Hetterich H, Hoffmann V, Yuan C, Dichgans M, Poppert H, Koeppel T, Hoffmann U, Reiser MF, Bamberg F. Meta-analysis and systematic review of the predictive value of carotid plaque hemorrhage on cerebrovascular events by magnetic resonance imaging. J Am Coll Cardiol 2013;62:1081-1091.

Schulte-Altedorneburg G, Droste DW, Haas N, Kemeny V, Nabavi DG, Fuzesi L, Ringelstein EB. Preoperative B-mode ultrasound plaque appearance compared with carotid endarterectomy specimen histology. Acta Neurol Scand 2000;101:188-194.

Steinbuch J, Hoeks AP, Hermeling E, Truijman MT, Schreuder FH, Mess WH. Standard B-Mode Ultrasound Measures Local Carotid Artery Characteristics as Reliably as Radiofrequency Phase Tracking in Symptomatic Carotid Artery Patients. Ultrasound Med Biol 2016a;42:586-595.

Steinbuch J, Van Dijk AC, Schreuder FHBM, Truijman MTB, De Rotte AAJ, Nederkoorn PJ, Van der Lugt A, Hermeling E, Hoeks APG, Mess WH. High spatial inhomogeneity in intima-media thickness of the common carotid artery is associated with a larger degree of stenosis in the internal carotid artery: The PARISK study. Ultraschall Med 2016b;

Steinbuch J, van Dijk AC, Schreuder F, Truijman M, Hendrikse J, Nederkoorn PJ, van der Lugt A, Hermeling E, Hoeks A, Mess WH. Definition of common carotid wall thickness affects risk classification in relation to degree of internal carotid artery stenosis: the Plaque At RISK (PARISK) study. Cardiovasc Ultrasound 2017;15:9.

Truijman MT, Kooi ME, van Dijk AC, de Rotte AA, van der Kolk AG, Liem MI, Schreuder FH, Boersma E, Mess WH, van Oostenbrugge RJ, Koudstaal PJ, Kappelle LJ, Nederkoorn PJ, Nederveen AJ, Hendrikse J, van der Steen AF, Daemen MJ, van der Lugt A. Plaque At RISK (PARISK): prospective multicenter study to improve diagnosis of high-risk carotid plaques. Int J Stroke 2014;9:747-754.

Xu C, Yuan C, Stutzman E, Canton G, Comess KA, Beach KW. Quest for the Vulnerable Atheroma: Carotid Stenosis and Diametric Strain-A Feasibility Study. Ultrasound Med Biol 2016;42:699-716.a

7

Carotid plaques do not modify orthogonal adventitia-adventitia diameter while relative lumen distension is negatively associated with plaque echogenicity

Steinbuch J, Schreuder FHBM, Reesink KD, Hoeks APG, Mess WH. Carotid plaques do not modify orthogonal adventitia-adventitia diameter while relative lumen distension is negatively associated with plaque echogenicity (submitted)

Abstract

To properly assess morphological and dynamic parameters of arteries and plaques, we propose the concept of orthogonal distance measurements, i.e. perpendicularly to the local lumen axis rather than along the ultrasound beam (vertical direction for a linear array). The aim of this study is to compare the orthogonal and vertical lumen diameter at the site of the plaque and to investigate the interrelationship of orthogonal diameters and plaque size and the association of artery parameters with plaque echogenicity in the common carotid artery (CCA). In 29 patients a longitudinal B-mode US-recording was acquired of CCA plaques at the posterior wall. Following semi-automatic segmentation, parameters were extracted orthogonally along the lumen axis. To establish inter-observer variability of parameters obtained at the location of maximal plaque thickness, a second observer repeated the analysis (subset N=21). Orthogonal adventitia-adventitia and lumen diameter and distension could be determined with good precision (coefficient of variation: 1-5% and 21-50%, respectively). Orthogonal lumen diameter was significantly smaller than the vertical lumen diameter (p-value<0.001). Surprisingly, the CCA plaques in our population did not cause outward remodeling, i.e., a local increase in adventitia-adventitia distance. The intra- and inter-observer precision of plaque compression were poor and of the same order as the standard deviation of plaque compression. The orthogonal relative lumen distension was significantly lower for echogenic plaques, indicating a higher stiffness, than for echolucent plaques (p-value<0.01). In conclusion, we demonstrated the feasibility to extract orthogonal CCA and plaque dimensions, albeit that the proposed approach was inadequate to quantify plaque compression.

Introduction

Understanding of mechanical plaque properties would be beneficial to improve plaque risk assessment. In a stroke population, the adventitia-adventitia distension of the common carotid artery (CCA) and the internal carotid artery (ICA) at the stenotic side is significantly lower than at the contralateral side (Giannattasio et al. 2001), indicating a stiffer vessel. Furthermore, decreased distension at plaque location is associated with advanced plaques (containing a lipid core, hemorrhage, calcifications or thrombus), as characterized by MRI (Beaussier et al. 2011). A plaque induces pressure wave reflections (Nichols et al. 2011). Moreover, it will locally increase blood flow velocity and, thereby, wall shear stress, stimulating the endothelium to release vasodilators to restore local wall shear stress to normal level (Glagov et al. 1997; Samijo et al. 1998; Dammers et al. 2003). As a consequence, it is expected that the adventitia-adventitia diameter at the plaque is larger, which is referred to as outward remodeling. Indeed, patients with CCA plaques who have type 2 diabetes, dyslipidemia or hypertension are associated with a decreased adventitia-adventitia distension and larger adventitia-adventitia diameter at the CCA plaque (Paini et al. 2007; Beaussier et al. 2008).

In standard transcutaneous ultrasound applications, echoes and scattered signals from tissue transitions are received as function of depth. Therefore, distance or displacement measurements of echo transitions to quantify e.g. lumen diameter or wall thickness are performed along the ultrasound beam (vertical direction for a B-mode linear array image), also ensuring best depth resolution. For tissue structures parallel to the skin surface, e.g., the CCA, distance measurements along the ultrasound beam will hardly deviate from distance measurements along the radius, even for a deviation of 10 degrees from perpendicular insonation. However, for tortuous structures oriented oblique to the skin surface, e.g., the carotid bifurcation and ICA, distance and displacement measurements along the ultrasound beam increasingly lose their relevance depending on the angle between ultrasound beam and the orientation of the structure under examination. Especially the presence of plaques, where the local relevant tissue orientation may reach angles of 45 degrees with respect to the beam direction, may lead to large differences between orthogonal, i.e. perpendicularly to the local lumen axis, and perpendicular distance assessment.

For proper assessment of local adventitia-adventitia and lumen diameters and distensions, distances and displacements between echo transitions should preferentially be measured along the vessel radius, i.e., perpendicular to the local orientation of the blood vessel or lumen axis. In this study, we propose the concept of orthogonal distance measurements and apply it to morphological CCA (plaque) measurements. It is based on semi-automatic outlining of the anterior and posterior lumen-intima and media-adventitia transitions. , Subsequently based on an iterative search for the shortest cross-sectional diameter, the local radius orientation and associated distances are automatically extracted at an interspacing of 1 mm along the length of the vessel. The procedure is executed for the diastolic as well as the systolic images of a B-mode video providing estimates of diastolic to systolic changes.

The dynamic parameters, i.e., lumen and adventitia-adventitia distension and plaque compression, are likely influenced by plaque composition and the pressure wave. Plaque composition can be qualified by plaque echogenicity (Elatrozy et al. 1998; Kakkos et al. 2007), quantified by the (normalized) grey-scale median (GSM). Echolucent plaques are associated with increased risk of cerebrovascular events (Biasi et al. 1999; Gronholdt et al. 2001; Mathiesen et al. 2001; Topakian et al. 2011). Patients with recurrent ischemic events have a plaque with a large lipid core and lower echogenicity (Salem et al. 2012), while plaque echogenicity increases with time from stroke or transient ischemic attack (TIA) onset (Martinez-Sanchez et al. 2012). The latter has consequences for the local dynamic behavior of lumen and plaque.

The aim of this study is to introduce the concept of orthogonal measurements and to investigate the association between dynamic parameters and plaque echogenicity for plaques in the common carotid artery. More specifically, 1) we will evaluate the intra- and inter-observer precision of morphological/dynamic parameters, i.e., adventitia-adventitia diameter, lumen diameter and distension and plaque compression, 2) evaluate the difference between orthogonal and vertical mean lumen diameter along the plaque, 3) we will consider plaque thickness and compare parameters at the site of the plaque with those of the adjacent proximal or distal segments and 4) we will associate dynamic plaque parameters with normalized grey scale values specifically for plaques with a high echogenicity.

Methods

Study subjects

The Plaque At RISK (PARISK) study (clinical trials.gov NCT01208025) is an ongoing multi-center cohort study with 2-year follow-up (Truijman et al. 2014). The study was approved by the Medical Ethics Committees of the participating centers and all patients gave written informed consent. For the current substudy, we selected the B-mode ultrasound recordings of 29 patients (70±9 yrs) with at least one plaque present at the posterior wall in either left or right CCA.

Data acquisition

During the ultrasound examination, the patient lay in supine position with the head slightly tilted to the side opposite to the one investigated. A Philips iU22 scanner (Philips Medical Systems, Bothell, USA) with a 9-3 MHz linear array probe (width 40 mm), operating at a frame rate of approximately 40 frames per second, was used to locate the CCA plaque and to select a plane of observation with maximum plaque cross-section. Subsequently, a single longitudinal B-mode ultrasound recording of about 6 seconds was acquired. Subject characteristics and relevant clinical data (e.g., age, gender, clinical reason for ultrasound examination) were collected.

Image analysis: Manual edge tracking

To identify end-diastolic and systolic frames, an artery section proximal or distal to the plaque (or with a minimum of plaque interference) is selected. This section is divided into half-overlapping segments with a width of 2 mm which is on the order of 2 times the lateral ultrasound resolution (about 1.3 mm). The diameter waveform of each segment is extracted by automatic edge tracking of the media-adventitia transitions of the anterior and posterior wall using a threshold of 65% of the maximal grey value of the local adventitia, as previously described (Steinbuch et al. 2016a; Steinbuch et al. 2016b). The end-diastolic and systolic frames follow from the local minima and maxima of the spatial average of the diameter waveforms of all segments.

Before manual outlining an artery, image frames are interpolated by a factor of 2 in depth and width. Subsequently, the positions of the lumen-intima and media-adventitia transitions for both the anterior and posterior walls are manually identified (Fig.1) for the first diastolic frame at 1 mm spacing (note: smaller than the lateral resolution). Media-adventitia and lumen-intima transitions are smoothed with Savitsky-Golay filter of the 3rd order and with a span of seven wall markers (7 mm), providing continuous outlines (Figure 1). Next, a first guess is made for the adventitia-adventitia and lumen centerline by averaging corresponding anterior and posterior endpoints along the (vertical) depth axis. Subsequently, the anterior and posterior endpoints are shifted in opposite direction (diameter rotation) until the distance between anterior and posterior outlines reaches a minimum, providing the orthogonal orientation and orthogonal diameters. If either endpoint enters a margin of 3 mm at any side of the image segment, it is excluded. Finally, the centerlines are recalculated. The final result (Figure 1) serves as a template for the next frame which improves precision and reduces process time.

The local wall and (hence) plaque thickness is defined as the difference between the media-adventitia and lumen-intima transitions along the orthogonal orientation at both the anterior or posterior wall, respectively. The local orthogonal adventitia-adventitia and lumen distensions are the difference between corresponding orthogonal systolic and end-diastolic diameters. Relative distension is the ratio of distension and end-diastolic diameter. The diameter and distension are determined both at the location of maximal plaque thickness and over the entire image segment by taking the median over all orthogonal diameters or distensions.

The plaque compression at either anterior or posterior wall is defined as the difference between systolic and end-diastolic vessel wall thickness at the location of maximal plaque thickness. All parameters are averaged (median) over all available heart beats.

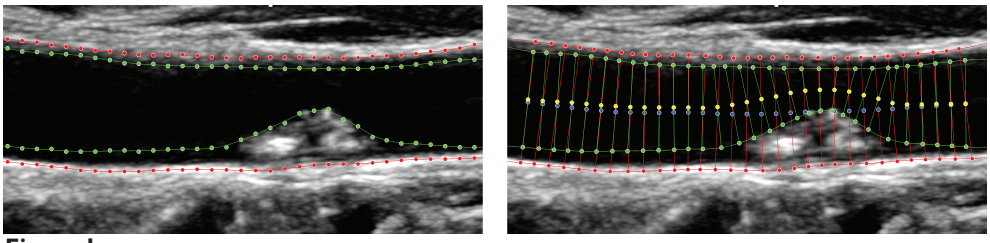

Figure 1

Manual outlining (left) at an interspacing of 1 mm of the anterior and posterior lumen-intima (green dots) and media-adventitia transitions (red dots) of a CCA plaque. Manual outlining (left) is followed by automatic extraction (right) of the local radius orientation (red and green lines) and associated distances using the lumen (yellow dots) or adventitia-adventitia centerlines (blue dots).

Grey-scale median analysis

Grey scale analysis is performed by a trained observer blinded for the results of artery outlining. At each end-diastolic and systolic frame, the plaque contour is manually segmented. For normalization, a reference box is positioned at the lumen-intima transition covering both the adventitia vessel wall and lumen. The grey value of the lumen within the reference box is set to 0 and the adventitia value is set to 199. Grey scale values of the plaque are normalized accordingly. The calcium content of the plaque likely determines most of the local vessel stiffness and is reflected by a higher echogenicity, quantified by the 75th percentile of the normalized grey value (GS75), and averaged (median) over all heartbeats.

Statistical analysis

Manual outlining of the CCA was performed twice by an observer without knowledge of the grey scale results. The analysis was repeated by a second observer for a subset of the patient population (N=21). Intra- and inter-observer precision of morphological and dynamic parameters, i.e., adventitia-adventitia and lumen diameters and distensions, and plaque compression, were quantified by the standard deviation of the differences between the observer and the assumed ground truth, i.e., the observed subject average. To compare the orthogonal and vertical lumen diameters along the plaque, the mean lumen diameter of the 40% smallest diameters along the radius of the CCA was calculated. Subsequently, the vertical lumen diameter was calculated for the same points. A paired t-test was used to compare the orthogonal and vertical lumen diameter and to compare the orthogonal diameter and plaque thickness with that of segments proximally or distally with an average intima-media thickness less than 1500 μm. The relation between parameters at maximal plaque thickness and the 75th percentile of the normalized grey scale value (GS75) was tested by Pearson correlation and Student t-test. Significance level was set at $p<0.05$. Values are presented as mean ± standard variation (SD).

Results

In total, 6 patients were excluded due to insufficient image quality (N=2), unclear media-adventitia wall because of a shadow (N=1) or out of plane motion of the plaque (N=3). In total, CCA images of 23 patients (age 70±9 yrs) were analyzed. The degree of stenosis according to the European Carotid Surgery Trial (ECST) criterion (European Carotid Surgery Trialists' Collaborative 1998) was 48±13%. Six patients (26%) had a plaque covering more than the width of the ultrasound image (40 mm). Patient characteristics are listed in Table 1. After exclusion of the 6 patients, the intra- and inter-observer precision was determined in 15 subjects of the selected subset (N=21).

Intra- and inter-observer precision

The mean morphological parameters and their intra- and inter-observer precision are shown in Table 2 and 3. The distribution of values observed over the entire ROI and at the site of the plaque does not show any trend with respect to the mean value observed by a single or both observers. The intra- and inter-observer precision of diameters is good (coefficient of variation: 1-5%) whereas the precision of distension is poor (coefficient of variation: 21-50%). Except for plaque compression, intra-observer precision of all parameters is considerably smaller than inter-observer precision. The intra- and inter-observer coefficient of variation (CV) of lumen diameter (2% and 5%) and distension (28% and 41%), as obtained over the entire region of interest, are larger than those of the adventitia-adventitia diameter (1% and 3%) and its distension (21% and 39%). Both intra- and inter-observer precision of adventitia-adventitia and lumen diameter and distension are smaller than the standard deviation of our patient population. However, intra- and inter-observer precision of plaque compression are higher than the mean compression and are of the same order as the standard deviation of plaque compression of our patient population. Therefore, plaque compression cannot be precisely determined and will not be considered for further analysis.

Table 1

Patient characteristics. Data are presented as mean ± standard deviation or number (%).

N	23
Age	70±9 years
Male	23 (66%)
Degree of stenosis	48±13%
Plaque location	
Posterior wall only	8 (35%)
Both walls	15 (65%)
Indication	
Stroke	7 (30%)
TIA	7 (30%)
Amaurosis fugax	1 (4%)
Other	8 (35%)

Orthogonal and vertical lumen diameter

The mean lumen diameter (smallest 40%) along the radius of the 23 patients is 4720±1176 µm whereas the lumen diameter along the ultrasound beam is 5344±1094 µm. Therefore, the orthogonal lumen diameter is significantly smaller than the vertical diameter (mean difference 625 µm, p-value<0.001) and reflects more properly local lumen narrowing, indicating the importance of orthogonal measurements.

Dynamic parameters at the CCA with and without plaque

Fourteen of the 23 patients had a mean posterior wall thickness lower than 1500 µm proximal as well as distal to the largest plaque. As expected, the end-diastolic lumen diameter at the plaque is significantly lower than proximal or distal to the plaque (Table 4; mean difference 1544 and 1903 µm, p-value=0.001 and <0.001, respectively). The end-diastolic adventitia-adventitia diameter at the plaque is significantly larger than at the CCA proximal to the plaque (mean difference 411 µm; p-value=0.009), suggesting outward remodeling. However, the end-diastolic adventitia-adventitia diameter at the CCA distal to the plaque is even borderline significantly larger than at the site of the plaque (mean difference 183 µm; p-value=0.087), which is in line with a diverging CCA towards the bifurcation and contradicting outward re-

Table 2

Intra-observer precision and mean values of diameter and distension estimates. Adventitia-adventitia and lumen diameters and distensions could be determined with good intra-observer precision. However, intra-observer precision of plaque compression is larger than the mean compression and is of the same order as the standard deviation of plaque compression of our patient population. Therefore, plaque compression cannot be precisely determined. Values are presented as mean ± standard deviation. Intra-observer precision is defined as the standard deviation of differences between repeated measurements and their average. CV, Coefficient of variation.

	N=15		**Mean**	**Intra-observer precision**	**CV [%]**
Entire region of interest	Adventitia to adventitia	End-diastolic diameter	8822±724 µm	59 µm	1
		Distension	193±128 µm	40 µm	21
	Lumen	End-diastolic diameter	5351±1030 µm	107 µm	2
		Distension	213±128 µm	59 µm	28
At maximal posterior plaque thickness	Adventitia to adventitia	End-diastolic diameter	8932±864 µm	78 µm	1
		Distension	200±160 µm	62 µm	31
	Lumen	End-diastolic diameter	4078±1049 µm	113 µm	3
		Distension	216±126 µm	67 µm	31
	Plaque	Compression	8±113 µm	141 µm	1763

modeling. Indeed, the plaque adventitia-adventitia diameter does not deviate from the mean of the proximal and distal adventitia-adventitia diameters (Table 4; p-value=0.23). The adventitia-adventitia and lumen distension at the plaque are similar to either the distension at the CCA proximal or distal to the plaque (mean difference <70 μm; p-value>0.15).

Dynamic parameters and grey scale values

Scatterplots of the relative adventitia-adventitia and lumen distension compared to the 75th percentile of the normalized grey scale value (GS75) are shown in Figure 2. The relative adventitia-adventitia and lumen distensions are negatively correlated to the GS75 (Pearson correlation=-0.35 and -0.5, p-value=0.097 and 0.015, respectively). The group median of the GS75 is 72 (on the normalized 0-199 scale). Patients with a GS75 higher than 72 (N=11) exhibited a (borderline) significantly lower relative adventitia-adventitia and lumen distension (p-value=0.084 and 0.009, respectively), indicating higher vessel wall stiffness.

Table 3

Diameter and distension determined by two observers. Adventitia-adventitia and lumen diameters and distensions could be determined with good inter-observer precision. However, inter-observer precision of plaque compression is larger than the mean compression and is of the same order as the standard deviation of plaque compression of our patient population. Therefore, plaque compression cannot be precisely determined. Values are presented as mean ± standard deviation. Inter-observer precision is defined as the standard deviation of differences between measurements and their average of all observers. CV, Coefficient of variation.

	N=15		**Mean**	**Inter-observer precision**	**CV [%]**
Entire region of interest	Adventitia to adventitia	End-diastolic diameter	8555±756 μm	289 μm	3
		Distension	213±153 μm	84 μm	39
	Lumen	End-diastolic diameter	5547±1066 μm	278 μm	5
		Distension	234±163 μm	95 μm	41
At maximal posterior plaque thickness	Adventitia-to-adventitia	End-diastolic diameter	8648±885 μm	330 μm	4
		Distension	189±158 μm	76 μm	40
	Lumen	End-diastolic diameter	4218±1036 μm	183 μm	4
		Distension	222±159 μm	112 μm	50
	Plaque	Compression	-6±130 μm	146 μm	2433

Figure 2

Orthogonal relative adventitia-adventitia (left) and lumen distension (right) are negatively correlated with the 75th percentile of the grey-scale value (Pearson correlation of -0.35 and -0.5, with p-value of 0.097 and 0.015, respectively).

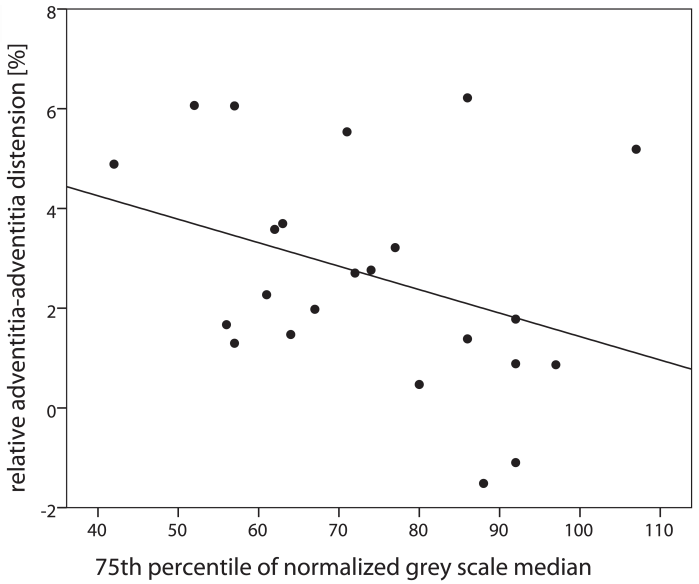

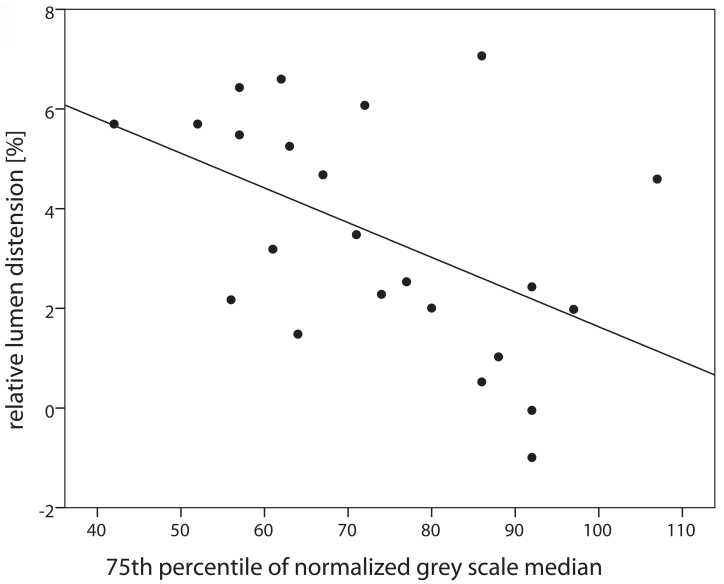

Table 4

Lumen and adventitia-adventitia diameters and distensions at three locations about the plaque site. Though the adventitia-adventitia diameter at the plaque is larger than at the CCA proximal to the plaque ([1]p-value), suggesting outward remodeling, the difference vanishes for the distal diameter ([2]p-value) or for the mean of both proximal and distal diameters ([3]p-value). No spatial differences are observed for the local distensions.

	N=14	Proximal	Plaque	Distal	p-value[1]	p-value[2]	p-value[3]
Diameter	Adventitia-adventitia	7826±863 μm	8237±842 μm	8419±843 μm	0.009	0.087	0.23
	Lumen	6233±1195 μm	4689±1071 μm	6592±1098 μm	0.001	<0.001	<0.001
Distension	Adventitia-adventitia	194±161 μm	216±161 μm	286±183 μm	0.49	0.15	0.46
	Lumen	311±196 μm	294±211 μm	351±235 μm	0.71	0.27	0.40

Discussion

The present study explored the option to extract from ultrasound images the orthogonal dimensions of the common carotid artery (CCA) and plaques, i.e., the values perpendicular to the local orientation of the artery centerline. Adventitia-adventitia and lumen diameters and distensions could be determined with good intra- and inter-observer precision. The orthogonal lumen diameter at the site of the plaque differs substantially from the one measured along the ultrasound beam (vertical direction for B-mode image obtained with a linear array). Since the intra- and inter-observer precision of plaque compression is of the same order as the standard deviation of the plaque compression of the patient population, plaque compression cannot be precisely determined. Contrary to the general concept of outward remodeling (induced by the locally increased wall shear strain) at the site of the plaque, we observed a gradually increasing adventitia-adventitia diameter across the CCA. Furthermore, orthogonal relative adventitia-adventitia and lumen distensions at the site of the plaque are negatively associated with the 75th percentile of the normalized grey scale value.

As expected, the observed intra-subject precision of the orthogonal adventitia-adventitia diameter is low (coefficient of variation 1%) and similar to the values reported in literature (coefficient of variation 1.5%) without correction for the angle of interrogation (Steinbuch et al. 2016a). The observed intra-subject precision of orthogonal distension (40 μm) is also similar to the CCA distension (44 μm) of patients with plaques in the internal carotid artery (Steinbuch et al. 2016a) and to the subgroups of Graf et. al. (Graf et al. 2010) with plaques in the ipsilateral or contralateral common or internal carotid artery. Note that we use the average of repeated measurements as reference for calculating the intra-subject precision whereas Graf et. al. only used one measurement as reference for the other, resulting in an intra-subject precision twice as high as in our approach. However, due to a smaller mean distension (193±128 μm) as a consequence of the plaque (Table 2), the coefficient of variation is substantially larger (21%) than reported values determined in the CCA without plaque (mean distension 377±122 μm; CV=12%) (Steinbuch et al. 2016a). The mean adventitia-adventitia distension (193 μm) is also substantially smaller than reported (>300 μm) by others for common carotid artery plaques (Paini et al. 2007; Beaussier et al. 2008; Beaussier et al. 2011). This is explained by the fact that we considered the orthogonal distension along the entire segment rather than the proximal value only where pulse pressures are higher because of pulse wave reflection (Hoeks et al. 2008).

The intra-observer coefficients of variation (CVs) of the orthogonal lumen diameter and distension are smaller than the inter-observer CVs. No specific rules were issued regarding the segmentation, allowing free interpretation of the observer and explaining larger inter-observer variations. The CVs of lumen diameter (2 and 5%) and distension (28 and 41%) are larger than the CVs of the adventitia-adventitia diameter (1 and 3%) and distension (21 and 39%) for both intra- and inter-observer variability. This is likely due to the problems associated with the determination of the lumen-intima transition at the near wall. Accordingly, the Mannheim consensus recommends assessment of intima-media thickness at the far wall only instead of near and far wall (Touboul et al. 2012). Since both intra- and inter-observer precision of adventi-

tia-adventitia and lumen diameters and distensions are substantially smaller than the observed standard deviation of those parameters in our patient population, orthogonal diameter and distension can be precisely determined from ultrasound images.

In contrast to the distension and diameter, orthogonal plaque compression cannot be precisely determined. This is because intra- and inter-observer precisions of plaque compression are higher than the actual compression and are of the same order as the standard deviation of compression in our patient population. The main reason for the high intra-and inter-observer variability is the ultrasound resolution (300 μm (Steinbuch et al. 2017)) in combination with the small variation of the plaque thickness. The variability which cannot be adequately improved by averaging over subsequent heart beats. Another option is to consider spatial averaging over adjacent plaque segments. However, plaque compression may vary across multiple plaque segments due to spatial variations of plaque thickness, composition and local pulse pressure.

In this study, we explored the possibility to extract the CCA dimensions and plaque thickness perpendicularly to the local orientation of either the adventitia-adventitia or lumen centerline. Since the CCA is commonly parallel to the skin surface, the orthogonal artery dimensions for segments without a plaque do not deviate from those obtained with standard procedures (Graf et al. 2010; Steinbuch et al. 2016a). However, at a stenotic segment the artery orientation will change with position along the stenotic segment (Figure 1). Consequently, the orthogonal dimensions at the proximal and distal plaque segments are lower than those observed along the ultrasound beam, despite the parallel orientation of the CCA. For artery segments with an oblique orientation, e.g., the ICA, larger differences may occur between orthogonal and perpendicular assessment.

As stated earlier, the presence of a stenosis will locally increase the blood flow velocity and, hence, the wall shear stress. This will stimulate the endothelium to release a vasodilating agent (NO) in an attempt to restore the local wall shear stress (Glagov et al. 1997; Samijo et al. 1998; Dammers et al. 2003). Consequently, the adventitia-adventitia diameter should be larger at the site of a stenosis (outward remodeling). To investigate this effect, we considered the adventitia-adventitia and lumen diameter and distension proximal and distal to a plaque in a subset (N=14). Because of the stenosis, the lumen diameter at the plaque is significantly smaller than either the corresponding lumen diameter proximal or distal to the plaque (Table 4). On the other hand, the adventitia-adventitia diameter at the plaque is significantly larger than the diameter proximal to the plaque (Table 4), suggesting outward remodeling. This is in line with studies where outward remodeling was observed for some of the CCA plaques considered (Paini et al. 2007; Beaussier et al. 2008; Beaussier et al. 2011). However, the adventitia-adventitia diameter at the plaque was borderline significantly smaller than the diameter distal to the plaque (Table 4) while there was no difference with the mean of proximal and distal diameters. Those observations are in line with a diverging CCA towards the bifurcation and contradicts the concept of outward remodeling. Since CCA plaques are relatively stable compared to plaques at the downstream bifurcation, outward remodeling may indeed

be limited, even though the average stenosis degree is 48% (Table 1). In addition, it should be realized that proximal or distal to a recording location plaques may exist which affect the parameters extracted from the recording.

Orthogonal adventitia-adventitia and lumen relative distension at the site of the plaque are negatively associated with the GS75. Thus, a locally stiffer vessel wall, as reflected by the decreased relative lumen distension, is associated with echogenic plaques, which is probably due to a higher calcium content. The current study is performed in a relatively small cohort (N=23) which might explain the borderline association between the adventitia-adventitia distension and GS75.

A limitation of this study is the stability of CCA plaques; CCA plaques will almost never lead to rupture. However, CCA plaque evaluation will contribute to the knowledge of plaque dynamics and the relation with plaque morphology and composition. In the near future, the association between the relative adventitia-adventitia and lumen distensions at the plaque within the carotid bulb and plaque progression and/or rupture risk will be investigated in the PARISK follow-up study (Truijman et al. 2014).

In conclusion, we demonstrated the feasibility to extract from a sequence of ultrasound B-mode frames the orthogonal dynamic dimensions of the common carotid artery and plaques, albeit that the proposed approach appears inadequate to establish plaque compression. At the site of the plaque the orthogonal lumen diameter is significantly smaller than the lumen diameter along the ultrasound beam. Surprisingly, we did not found outward remodeling with the CCA plaques. Orthogonal relative lumen distension is negatively associated with plaque echogenicity, which is in line with the known larger stiffness of lesions with increased echogenicity.

References

Beaussier H, Masson I, Collin C, Bozec E, Laloux B, Calvet D, Zidi M, Boutouyrie P, Laurent S. Carotid plaque, arterial stiffness gradient, and remodeling in hypertension. Hypertension 2008;52:729-736.

Beaussier H, Naggara O, Calvet D, Joannides R, Guegan-Massardier E, Gerardin E, Iacob M, Laloux B, Bozec E, Bellien J, Touze E, Masson I, Thuillez C, Oppenheim C, Boutouyrie P, Laurent S. Mechanical and structural characteristics of carotid plaques by combined analysis with echotracking system and MR imaging. JACC Cardiovasc Imaging 2011;4:468-477.

Biasi GM, Sampaolo A, Mingazzini P, De Amicis P, El-Barghouty N, Nicolaides AN. Computer analysis of ultrasonic plaque echolucency in identifying high risk carotid bifurcation lesions. Eur J Vasc Endovasc Surg 1999;17:476-479.

Dammers R, Stifft F, Tordoir JH, Hameleers JM, Hoeks AP, Kitslaar PJ. Shear stress depends on vascular territory: comparison between common carotid and brachial artery. J Appl Physiol (1985) 2003;94:485-489.

Elatrozy T, Nicolaides A, Tegos T, Griffin M. The objective characterisation of ultrasonic carotid plaque features. Eur J Vasc Endovasc Surg 1998;16:223-230.

European Carotid Surgery Trialists' Collaborative G. Randomised trial of endarterectomy for recently symptomatic carotid stenosis: final results of the MRC European Carotid Surgery Trial (ECST). The Lancet 1998;351:1379-1387.

Giannattasio C, Failla M, Emanuelli G, Grappiolo A, Boffi L, Corsi D, Mancia G. Local effects of atherosclerotic plaque on arterial distensibility. Hypertension 2001;38:1177-1180.

Glagov S, Bassiouny HS, Sakaguchi Y, Goudet CA, Vito RP. Mechanical determinants of plaque modeling, remodeling and disruption. Atherosclerosis 1997;131 Suppl:S13-14.

Graf IM, Schreuder FH, Mess WH, Reneman RS, Hoeks AP. Spatial distension variations are associated with focal atherosclerotic plaques. Cerebrovasc Dis 2010;29:199-205.

Gronholdt ML, Nordestgaard BG, Schroeder TV, Vorstrup S, Sillesen H. Ultrasonic echolucent carotid plaques predict future strokes. Circulation 2001;104:68-73.

Hoeks AP, Reesink KD, Hermeling E, Reneman RS. Local blood pressure rather than shear stress should be blamed for plaque rupture. J Am Coll Cardiol 2008;52:1107-1108; author reply 1108-1109.

Kakkos SK, Stevens JM, Nicolaides AN, Kyriacou E, Pattichis CS, Geroulakos G, Thomas D. Texture analysis of ultrasonic images of symptomatic carotid plaques can identify those plaques associated with ipsilateral embolic brain infarction. Eur J Vasc Endovasc Surg 2007;33:422-429.

Martinez-Sanchez P, Fernandez-Dominguez J, Ruiz-Ares G, Fuentes B, Alexandrov AV, Diez-Tejedor E. Changes in carotid plaque echogenicity with time since the stroke onset: an early marker of plaque remodeling? Ultrasound Med Biol 2012;38:231-237.

Mathiesen EB, Bonaa KH, Joakimsen O. Echolucent plaques are associated with high risk of ischemic cerebrovascular events in carotid stenosis: the tromso study. Circulation 2001;103:2171-2175.

Nichols WW, O'Rourke MF, Vlachopoulos C. McDonald's blood flow in arteries : theoretic, experimental, and clinical principles. 6th. Hodder Arnold, London, 2011.

Paini A, Boutouyrie P, Calvet D, Zidi M, Agabiti-Rosei E, Laurent S. Multiaxial mechanical characteristics of carotid plaque: analysis by multiarray echotracking system. Stroke 2007;38:117-123.

Salem MK, Sayers RD, Bown MJ, West K, Moore D, Nicolaides A, Robinson TG, Naylor AR. Patients with recurrent ischaemic events from carotid artery disease have a large lipid core and low GSM. Eur J Vasc Endovasc Surg 2012;43:147-153.

Samijo SK, Willigers JM, Barkhuysen R, Kitslaar PJ, Reneman RS, Brands PJ, Hoeks AP. Wall shear stress in the human common carotid artery as function of age and gender. Cardiovasc Res 1998;39:515-522.

Steinbuch J, Hoeks AP, Hermeling E, Truijman MT, Schreuder FH, Mess WH. Standard B-Mode Ultrasound Measures Local Carotid Artery Characteristics as Reliably as Radiofrequency Phase Tracking in Symptomatic Carotid Artery Patients. Ultrasound Med Biol 2016a;42:586-595.

Steinbuch J, Van Dijk AC, Schreuder FHBM, Truijman MTB, De Rotte AAJ, Nederkoorn PJ, Van der Lugt A, Hermeling E, Hoeks APG, Mess WH. High spatial inhomogeneity in intima-media thickness of the common carotid artery is associated with a larger degree of stenosis in the internal carotid artery: The PARISK study. Ultraschall Med 2016b;

Steinbuch J, van Dijk AC, Schreuder F, Truijman M, Hendrikse J, Nederkoorn PJ, van der Lugt A, Hermeling E, Hoeks A, Mess WH. Definition of common carotid wall thickness affects risk classification in relation to degree of internal carotid artery stenosis: the Plaque At RISK (PARISK) study. Cardiovasc Ultrasound 2017;15:9.

Topakian R, King A, Kwon SU, Schaafsma A, Shipley M, Markus HS, Investigators A. Ultrasonic plaque echolucency and emboli signals predict stroke in asymptomatic carotid stenosis. Neurology 2011;77:751-758.

Touboul PJ, Hennerici MG, Meairs S, Adams H, Amarenco P, Bornstein N, Csiba L, Desvarieux M, Ebrahim S, Hernandez Hernandez R, Jaff M, Kownator S, Naqvi T, Prati P, Rundek T, Sitzer M, Schminke U, Tardif JC, Taylor A, Vicaut E, Woo KS. Mannheim carotid intima-media thickness and plaque consensus (2004-2006-2011). An update on behalf of the advisory board of the 3rd, 4th and 5th watching the risk symposia, at the 13th, 15th and 20th European Stroke Conferences, Mannheim, Germany, 2004, Brussels, Belgium, 2006, and Hamburg, Germany, 2011. Cerebrovasc Dis 2012;34:290-296.

Truijman MT, Kooi ME, van Dijk AC, de Rotte AA, van der Kolk AG, Liem MI, Schreuder FH, Boersma E, Mess WH, van Oostenbrugge RJ, Koudstaal PJ, Kappelle LJ, Nederkoorn PJ, Nederveen AJ, Hendrikse J, van der Steen AF, Daemen MJ, van der Lugt A. Plaque At RISK (PARISK): prospective multicenter study to improve diagnosis of high-risk carotid plaques. Int J Stroke 2014;9:747-754.

8

General discussion

Introduction

This thesis is a step towards identification of plaques at risk with ultrasound and pertains to baseline ultrasound recordings (2010-2014) of the 2-year follow-up Plaque At RISK study (PARISK). The main aim of this thesis is to develop and validate new techniques to extract from ultrasound recordings the morphological and mechanical properties of carotid arteries and plaques in order to provide accurately and precisely characteristics specific for a plaque at risk. The first part of this thesis addresses the mechanical properties of the common carotid artery in association with distal plaques, while the second part of this thesis focuses on carotid plaques itself. For this purpose, we have developed and validated a method to extract mechanical properties of the carotid artery, such as diameter, distension, intima-media thickness, distension rise time characteristics, and the spatial inhomogeneity of these quantities. They were obtained with a novel edge detection technique facilitating tracking of tissue interfaces over time and applicable to image sequences as obtained in the clinic with a standard ultrasound echo system. In addition, we developed a novel technique to obtain morphological information of arteries and plaques along the relevant axis (center line lumen) rather than along the line of observation (ultrasound beam axis).

PARISK study

The Plaque At RISK (PARISK) study (clinical trials.gov NCT01208025) aims to evaluate plaques at risk with multiple non-invasive imaging techniques to improve, in a final application stage, identification of patients at increased risk of stroke, even before a first stroke or transient ischemic attack (TIA) has occurred (Truijman et al. 2014). More specifically, PARISK aims to identify suitable plaque parameters (including morphology, composition and mechanical parameters) that can be assessed with the selected imaging techniques with high sensitivity and specificity. The study involves cross-sectional as well as longitudinal clinical validation. Therefore, PARISK will eventually enable to 1) diagnose plaques at an early stage and monitor progression, 2) assess individual risk for stroke or TIA, 3) assess efficacy of individual drug therapy and intervention for (asymptomatic) patients at risk for a (recurrent) stroke or TIA and 4) develop surrogate endpoints of non-invasive imaging techniques in novel drug development.

Current status of the PARISK study

240 patients who recently had an ischemic stroke or transient ischemic attack (TIA) and a mild-to-moderate stenosis (30-70%) in the ipsilateral carotid bifurcation or internal carotid artery (ICA) were included within three months after the clinical event. Image modality recordings, i.e., Magnetic Resonance Imaging (MRI), multidetector Computed Tomography Angiogram (MDCT), ultrasound and Transcranial Doppler (TCD), were performed after inclusion. Currently, baseline results of the PARISK study are available (Figure 1). Average time between the clinical event and ultrasound recording is relatively long (N=233; 55±73 days). To assess determinants for plaque progression and assess changes in baseline and follow-up parameters, all image modalities were reapplied in the first 150 patients after two years. Analysis will be completed shortly. To determine the primary endpoints, i.e., which patients endured a new recurrent stroke or transient ischemic attack, patients will be evaluated clinically when a follow-up brain MRI is repeated two years after inclusion in all patients in order to also detect clinically silent infarctions.

This thesis mainly describes (the integration of) morphological and mechanical characterization of the common carotid artery with or without plaque as determined with ultrasound. Analysis of internal carotid artery ultrasound recordings is only performed for grey-scale median values. In the future, the mechanical properties of the internal carotid artery plaques will also be investigated.

Compatibility between centers

PARISK focusses on multiple existing non-invasive imaging techniques such as magnetic resonance imaging (MRI), multidetector computed tomography angiogram (MDCTA), ultrasound (US) and transcranial Doppler (TCD). All imaging techniques are already rather standard in the clinic, which makes it feasible to translate the findings of the PARISK study directly into daily practice. The imaging modalities were recorded in four centers in the Netherlands, i.e., Maastricht University Medical Center, Erasmus Medical Center, University Medical Center Utrecht and Amsterdam Medical Center. Multiple participating centers are necessary to provide a large sample size to ensure enough power for the primary endpoints, i.e., which patients endured a new ipsilateral recurrent ischemic stroke or transient ischemic attack. On the other hand, multiple centers might contribute to a higher variability. To reduce the variability between centers, similar devices were used for all image modalities. For the ultrasound recordings, all centers used a standard echo machine, the Philips iU22 scanner (Philips Medical Systems, Bothell, USA), operating at a frame rate of approximately 40 fps. However, different transducers were used depending on the depth of the carotid artery (either 17-5, 12-5 or 9-3 MHz probe) reflecting the daily practice. In addition, settings were not standardized across centers leading to more diversity and easier translation to other devices. Pooling data and translation of the results is only possible if inter-subject values between centers are not significantly different. The inter-subject values of morphological and mechanical characteristics derived from ultrasound recordings (end-diastolic diameter, distension, intima-media thickness, its inhomogeneity) of the common carotid artery were similar between the different centers (**Chapter 4**; ANOVA: p-value=>0.1). However, risetime and its inhomogeneity across the distension distribution were significantly lower for one center (**Chapter 6**; ANOVA: p-value<0.001 and 0.008, respectively), which might be caused by presence of more vulnerable plaques as confirmed by the MRI.

Severe stenosis cohort

In addition to the large cohort follow-up study (clinicaltrials.gov: NCT01208025), a small second cohort was included in the PARISK study (clinicaltrials.gov: NCT01709045) by the Maastricht University Medical Center. This subcohort consists of 71 patients with a recent stroke or transient ischemic attack and severe stenosis (>70%), undergoing carotid endarterectomy. The same imaging modalities as in the large cohort (see above) were applied one day before the surgery. This small cohort allows investigation of severe plaques and enables eventually comparison and validation of the imaging results against histology of the surgically removed (plaque) tissue.

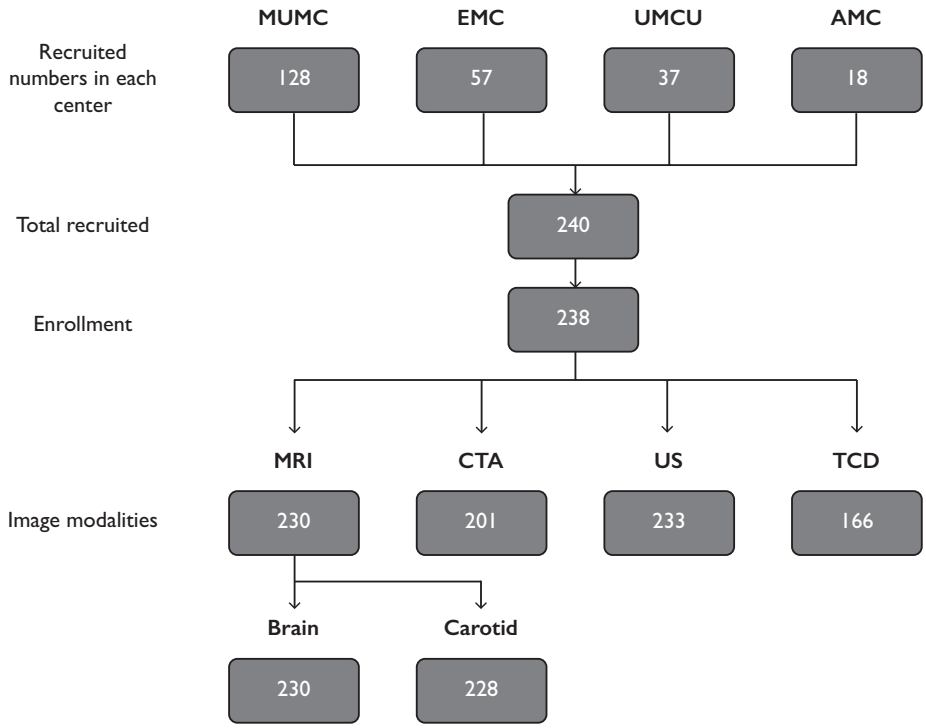

Figure 1

Flow chart of patient recruitment and inclusion, and numbers investigated for each imaging modality, i.e., Magnetic Resonance Imaging (MRI), multidetector Computed Tomography Angiogram (CTA), ultrasound (US) and Transcranial Doppler (TCD). In total, 240 patients were recruited. Two patients were excluded due to withdrawal of the informed consent during the measurements, resulting in 238 patients. Exclusions of the different imaging modalities were mainly due to contra-indications or technical recording failure. Participating centers are Maastricht University Medical Center (MUMC), Erasmus Medical Center (EMC), University Medical Center Utrecht (UMCU) and Amsterdam Medical Center (AMC).

CCA plaque study

In the PARISK study, two-dimensional (2D) ultrasound images of the common carotid artery (CCA) and internal carotid artery (ICA) were collected of patients with a plaque in the carotid bifurcation or ICA. As a first step towards plaque characterization in the ICA, we set up a small pilot study (N=40) in the Maastricht Medical University Center to evaluate our method in CCAs with plaque (**Chapter 7**). It should be noted that CCA plaques are rare and relatively stable (Figure 2).

Since CCA plaques are easily accessible for ultrasound, CCA plaques can enhance our knowledge of plaque and plaque imaging. However, we realize that CCA plaque do usually not rupture and, hence, hardly contribute to relevant stroke risk assessment. We will return to this issue after we have discussed the proposed analysis methods in detail.

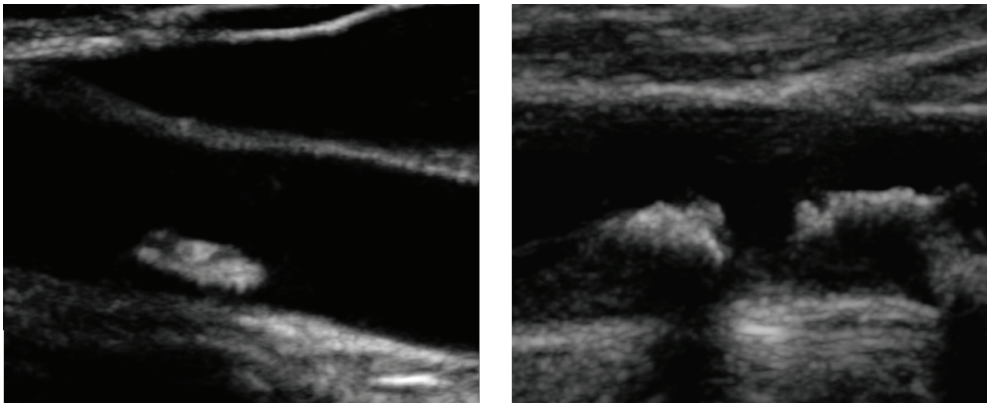

Figure 2

Minor plaque (left) and severe plaque (right) in the common carotid artery. These plaques are relatively stable, as can be deduced from the echogenic appearance (normalized grey scale median: 56±46 and 45±42, respectively).

B-mode edge detection/tracking in the common carotid artery

Since the internal carotid artery is usually curved at a variable depth, we validated our novel edge detection and tracking technique (**Chapter 3**) in the common carotid artery (CCA). In addition, mechanical characteristics of the CCA were determined (**Chapter 3-6**). These characteristics might be risk factors for plaque formation.

B-mode wall edge tracking accuracy and precision

Arterial stiffness of the common carotid artery, determined by the distensibility coefficient, i.e., the relative change in diameter normalized to the driving pulse pressure, is associated with coronary heart and vascular disease (Leone et al. 2008; van Sloten et al. 2014). Local distension, defined as the local diameter change over the cardiac cycle, is commonly extracted with radiofrequency phase tracking applied to recordings obtained at a high frame rate (Meinders et al. 2001). Because this technique requires an expensive and dedicated ultrasound machine, its application is restricted to a limited number of specialized hospitals. We showed in **Chapter 3** that the local diameter, and hence its change over the cardiac cycle (distension) can be extracted with semi-automatic edge tracking applied to standard B-mode echo images acquired at a video frame rate of approximately 40 Hz. More specifically, in an elderly patient population, which often has curved vessels with motion artefacts, the proposed method provides distension as precise and accurate as radiofrequency phase tracking applied to high frame rate echo sequences. Since distension can be properly extracted in this technically most challenging patient group, it is likely that our edge tracking technique will also work adequately in younger patients or those without atherosclerotic disease.

Common carotid wall thickness parameters as risk factors

Mean and maximal intima-media thickness (IMT) are potential risk markers for atherosclerotic disease. Although increased mean and/or maximal IMT are associated with presence of an atherosclerotic plaque in the internal carotid artery (ICA) (Persson et al. 1994; Bonithon-Kopp et al. 1996; Rundek et al. 2015) and with increased risk on a first or recurrent stroke in a large population (O'Leary et al. 1999; Tsivgoulis et al. 2006; Talelli et al. 2007; Silvestrini et al. 2010; Roquer et al. 2011), recent literature shows that mean or maximal IMT is not suitable to predict for an individual patient the risk of (future) cardiovascular events (Lorenz et al. 2010; den Ruijter et al. 2013; van den Oord et al. 2013; Bots et al. 2014). IMT inhomogeneity, defined as the spatial standard deviation of IMT over the recorded B-mode image, may be a good alternative for mean or maximal IMT, because it reflects the irregular appearance of the lumen-intima interface. To investigate IMT and its inhomogeneity, we included the detection of the posterior lumen-intima transition (Figure 3) in our semi-automatic edge tracking program (**Chapter 4**).

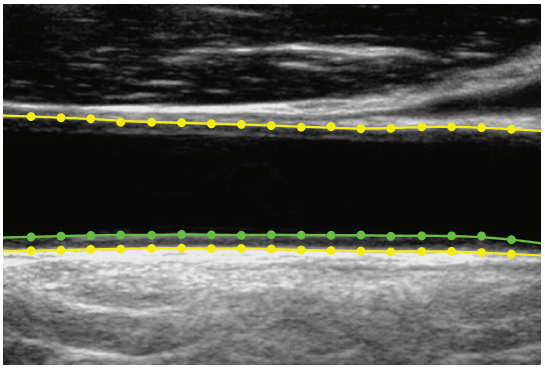

Figure 3

To extract the intima-media thickness and its inhomogeneity, the lumen-intima (green line) and media-adventitia transitions (yellow lines) of the common carotid artery are determined by edge detection.

We demonstrated that common carotid arteries (CCAs) with a high relative IMT inhomogeneity are associated with a larger median IMT (p-value<0.001), distension inhomogeneity (p-value=0.01) and degree of ICA stenosis (p-value=0.023). Furthermore, after adjustment for traditional risk factors, i.e., age, Body Mass Index, smoking, diabetes mellitus and hypertension, relative IMT inhomogeneity remained independently associated with the degree of ipsilateral ICA stenosis (stepwise linear regression, standardized β=0.18, p=0.016). However, in **Chapter 5** it appeared that mainly CCA plaques dominate the association with the degree of ipsilateral ICA stenosis (p-value<0.001). Henceforth, we conclude that IMT inhomogeneity does not add extra information on top of maximal IMT.

Although **Chapter 4** and **Chapter 5** indicate a relation between wall thickness parameters and the degree of stenosis, it remains unclear whether the wall parameters are abnormal previous to plaque formation. It seems reasonable that the vessel wall first exhibits IMT irregularity followed by plaque formation. However, it is also possible that IMT and plaque formation are different and independent processes (Spence and Hegele 2004; Hegele et al. 2005; Spence 2008). It requires a longitudinal study in a large asymptomatic population to evaluate changes in wall parameters prior to plaque formation. Eventually the PARISK follow-up study will provide wall thickness parameters in relation to plaque progression and recurrent stroke.

An important finding of our study is that risk classification for having a distal moderate stenosis (>50%) is affected when wall thickness in relation to the actual common carotid artery diameter is considered rather than its absolute value (**Chapter 5**). This is in line with the physiological consideration that wall tension will be the same for a constant ratio of wall thickness and diameter as expressed by the Lamé equation (Liang et al. 2001; Nichols et al. 2011). To rate wall thickness properly, it is advised always to use relative instead of absolute IMT. The potentially greater relevance of the relative compared to absolute wall thickness parameters in association with plaque progression and stroke recurrence is further investigated in the PARISK follow-up study.

Vulnerable plaque identification

Common features of vulnerable plaques, i.e., plaques prone to rupture, are a lipid-rich necrotic core with a thin fibrous cap (<65 μm), accumulation of macrophages and lack of smooth muscle cells (Lusis 2000; Virmani et al. 2000; Virmani et al. 2006). Plaque deformation, and eventually plaque rupture, will vary with plaque morphology (size and shape) and composition, as well as the mechanical load exerted by (transmural) blood pressure, pulse pressure, and wave reflections (Hoeks et al. 2008). The ability to assess by ultrasound the composition of (vulnerable) plaque will be beneficial since it simplifies procedures by bypassing Magnetic Resonance Imaging or Computed Tomographic scans and thereby may reduce healthcare costs.

Degree of stenosis

The degree of stenosis of the internal carotid artery (ICA) can be determined by ultrasound, Computed Tomographic (CT) or Magnetic Resonance Angiography according to either the European Carotid Surgery Trial (ECST) criterion (European Carotid Surgery Trialists' Collaborative 1998) or the North American Symptomatic Carotid Endarterectomy Trial (NASCET) criterion (North American Symptomatic Carotid Endarterectomy Trial 1991). The ECST criterion divides the lumen diameter at the site of the plaque by the assumed original vessel diameter at the same location, whereas the NASCET criterion considers the ratio of the lumen diameter at the site of the plaque by the vessel diameter just distally to the plaque location. In the Netherlands, the degree of stenosis is commonly classified in the clinic by the highest peak velocity of the Doppler ultrasound signal, most likely obtained within or just distal to a stenosis, and linked to the NASCET criterion (Grant et al. 2003). However, the degree of stenosis from ultrasound Doppler velocities is only available as categorical rather than continuous data. Moreover, plaques with less than 50% degree of stenosis hardly affect peak velocities, so this method is unsuited for minor plaques. However, half our patient population has an average degree of ICA stenosis below 50%. In addition, Doppler velocities as well as NASCET criterion underestimate the actual burden of atherosclerosis (Staikov et al. 2000; Sabeti et al. 2004; Schreuder et al. 2009). Therefore, we advocate the use the degree of ICA stenosis on a continuous scale as determined with the ECST criterion on CT recordings.

Plaque composition

Plaque composition can be determined either by Magnetic Resonance Imaging (MRI) (Yuan et al. 2001; Cappendijk et al. 2004; Cappendijk et al. 2005; Saam et al. 2005) or ultrasound applying grey scale median (GSM) values (El-Barghouty et al. 1996; Tegos et al. 2000; Lal et al. 2002; Goncalves et al. 2004; Sztajzel et al. 2005). Echolucent plaques, i.e., plaques with relatively low echo amplitude, tend to be rather homogeneous of composition (**Chapter 2**) and are associated with increased risk of cerebrovascular events (Biasi et al. 1999; Gronholdt et al. 2001; Mathiesen et al. 2001; Topakian et al. 2011). However, plaque echogenicity alone is not powerful enough to select patients for carotid endarterectomy (Gupta et al. 2015). The predictive value of MRI plaque composition for determining plaques at risk is further investigated in the PARISK follow-up.

Distance and displacement measurements

In standard transcutaneous ultrasound applications, echoes and scattered signals from tissue transitions are received as function of depth. This implies that a (change in) distance between echo transitions will be measured along the ultrasound beam. For structures parallel to the skin surface, e.g., the common carotid artery, the signals obtained will adequately reflect the actual properties of the structures under study. Even a deviation of 10 degrees from perpendicular insonation will hardly affect distance measurement of, for example, lumen diameter, wall thickness or plaque thickness. The situation changes drastically (Figure 4) for the carotid bifurcation and internal carotid artery that are oriented oblique to the skin surface and are frequently tortuous. The situation is aggravated by plaques where the local relevant tissue orientation may reach angles of 45 degrees. Under these conditions, distance and displacement measurements along the ultrasound beam lose their relevance.

For a proper assessment of local lumen diameter and wall thickness, distance measurements should preferentially be performed along the radius, i.e., perpendicular to the local orientation of the lumen axis. In **Chapter 7**, the concept of orthogonal distance measurements was introduced. It is based on manual outlining of the anterior and posterior lumen-intima and media-adventitia transitions, followed by automatic extraction of the local radius orientation, at an interspacing of 1 mm, and associated distances (Figure 5). This procedure is executed for the diastolic as well as the systolic images of a B-mode video sequence (established using the method as proposed in **Chapter 7**). For each video sequence, the result is a large compilation of measurements, even involving diastolic to systolic longitudinal motion of the observed artery segment based on the cross-correlation of the lumen shape.

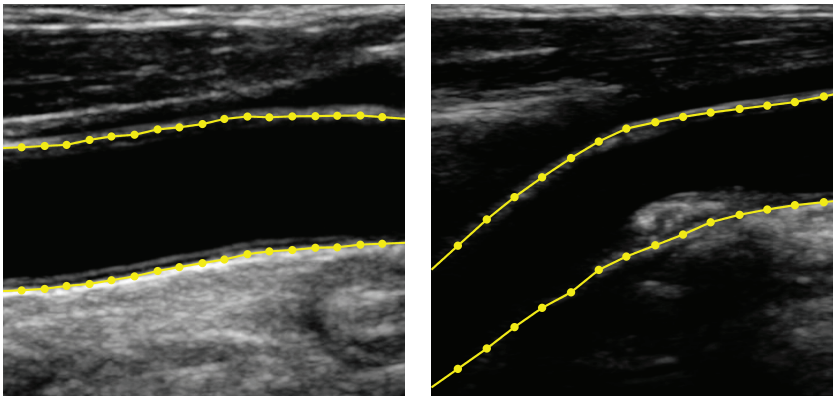

Figure 4

The common carotid artery (left) and internal carotid artery (right) of the same patient. The common carotid artery is observed perpendicularly (ultrasound probe at top) whereas the internal carotid artery changes continuously in orientation leading to errors in distance and displacement measures.

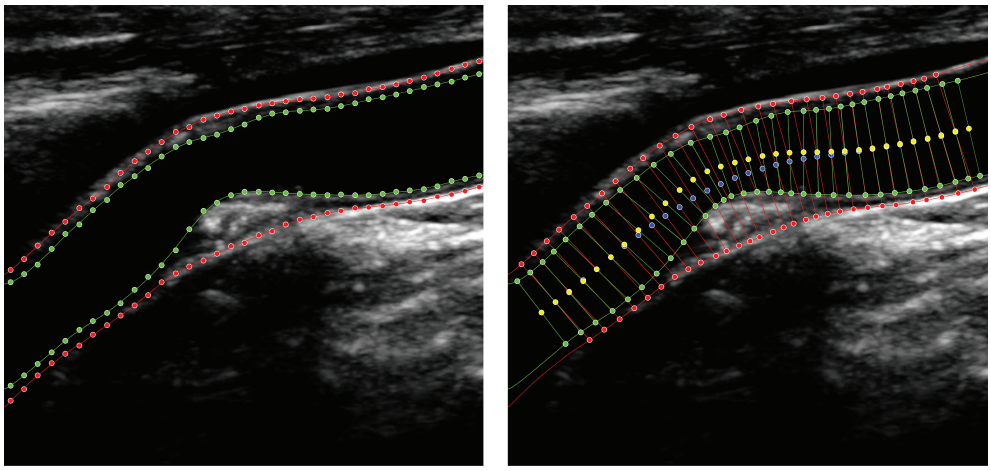

Figure 5

Manual outlining of the anterior and posterior lumen-intima (green dots) and media-adventitia transitions (red dots) of the internal carotid artery with a posterior plaque. Manual outlining (left) is followed by automatic extraction (right) of the local radius orientation (red and green lines) at an interspacing of 1 mm using the lumen (yellow dots) or adventitia-adventitia centerlines (blue dots).

A complicating factor for orthogonal distance assessment is that for tissue interfaces not perpendicular to the ultrasound beam the character of the received echo signals shifts from reflection to scattering. Moreover, the lateral ultrasound resolution imposed by the beam width (**Chapter 2**), which is about a factor 5 poorer than the depth resolution along the beam, will blur images. As a consequence, tissue transitions may be less distinct, complicating manual outlining of tissue interfaces. To separate sources of error, i.e., manual outlining and image quality, we first applied the proposed method to common carotid arteries with plaques.

The orthogonal approach facilitates, with good intra- and inter-observer precision (coefficient of variation: diameter 3-5%), assessment of the external and internal diameter of the vessel near and at the CCA plaque (**Chapter 7**). However, intra- and inter -observer precisions are limited by the US resolution in depth (around 300 µm). This is of specific relevance for the assessment of diastolic to systolic changes in distances (coefficient of variation: distension 40-60%). For example the plaque compression, i.e. the relative change in plaque thickness from diastole to systole, cannot be determined precisely. The intra- and inter-subject precision is 141 and 146 µm, respectively, which is higher than the actual compression (should be below 10%). Averaging over adjacent plaque segments might improve the inter- and intra-observer precision, though compressibility values might vary across plaque segments due to plaque structure and composition (especially near plaque borders). Alternatively one may consider plaque motion based on the movement of the plaque center, which is likely less resolution dependent. Baseline results of center movement of plaques in the internal carotid artery will be available soon.

Integrating morphological and biomechanical characteristics

As shown in **Chapter 3**, edge detection of anterior and posterior wall-lumen transition for a sequence of B-mode images provides the distribution of diameter distension waveforms over the observed artery segment. The local transmural blood pressure is cushioned by the artery compliance which is inversely related to wall stiffness (Nichols et al. 2011). It is, therefore, anticipated that the diastolic to systolic risetime of the distension waveform is long for young subjects with highly compliant arteries and shortens with age. The relevant distension segment, obtained from a standard B-mode video sequence, contains only a few sample points. Therefore, determination of diastolic and systolic time points (minimum and maximum) always has a low precision. That is why we proposed in **Chapter 6** to interpolate the distension waveform distribution by a factor of 25 and considered the time points for 20 and 80% of the systolic upstroke as relevant for the risetime. Based on repeated recordings we could show that, following this approach, we could achieve a precision of 7 ms for the median risetime (**Chapter 6**), which is well below the B-mode interframe spacing of about 25 ms.

To assess the effect of wave reflections on the distension waveform distribution, median risetime and its inhomogeneity over the common carotid artery were compared with the degree of stenosis and plaque composition of the internal carotid artery (**Chapter 6**). Both a mild stenosis (<50% according to ECST criterion) and moderate stenosis (50-70% according to ECST and NASCET criterion, respectively) in the internal carotid artery did not have a notable effect on the common carotid artery risetime and its inhomogeneity (**Chapter 6**; Student t-test: p-value>0.7). The magnitude of wave reflections is directly related to changes in hemodynamic impedance caused by a stenosis, explaining why the association between risetime and stenosis degree did not reach significance for mild and moderate stenoses. Hence, median risetime should be specifically investigated for severe plaques (>70% according to NASCET criterion). This is eventually possible for the second small cohort of the PARISK study, i.e., patients with a recent stroke or transient ischemic attack and severe stenosis undergoing carotid endarterectomy.

However, the risetime inhomogeneity of the common carotid artery distension waveform distribution is higher for a stable, hard distal plaques than for a soft plaque, having substantial proximal lipid-rich necrotic core (LRNC) and thin/ruptured fibrous cap (**Chapter 6**; mean difference 4.5 ms, Student t-test: p-value=0.001). In the latter case, the risetime inhomogeneity was of the same order as the baseline value, based on the contralateral common carotid artery with a small degree of distal stenosis (<30% according to ECST criterion). These observations corroborate the cushioning effect of a lipid rich necrotic core at the proximal part of a plaque on wave reflections. Therefore, risetime inhomogeneity of the distension waveform distribution seems to offer a non-invasive and inexpensive method to characterize the nature of a distal plaque. To assess the possibility of vulnerable plaque discrimination with risetime inhomogeneity in a patient population, a cut-off value for risetime inhomogeneity needs to be defined in relation to histology of the plaque.
We observed across our patient population a high standard deviation of the risetime inhomo-

geneity of the distension waveform. Moreover, a low risetime inhomogeneity on the order of the baseline values was also observed for patients without a lipid rich necrotic core. Hence, the specificity and sensitivity of risetime inhomogeneity will be likely too low for predicting plaque vulnerability for individual patients. However, these issues (effect of severe stenosis, true baseline value, and histology comparison) will enhance our understanding of the mutual interaction of, on the one hand, pressure waves and associated wave reflection and, on the other hand, morphology, structure and, composition of arteries and plaques.

The grey scale medium (GSM) value of a plaque is predominantly determined by the elastin and calcium content of the plaque (Goncalves et al. 2004) and is affected by acoustic shadowing in case of strong calcification of a plaque. Hence, risetime inhomogeneity might provide more potential than GSM values to identify non-invasively the nature of a plaque and thereby plaque vulnerability. On the other hand, risetime inhomogeneity was only borderline significantly lower for vulnerable plaques (N=59), containing a LRNC, intraplaque haemorrhage and thin or rupture fibrous cap, compared to stable plaques (N=75; no LRNC; Student t-test p-value=0.06). If the analysis is restricted to subjects with a LRNC of more than 10% (N=45) the association with risetime inhomgeneity becomes highly significant (p-value=0.008). Surprisingly, risetime inhomogeneity is not associated with GSM values (Pearson coefficient=0.05, p-value=0.3). This observation is likely due to the fact that GSM is a composite reflection of the total plaque composition including calcifications, a LRNC and intraplaque hemorrhage whereas risetime inhomogeneity is mainly associated with LRNC at the proximal part of the plaque (**Chapter 6**).

We hypothesized that the plaque composition may affect its compressibility and hence the local artery distension (Paini et al. 2007; Beaussier et al. 2008; Beaussier et al. 2011). For this purpose, external and internal relative distension of the vessel wall at the maximal posterior plaque in the common carotid artery (CCA) were determined in 23 patients (**Chapter 7**). Since it is likely that calcium content of the plaque mostly determines the local vessel stiffness, we looked at the 75th percentile of the normalized GSM values. Although the patient number is relatively low, patients with a high 75th percentile of the normalized GSM values (>72; N=11) of the CCA plaque had a (borderline) significantly lower external and internal relative distension of the vessel wall at the CCA plaque (Student t-test: p-value=0.084 and 0.009, respectively) compared to patients with a low 75th percentile of the normalized GSM values (<72; N=11). Therefore, plaque echogenicity is associated with a stiffer vessel wall. This study was performed in a relatively small cohort with CCA plaques (N=23). The association between morphological characteristics (degree of stenosis, grey scale median) and mechanical characteristics (distension, plaque movement) of the internal carotid artery plaque in the large PARISK cohort will be further investigated. In addition, compliant plaques might be more vulnerable for rupture. Therefore, the association between external or internal relative distension at the plaque and plaque progression and/or risk of rupture will be investigated in the PARISK follow-up study.

Table 1

Lumen and adventitia-adventitia diameter at three locations, i.e., proximal to the plaque, at the plaque and distal to the plaque.

	Proximal	Plaque	Distal	p-value[1]	p-value[2]
Lumen diameter	6233±1195 μm	4689±1071 μm	6592±1098 μm	0.001	<0.001
adventitia-adventitia diameter	7826±863 μm	8237±842 μm	8419±843 μm	0.009	0.087

[1]p-value between the diameter at the plaque and proximal to the plaque. [2]p-value between the diameter at the plaque and distal to the plaque.

One of the features of a plaque is outward remodeling (Naghavi et al. 2003), i.e. an enlarged adventitia-adventitia diameter at the site of the plaque compared to the nearby proximal or distal artery segment, to restore lumen diameter and hence wall shear stress (Glagov et al. 1997). To investigate the relevance of outward remodeling of the CCA plaques, the adventitia-adventitia and lumen diameter proximal and distal to the CCA plaque were analyzed in a subset of the CCA plaque study (N=14; **Chapter 7**). The lumen diameter at the plaque was significantly smaller than either the lumen diameter proximal (Table 1; paired t-test p-value=0.001) or distal (Table 1; paired t-test p-value<0.001) to the plaque.The adventitia-adventitia diameter at the plaque was significantly larger than the corresponding diameter proximal to the plaque (Table 1; paired t-test p-value=0.009), corroborating the concept of outward remodeling. However, the adventitia-adventitia diameter at the plaque was borderline significantly smaller than distal to the plaque (Table 1; paired t-test p-value=0.087), indicating diverging of the vessel towards the bifurcation and contradicting outward remodeling. Therefore, in contrast to literature where outward remodeling was observed for some of the CCA plaques considered (Paini et al. 2007; Beaussier et al. 2008; Beaussier et al. 2011), outward remodeling of the plaques is either not present or obscured by diverging. Since CCA plaques are relatively stable (**Chapter 2**), it is likely that outward remodeling is limited.

Limitations

2D imaging

Out of plane motion of the vessel wall or plaque can occur, complicating analysis of 2D recordings. For circular structures in straight healthy vessels, for example the intima and media layers of the common carotid artery, out of plane motion is limited and will not affect the outcome of intima-media thickness since the received echo primarily originates from a segment perpendicular to the ultrasound beam. However, assessment of plaque compression or center movement in a 2D recording, especially for plaques located in curved twisting vessels, will not only depend on the pressure wave and plaque composition, but might also be influence by the out of plane motion of the plaque, complicating interpretation. As demonstrated in **Chapter 7**, reliable segmentation of a simple 2D echo image with a minimum of observation and motion artefacts remains problematic. This can be attributed to the nature of ultrasound echo signals (originating from tissue interfaces; **Chapter 2**), to the depth-dependent shape of the point spread function (leading part and trailing part of an echo have a different shape), and to reverberations mixing with true echoes. Recently, using plane wave imaging 3D ultrasound imaging with an exceptional high frame rate (>1000 Hz) became possible (Jensen et al. 2006; Tanter and Fink 2014). 3D imaging eventually allows determination of plaque motion in either direction if procedures for proper segmentation of the artery trajectory in space and in time become available. Disadvantages of 3D imaging are the costs, compromised lateral resolution because of tissue dependent time of flight, and dedicated operation. Due to resolution limitations, it is questionable whether 3D recordings would indeed improve plaque motion assessment.

Manual plaque segmentation

In the presence of plaques, the tracking of vessel walls in 2D images over time is complicated because of echogenicity, shadowing and out of plane movement. Therefore, we choose to manually segment the vessel wall (Figure 6) including plaques at diastolic and systolic frames to arrive at (dynamic) characteristics for artery diameter, lumen and plaques (**Chapter 7**) or the plaque itself to obtain grey scale median values (**Chapter 7**).

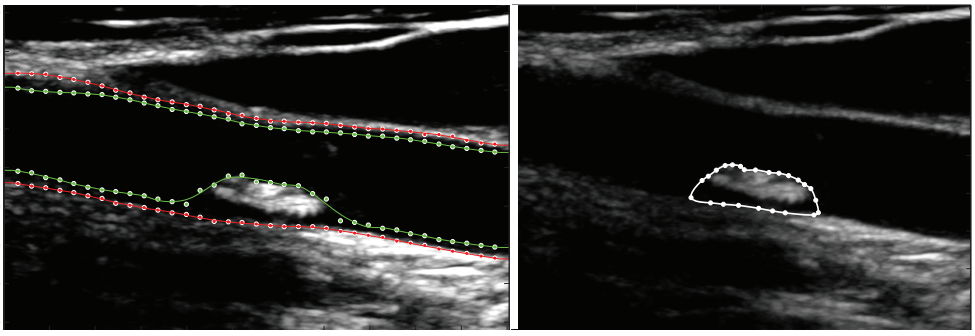

Figure 6

Manual segmentation of vessel walls (left) or plaque (right) of the common carotid artery to determine either the vessel wall characteristics or grey scale median value of the echogenic plaque. Green dots indicate the lumen-intima transitions, red dots the media-adventitia transitionsand white dots indicate the plaque boundary. Automatic tracking is hampered by the echogenic and echolucent parts of the plaque.

The use of electrocardiogram as time reference is avoided by lumen tracking for a vessel segment without a plaque for the determination of diastolic and systolic frames from the average distension waveform prior to the manual segmentation. Manual segmentation makes the process more time-consuming and observer- dependent (cf. **Chapter 7**). As stated earlier, the nature of ultrasound, lumen orientation relative to the ultrasound beam, and shadowing and plaque echogenicity renders automatic tracking nearly impossible; manual corrections will always be necessary to accurately segment the vessel wall at the plaque and the plaque itself. Semi-automatic interactive tracking will reduce observer dependency and might be the best possible option.

Future clinical perspectives

Plaque progression shortly after a cerebrovascular event

As mentioned in the Introduction, it is beneficial to operate patients with a severe stenosis (>70%) in the carotid bifurcation (North American Symptomatic Carotid Endarterectomy Trial 1991; Barnett et al. 1998; European Carotid Surgery Trialists' Collaborative 1998; Rothwell et al. 2003), whereas it is only moderately beneficial to operate patients with a moderate stenosis (50-70%) (Barnett et al. 1998; Rothwell et al. 2003). However, the benefit of surgery also depends on its timing after the last event: operating within two weeks after the last event is most beneficial whereas the benefit of the surgery rapidly decreases with a longer time delay (Rothwell et al. 2004). Apparently, most carotid artery plaques stabilize within a few weeks after stroke.

As stated earlier, the time between an event and image recording in the PARISK study is relatively long (55±73 days) after which most plaques would have already stabilized. The mechanism of early plaque development, destabilization and restabilization is still unclear, especially in the first weeks after stroke. Periodic imaging after a stroke or transient ischemic attack will help to understand plaque progression and regression shortly after stroke. Since ultrasound is an affordable and harmless imaging technique, which is readily accessible even in an ambulatory fashion due to high quality portable devices, it provides a good platform for repeated examinations within a short time window.

PARISK Follow-up

This thesis focuses on the baseline results of the PARISK study. All non-invasive imaging techniques were reapplied in 150 patients 2 years after inclusion (Truijman et al. 2014). From these follow-up data, plaque progression as quantified by its size can be extracted, allowing its association with potential risk factors as obtained with the non-invasive imaging techniques, i.e. ultrasound, Magnetic Resonance Imaging (MRI) and Computed Tomography, at baseline. In addition, changes in the investigated parameters between baseline and follow-up can also be assessed. Furthermore, the primary endpoints of the follow-up study (which patients endured a new ipsilateral recurrent ischemic stroke or transient ischemic attack) will be available in the summer of 2016. Since the expected incidence of ischemic stroke is rather low (2,5% per year), new silent ischemic brain lesions (around 19%) on MRI at follow-up will also be considered as primary endpoint (Truijman et al. 2014). In addition, the follow-up time of PARISK study is extended for another three years. At the end of the PARISK follow-up study, potential risk factors to predict recurrent stroke or transient ischemic attack and therefore plaque rupture can be determined. In addition, results from all multiple non-invasive imaging techniques will be compared and the best possible individual risk stratification can be considered. One may question whether the results of the PARISK study can also be directly translated to the clinic, when other ultrasound systems are used. Since settings were not standardized and inter-subject values were similar across centers for the ultrasound recordings, another device will probably not change the outcome. After determination of the potential risk factors, a large randomized longitudinal trial will be necessary to prove the predictive value of the potential risk factors prior to eventually incorporating the new approach in the clinical workflow.

General conclusion

This thesis is a step towards identification of plaques at risk with ultrasound and pertains to the baseline ultrasound recordings (2010-2014) of the 2-year follow-up PARISK study. The morphological and mechanical characteristics of the carotid artery walls and plaques were investigated by ultrasound. We developed analysis techniques to extract these characteristics with a novel edge detection algorithm which performed properly on standard ultrasound echo images as recorded in the clinic. Wall thickness parameters of the common carotid artery are associated with the degree of internal carotid artery stenosis. Integrating mechanical and morphological characteristics showed associations between the mechanical characteristics, i.e., the risetime inhomogeneity of the common carotid artery and the relative distension of the internal carotid artery, and the plaque composition determined by either Magnetic Resonance imaging or ultrasound, respectively. In conclusion, integrating mechanical and morphological characteristics might provide predictors for plaque vulnerability. The predictive value of vessel wall and plaque characteristics for plaque progression and cerebrovascular events will be evaluated in the follow-up phase of the PARISK study.

References

Barnett HJ, Taylor DW, Eliasziw M, Fox AJ, Ferguson GG, Haynes RB, Rankin RN, Clagett GP, Hachinski VC, Sackett DL, Thorpe KE, Meldrum HE, Spence JD. Benefit of carotid endarterectomy in patients with symptomatic moderate or severe stenosis. North American Symptomatic Carotid Endarterectomy Trial Collaborators. N Engl J Med 1998;339:1415-1425.

Beaussier H, Masson I, Collin C, Bozec E, Laloux B, Calvet D, Zidi M, Boutouyrie P, Laurent S. Carotid plaque, arterial stiffness gradient, and remodeling in hypertension. Hypertension 2008;52:729-736.

Beaussier H, Naggara O, Calvet D, Joannides R, Guegan-Massardier E, Gerardin E, Iacob M, Laloux B, Bozec E, Bellien J, Touze E, Masson I, Thuillez C, Oppenheim C, Boutouyrie P, Laurent S. Mechanical and structural characteristics of carotid plaques by combined analysis with echotracking system and MR imaging. JACC Cardiovasc Imaging 2011;4:468-477.

Biasi GM, Sampaolo A, Mingazzini P, De Amicis P, El-Barghouty N, Nicolaides AN. Computer analysis of ultrasonic plaque echolucency in identifying high risk carotid bifurcation lesions. Eur J Vasc Endovasc Surg 1999;17:476-479.

Bonithon-Kopp C, Touboul PJ, Berr C, Leroux C, Mainard F, Courbon D, Ducimetiere P. Relation of intima-media thickness to atherosclerotic plaques in carotid arteries. The Vascular Aging (EVA) Study. Arterioscler Thromb Vasc Biol 1996;16:310-316.

Bots ML, Groenewegen KA, Anderson TJ, Britton AR, Dekker JM, Engstrom G, Evans GW, de Graaf J, Grobbee DE, Hedblad B, Hofman A, Holewijn S, Ikeda A, Kavousi M, Kitagawa K, Kitamura A, Ikram MA, Lonn EM, Lorenz MW, Mathiesen EB, Nijpels G, Okazaki S, O'Leary DH, Polak JF, Price JF, Robertson C, Rembold CM, Rosvall M, Rundek T, Salonen JT, Sitzer M, Stehouwer CD, Franco OH, Peters SA, den Ruijter HM. Common carotid intima-media thickness measurements do not improve cardiovascular risk prediction in individuals with elevated blood pressure: the USE-IMT collaboration. Hypertension 2014;63:1173-1181.

Cappendijk VC, Cleutjens KB, Heeneman S, Schurink GW, Welten RJ, Kessels AG, van Suylen RJ, Daemen MJ, van Engelshoven JM, Kooi ME. In vivo detection of hemorrhage in human atherosclerotic plaques with magnetic resonance imaging. J Magn Reson Imaging 2004;20:105-110.

Cappendijk VC, Cleutjens KB, Kessels AG, Heeneman S, Schurink GW, Welten RJ, Mess WH, Daemen MJ, van Engelshoven JM, Kooi ME. Assessment of human atherosclerotic carotid plaque components with multisequence MR imaging: initial experience. Radiology 2005;234:487-492.

den Ruijter HM, Peters SA, Groenewegen KA, Anderson TJ, Britton AR, Dekker JM, Engstrom G, Eijkemans MJ, Evans GW, de Graaf J, Grobbee DE, Hedblad B, Hofman A, Holewijn S, Ikeda A, Kavousi M, Kitagawa K, Kitamura A, Koffijberg H, Ikram MA, Lonn EM, Lorenz MW, Mathiesen EB, Nijpels G, Okazaki S, O'Leary DH, Polak JF, Price JF, Robertson C, Rembold CM, Rosvall M, Rundek T, Salonen JT, Sitzer M, Stehouwer CD, Witteman JC, Moons KG, Bots ML. Common carotid intima-media thickness does not add to Framingham risk score in individuals with diabetes mellitus: the USE-IMT initiative. Diabetologia 2013;56:1494-1502.

El-Barghouty NM, Levine T, Ladva S, Flanagan A, Nicolaides A. Histological verification of computerised carotid plaque characterisation. Eur J Vasc Endovasc Surg 1996;11:414-416.

European Carotid Surgery Trialists' Collaborative G. Randomised trial of endarterectomy for recently symptomatic carotid stenosis: final results of the MRC European Carotid Surgery Trial (ECST). The Lancet 1998;351:1379-1387.

Glagov S, Bassiouny HS, Sakaguchi Y, Goudet CA, Vito RP. Mechanical determinants of plaque modeling, remodeling and disruption. Atherosclerosis 1997;131 Suppl:S13-14.

Goncalves I, Lindholm MW, Pedro LM, Dias N, Fernandes e Fernandes J, Fredrikson GN, Nilsson J, Moses J, Ares MP. Elastin and calcium rather than collagen or lipid content are associated with echogenicity of human carotid plaques. Stroke 2004;35:2795-2800.

Grant EG, Benson CB, Moneta GL, Alexandrov AV, Baker JD, Bluth EI, Carroll BA, Eliasziw M, Gocke J, Hertzberg BS, Katarick S, Needleman L, Pellerito J, Polak JF, Rholl KS, Wooster DL, Zierler E, Society of Radiologists in U. Carotid artery stenosis: grayscale and Doppler ultrasound diagnosis--Society of Radiologists in Ultrasound consensus conference. Ultrasound Q 2003;19:190-198.

Gronholdt ML, Nordestgaard BG, Schroeder TV, Vorstrup S, Sillesen H. Ultrasonic echolucent carotid plaques predict future strokes. Circulation 2001;104:68-73.

Gupta A, Kesavabhotla K, Baradaran H, Kamel H, Pandya A, Giambrone AE, Wright D, Pain KJ, Mtui EE, Suri JS, Sanelli PC, Mushlin AI. Plaque echolucency and stroke risk in asymptomatic carotid stenosis: a systematic review and meta-analysis. Stroke 2015;46:91-97.

Hegele RA, Al-Shali K, Khan HMR, Hanley AJG, Harris SB, Mamakeesick M, Zinman B, Fenster A, Spence JD, House AA. Carotid Ultrasound in One, Two and Three Dimensions. Vasc Dis Prev 2005;2:87-91.

Hoeks AP, Reesink KD, Hermeling E, Reneman RS. Local blood pressure rather than shear stress should be blamed for plaque rupture. J Am Coll Cardiol 2008;52:1107-1108; author reply 1108-1109.

Jensen JA, Nikolov SI, Gammelmark KL, Pedersen MH. Synthetic aperture ultrasound imaging. Ultrasonics 2006;44 Suppl 1:e5-15.

Lal BK, Hobson RW, 2nd, Pappas PJ, Kubicka R, Hameed M, Chakhtoura EY, Jamil Z, Padberg FT, Jr., Haser PB, Duran WN. Pixel distribution analysis of B-mode ultrasound scan images predicts histologic features of atherosclerotic carotid plaques. J Vasc Surg 2002;35:1210-1217.

Leone N, Ducimetiere P, Gariepy J, Courbon D, Tzourio C, Dartigues JF, Ritchie K, Alperovitch A, Amouyel P, Safar ME, Zureik M. Distension of the carotid artery and risk of coronary events: the three-city study. Arterioscler Thromb Vasc Biol 2008;28:1392-1397.

Liang YL, Shiel LM, Teede H, Kotsopoulos D, McNeil J, Cameron JD, McGrath BP. Effects of Blood Pressure, Smoking, and Their Interaction on Carotid Artery Structure and Function. Hypertension 2001;37:6-11.

Lorenz MW, Schaefer C, Steinmetz H, Sitzer M. Is carotid intima media thickness useful for individual prediction of cardiovascular risk? Ten-year results from the Carotid Atherosclerosis Progression Study (CAPS). Eur Heart J 2010;31:2041-2048.

Lusis AJ. Atherosclerosis. Nature 2000;407:233-241.

Mathiesen EB, Bonaa KH, Joakimsen O. Echolucent plaques are associated with high risk of ischemic cerebrovascular events in carotid stenosis: the tromso study. Circulation 2001;103:2171-2175.

Meinders JM, Brands PJ, Willigers JM, Kornet L, Hoeks AP. Assessment of the spatial homogeneity of artery dimension parameters with high frame rate 2-D B-mode. Ultrasound Med Biol 2001;27:785-794.

Naghavi M, Libby P, Falk E, Casscells SW, Litovsky S, Rumberger J, Badimon JJ, Stefanadis C, Moreno P, Pasterkamp G, Fayad Z, Stone PH, Waxman S, Raggi P, Madjid M, Zarrabi A, Burke A, Yuan C, Fitzgerald PJ, Siscovick DS, de Korte CL, Aikawa M, Juhani Airaksinen KE, Assmann G, Becker CR, Chesebro JH, Farb A, Galis ZS, Jackson C, Jang IK, Koenig W, Lodder RA, March K, Demirovic J, Navab M, Priori SG, Rekhter MD, Bahr R, Grundy SM, Mehran R, Colombo A, Boerwinkle E, Ballantyne C, Insull W, Jr., Schwartz RS, Vogel R, Serruys PW, Hansson GK, Faxon DP, Kaul S, Drexler H, Greenland P, Muller JE, Virmani R, Ridker PM, Zipes DP, Shah PK, Willerson JT. From vulnerable plaque to vulnerable patient: a call for new definitions and risk assessment strategies: Part I. Circulation 2003;108:1664-1672.

Nichols WW, O'Rourke MF, Vlachopoulos C. McDonald's blood flow in arteries : theoretic, experimental, and clinical principles. 6th. Hodder Arnold, London, 2011.

North American Symptomatic Carotid Endarterectomy Trial C. Beneficial effect of carotid endarterectomy in symptomatic patients with high-grade carotid stenosis. N Engl J Med 1991;325:445-453.

O'Leary DH, Polak JF, Kronmal RA, Manolio TA, Burke GL, Wolfson SK, Jr. Carotid-artery intima and media thickness as a risk factor for myocardial infarction and stroke in older adults. Cardiovascular Health Study Collaborative Research Group. N Engl J Med 1999;340:14-22.

Paini A, Boutouyrie P, Calvet D, Zidi M, Agabiti-Rosei E, Laurent S. Multiaxial mechanical characteristics of carotid plaque: analysis by multiarray echotracking system. Stroke 2007;38:117-123.

Persson J, Formgren J, Israelsson B, Berglund G. Ultrasound-determined intima-media thickness and atherosclerosis. Direct and indirect validation. Arterioscler Thromb 1994;14:261-264.

Roquer J, Segura T, Serena J, Cuadrado-Godia E, Blanco M, Garcia-Garcia J, Castillo J, Study A. Value of carotid intima-media thickness and significant carotid stenosis as markers of stroke recurrence. Stroke 2011;42:3099-3104.

Rothwell PM, Eliasziw M, Gutnikov SA, Fox AJ, Taylor DW, Mayberg MR, Warlow CP, Barnett HJM. Analysis of pooled data from the randomised controlled trials of endarterectomy for symptomatic carotid stenosis. The Lancet 2003;361:107-116.

Rothwell PM, Eliasziw M, Gutnikov SA, Warlow CP, Barnett HJM. Endarterectomy for symptomatic carotid stenosis in relation to clinical subgroups and timing of surgery. The Lancet 2004;363:915-924.

Rundek T, Gardener H, Della-Morte D, Dong C, Cabral D, Tiozzo E, Roberts E, Crisby M, Cheung K, Demmer R, Elkind MS, Sacco RL, Desvarieux M. The relationship between carotid intima-media thickness and carotid plaque in the Northern Manhattan Study. Atherosclerosis 2015;241:364-370.

Saam T, Ferguson MS, Yarnykh VL, Takaya N, Xu D, Polissar NL, Hatsukami TS, Yuan C. Quantitative evaluation of carotid plaque composition by in vivo MRI. Arterioscler Thromb Vasc Biol 2005;25:234-239.

Sabeti S, Schillinger M, Mlekusch W, Willfort A, Haumer M, Nachtmann T, Mullner M, Lang W, Ahmadi R, Minar E. Quantification of internal carotid artery stenosis with duplex US: comparative analysis of different flow velocity criteria. Radiology 2004;232:431-439.

Schreuder FH, Mess WH, Hoeks AP. Ageing affects the accuracy of duplex ultrasonography in grading carotid artery stenosis. Cerebrovasc Dis 2009;27:75-83.

Silvestrini M, Cagnetti C, Pasqualetti P, Albanesi C, Altamura C, Lanciotti C, Bartolini M, Mattei F, Provinciali L, Vernieri F. Carotid wall thickness and stroke risk in patients with asymptomatic internal carotid stenosis. Atherosclerosis 2010;210:452-457.

Spence JD. The importance of distinguishing between diffuse carotid intima-media thickening and focal plaque. Can J Cardiol 2008;24:61C-64C.

Spence JD, Hegele RA. Noninvasive phenotypes of atherosclerosis: similar windows but different views. Stroke 2004;35:649-653.

Staikov IN, Arnold M, Mattle HP, Remonda L, Sturzenegger M, Baumgartner RW, Schroth G. Comparison of the ECST, CC, and NASCET grading methods and ultrasound for assessing carotid stenosis. European Carotid Surgery Trial. North American Symptomatic Carotid Endarterectomy Trial. J Neurol 2000;247:681-686.

Sztajzel R, Momjian S, Momjian-Mayor I, Murith N, Djebaili K, Boissard G, Comelli M, Pizolatto G. Stratified gray-scale median analysis and color mapping of the carotid plaque: correlation with endarterectomy specimen histology of 28 patients. Stroke 2005;36:741-745.

Talelli P, Terzis G, Katsoulas G, Chrisanthopoulou A, Ellul J. Recurrent stroke: the role of common carotid artery intima-media thickness. J Clin Neurosci 2007;14:1067-1072.

Tanter M, Fink M. Ultrafast imaging in biomedical ultrasound. IEEE Trans Ultrason Ferroelectr Freq Control 2014;61:102-119.

Tegos TJ, Sohail M, Sabetai MM, Robless P, Akbar N, Pare G, Stansby G, Nicolaides AN. Echomorphologic and histopathologic characteristics of unstable carotid plaques. AJNR Am J Neuroradiol 2000;21:1937-1944.

Topakian R, King A, Kwon SU, Schaafsma A, Shipley M, Markus HS, Investigators A. Ultrasonic plaque echolucency and emboli signals predict stroke in asymptomatic carotid stenosis. Neurology 2011;77:751-758.

Truijman MT, Kooi ME, van Dijk AC, de Rotte AA, van der Kolk AG, Liem MI, Schreuder FH, Boersma E, Mess WH, van Oostenbrugge RJ, Koudstaal PJ, Kappelle LJ, Nederkoorn PJ, Nederveen AJ, Hendrikse J, van der Steen AF, Daemen MJ, van der Lugt A. Plaque At RISK (PARISK): prospective multicenter study to improve diagnosis of high-risk carotid plaques. Int J Stroke 2014;9:747-754.

Tsivgoulis G, Vemmos K, Papamichael C, Spengos K, Manios E, Stamatelopoulos K, Vassilopoulos D, Zakopoulos N. Common carotid artery intima-media thickness and the risk of stroke recurrence. Stroke 2006;37:1913-1916.

van den Oord SC, Sijbrands EJ, ten Kate GL, van Klaveren D, van Domburg RT, van der Steen AF, Schinkel AF. Carotid intima-media thickness for cardiovascular risk assessment: systematic review and meta-analysis. Atherosclerosis 2013;228:1-11.

van Sloten TT, Schram MT, van den Hurk K, Dekker JM, Nijpels G, Henry RM, Stehouwer CD. Local stiffness of the carotid and femoral artery is associated with incident cardiovascular events and all-cause mortality: the Hoorn study. J Am Coll Cardiol 2014;63:1739-1747.

Virmani R, Burke AP, Farb A, Kolodgie FD. Pathology of the vulnerable plaque. J Am Coll Cardiol 2006;47:C13-18.

Virmani R, Kolodgie FD, Burke AP, Farb A, Schwartz SM. Lessons from sudden coronary death: a comprehensive morphological classification scheme for atherosclerotic lesions. Arterioscler Thromb Vasc Biol 2000;20:1262-1275.

Yuan C, Mitsumori LM, Ferguson MS, Polissar NL, Echelard D, Ortiz G, Small R, Davies JW, Kerwin WS, Hatsukami TS. In vivo accuracy of multispectral magnetic resonance imaging for identifying lipid-rich necrotic cores and intraplaque hemorrhage in advanced human carotid plaques. Circulation 2001;104:2051-2056.

Summary

Summary

In Europe, around 1 million people die annually of stroke which is the second most common cause of death (Nichols et al. 2012). The most common type of stroke is an ischemic stroke, caused by an occluded artery due to a thrombosis or embolism. 15-20% of ischemic strokes are caused by the rupture of a vulnerable atherosclerotic plaque in the carotid bifurcation or internal carotid artery (Chaturvedi et al. 2005). In the Netherlands, around 6,000 people die annually of ischemic stroke and around 33,000 people are annually hospitalized for more than one day (Koopman et al. 2014), leading to high health care costs.

To prevent a stroke or transient ischemic attack (TIA), patients are either only medically treated, i.e., with cholesterol synthesis inhibitors (statins) and anti-thrombotic therapy, or are additionally selected for a carotid endarterectomy (CEA). During a CEA procedure, the atherosclerotic plaque is surgically removed. Current clinical guidelines only consider the degree of stenosis when selecting patients for CEA. Previous trials have shown that patients with more than 70% degree of stenosis benefit from CEA (number to treat = 6), whereas patients with a 50-70% degree of stenosis only moderately benefit from CEA (Barnett et al. 1998; Rothwell et al. 2003). The benefit of surgery is also related to age and the time between the ischemic stroke or TIA and the CEA (Rothwell et al. 2004a; Rothwell et al. 2004b). However, it has been reported that 15% of the medically treated women with a moderate stenosis (50-69%) will experience a recurrent ipsilateral stroke within five years after the first event (Barnett et al. 1998). Nowadays, the risk of recurrent stroke is lower due to better medical treatment (Park and Ovbiagele 2015), which challenges the effectiveness of CEA and, hence, requires the best possible selection of patients who will undergo surgery.

The possibility to assess the risk of plaque rupture will have tremendous impact in clinical decision making and may help to reduce healthcare costs. Previous studies have shown a good correlation between imaging to assess plaque vulnerability and histological and/or clinical characteristics. However, these studies considered only one or two non-invasive imaging techniques in relatively small cohorts and did not deliver the necessary evidence to change the current clinical guidelines (Nederlandse vereniging voor Neurologie 2008).

The Plaque At RISK (PARISK) study aims to evaluate plaques at risk with multiple non-invasive imaging techniques to improve identification of patients at increased risk of stroke, even before a first stroke or TIA has occurred (Truijman et al. 2014). PARISK is an ongoing, multicenter follow-up study. Patients who recently had an ischemic stroke or a TIA and had a mild-to-moderate stenosis (30-70%) in the ipsilateral internal carotid artery are included within three months after the clinical event. Participants do receive medical treatment and are enrolled in a 2-year follow-up study.

Ultrasound imaging is affordable and versatile, widely accessible and can be used readily after observation of complaints. Therefore, the present PhD thesis focuses on extraction of morphological and mechanical properties by means of ultrasound recordings of carotid arteries and plaques, to improve non-invasive characterization of plaques at risk. For this purpose, we developed and validated image analysis programs to determine miscellaneous carotid

artery properties, such as diameter, distension and intima-media thickness, with a novel edge detection technique applied to standard ultrasound echo images as recorded in the clinic, favoring widespread application.

To support thorough understanding of all chapters of this thesis, **Chapter 2** provides a description of the underlying ultrasound principles.

Since the internal carotid artery (ICA) is located deeply and is usually curved and angulated with respect to the line of sight, we have validated our edge tracking method for the relatively straight common carotid artery (CCA). The local diameter change over the cardiac cycle (distension) is commonly extracted with radiofrequency phase tracking applied to high frame rate echo recordings (>300 fps) (Meinders et al. 2001). Because this technique requires an expensive and dedicated ultrasound machine, its application is restricted to a limited number of specialized hospitals. We show in **Chapter 3** that the local diameter and distension can also be extracted with edge tracking applied to standard echo recordings acquired at a video frame rate of approximately 40 fps. In a relevant patient population (N=30) the CCA distension obtained with edge tracking is as precise and accurate as the CCA distension obtained with radiofrequency phase tracking. Since our proposed method based on standard equipment functions properly in this technically most challenging patient group, it allows more widespread use of distension recordings.

Mean or maximal intima-media thickness (IMT) are not suitable to predict the risk of cardiovascular events for an individual patient (Lorenz et al. 2010; den Ruijter et al. 2013; van den Oord et al. 2013; Bots et al. 2014). However, the spatial inhomogeneity of the IMT, a measure of the irregularity, could be a promising alternative. We showed in **Chapter 4** that common carotid arteries with a high relative IMT inhomogeneity are associated with a larger median IMT, distension inhomogeneity and degree of ICA stenosis. Furthermore, after adjustment for traditional risk factors, relative IMT inhomogeneity remains independently associated with the degree of ICA stenosis.

Mean or maximal IMT is commonly used as surrogate endpoint in intervention studies. However, the effect of normalization to surrounding IMT, to median IMT, or to diameter is unknown. In addition, it is unclear whether IMT inhomogeneity is a useful predictor beyond common arterial wall parameters like maximal wall thickness, whether absolute or normalized to IMT or to lumen size. Therefore, we compared multiple wall thickness parameters of the CCA in relation to the degree of ipsilateral ICA stenosis in **Chapter 5.** Mainly CCA plaques dominate the association with the degree of ipsilateral ICA stenosis. Henceforth, IMT inhomogeneity does not add extra information on top of maximal IMT. An important finding is that risk classification for having a distal moderate stenosis (>50%) is affected, when wall thickness relative to the actual CCA adventitia-adventitia diameter is considered rather than its absolute value. It is more reasonable to normalize maximal wall thickness to end-diastolic adventitia-adventitia diameter rather than to surrounding IMT, affecting risk classification.

CCA rise time characteristics of the distension waveform may be influenced by pressure wave reflections from distal plaques. Therefore, we investigated the associations between CCA rise time characteristics, degree of ICA stenosis and MRI plaque features in **Chapter 6.** CCA risetime inhomogeneity is significantly higher for stable plaques as compared to vulnerable ICA plaques (lipid-rich necrotic core >10% and thin/ruptured fibrous cap). Surprisingly, for the latter group the risetime inhomogeneity was close to baseline indicating a cushioning effect of the lipid-rich necrotic core on wave reflection. This might offer a non-invasive and inexpensive method to characterize the composition/stability of distal plaques.
For proper assessment of local morphological and dynamic parameters of the artery, distance measurements should preferentially be considered along the artery radius. Therefore, we introduced the concept of orthogonal distance measurements in **Chapter 7**. To make a step towards wall tracking of a carotid bifurcation with plaques, we considered CCA plaques in a relatively small cohort (N=23). Since automatic edge detection in the presence of plaques is challenging, vessel wall and CCA plaques were manually segmented. We demonstrated the feasibility to extract orthogonal dimensions of the CCA and plaques. At the site of the plaque the orthogonal lumen diameter was significantly smaller than the vertical lumen diameter, i.e., along the line of view. However, the proposed approach, because of its poor precision, appears inadequate to establish plaque compression. Surprisingly, the CCA plaques in our population did not show evidence of outward remodeling. In addition, orthogonal relative lumen distension was significantly lower for artery segments with echogenic plaques, indicating a higher stiffness, than those with echolucent plaques.

In **Chapter 8**, an overall discussion of the major findings and final conclusion of the PhD thesis are presented. In addition, future perspectives for integrated morphological and dynamic characterization of plaques are described.

References

Barnett HJ, Taylor DW, Eliasziw M, Fox AJ, Ferguson GG, Haynes RB, Rankin RN, Clagett GP, Hachinski VC, Sackett DL, Thorpe KE, Meldrum HE, Spence JD. Benefit of carotid endarterectomy in patients with symptomatic moderate or severe stenosis. North American Symptomatic Carotid Endarterectomy Trial Collaborators. N Engl J Med 1998;339:1415-1425.

Bots ML, Groenewegen KA, Anderson TJ, Britton AR, Dekker JM, Engstrom G, Evans GW, de Graaf J, Grobbee DE, Hedblad B, Hofman A, Holewijn S, Ikeda A, Kavousi M, Kitagawa K, Kitamura A, Ikram MA, Lonn EM, Lorenz MW, Mathiesen EB, Nijpels G, Okazaki S, O'Leary DH, Polak JF, Price JF, Robertson C, Rembold CM, Rosvall M, Rundek T, Salonen JT, Sitzer M, Stehouwer CD, Franco OH, Peters SA, den Ruijter HM. Common carotid intima-media thickness measurements do not improve cardiovascular risk prediction in individuals with elevated blood pressure: the USE-IMT collaboration. Hypertension 2014;63:1173-1181.

Chaturvedi S, Bruno A, Feasby T, Holloway R, Benavente O, Cohen SN, Cote R, Hess D, Saver J, Spence JD, Stern B, Wilterdink J, Therapeutics, Technology Assessment Subcommittee of the American Academy of N. Carotid endarterectomy--an evidence-based review: report of the Therapeutics and Technology Assessment Subcommittee of the American Academy of Neurology. Neurology 2005;65:794-801.

den Ruijter HM, Peters SA, Groenewegen KA, Anderson TJ, Britton AR, Dekker JM, Engstrom G, Eijkemans MJ, Evans GW, de Graaf J, Grobbee DE, Hedblad B, Hofman A, Holewijn S, Ikeda A, Kavousi M, Kitagawa K, Kitamura A, Koffijberg H, Ikram MA, Lonn EM, Lorenz MW, Mathiesen EB, Nijpels G, Okazaki S, O'Leary DH, Polak JF, Price JF, Robertson C, Rembold CM, Rosvall M, Rundek T, Salonen JT, Sitzer M, Stehouwer CD, Witteman JC, Moons KG, Bots ML. Common carotid intima-media thickness does not add to Framingham risk score in individuals with diabetes mellitus: the USE-IMT initiative. Diabetologia 2013;56:1494-1502.

Koopman C, van Dis I, Vaartjes I, Visseren FLJ, Bots ML. Hart- en vaatziekten in Nederland 2014, cijfers over kwaliteit van leven, ziekte en sterfte. 2014

Lorenz MW, Schaefer C, Steinmetz H, Sitzer M. Is carotid intima media thickness useful for individual prediction of cardiovascular risk? Ten-year results from the Carotid Atherosclerosis Progression Study (CAPS). Eur Heart J 2010;31:2041-2048.

Meinders JM, Brands PJ, Willigers JM, Kornet L, Hoeks AP. Assessment of the spatial homogeneity of artery dimension parameters with high frame rate 2-D B-mode. Ultrasound Med Biol 2001;27:785-794.

Nederlandse vereniging voor Neurologie. Richtlijn Diagnostiek, behandeling en zorg voor patienten met een beroerte. 2008

Nichols M, Townsend N, Luengo-Fernandez R, Leal J, Gray A, Scarborough P, Rayner M. European cardiovascular disease statistics 2012. European Heart Network, Brussels, European Society of Cardiology, Sophia Antipolis 2012;

Park JH, Ovbiagele B. Optimal combination secondary prevention drug treatment and stroke outcomes. Neurology 2015;84:50-56.

Rothwell PM, Eliasziw M, Gutnikov SA, Fox AJ, Taylor DW, Mayberg MR, Warlow CP, Barnett HJM. Analysis of pooled data from the randomised controlled trials of endarterectomy for symptomatic carotid stenosis. The Lancet 2003;361:107-116.

Rothwell PM, Eliasziw M, Gutnikov SA, Warlow CP, Barnett HJ. Sex difference in the effect of time from symptoms to surgery on benefit from carotid endarterectomy for transient ischemic attack and nondisabling stroke. Stroke 2004a;35:2855-2861.

Rothwell PM, Eliasziw M, Gutnikov SA, Warlow CP, Barnett HJM. Endarterectomy for symptomatic carotid stenosis in relation to clinical subgroups and timing of surgery. The Lancet 2004b;363:915-924.

Truijman MT, Kooi ME, van Dijk AC, de Rotte AA, van der Kolk AG, Liem MI, Schreuder FH, Boersma E, Mess WH, van Oostenbrugge RJ, Koudstaal PJ, Kappelle LJ, Nederkoorn PJ, Nederveen AJ, Hendrikse J, van der Steen AF, Daemen MJ, van der Lugt A. Plaque At RISK (PARISK): prospective multicenter study to improve diagnosis of high-risk carotid plaques. Int J Stroke 2014;9:747-754.

van den Oord SC, Sijbrands EJ, ten Kate GL, van Klaveren D, van Domburg RT, van der Steen AF, Schinkel AF. Carotid intima-media thickness for cardiovascular risk assessment: systematic review and meta-analysis. Atherosclerosis 2013;228:1-11.

Samenvatting

Samenvatting

In Europa sterven per jaar ongeveer 1 miljoen mensen aan een beroerte (Nichols et al. 2012). In Nederland overlijden er ongeveer 6.000 mensen per jaar ten gevolge van een ischemische beroerte en ongeveer 33.000 mensen per jaar moeten meer dan één dag in het ziekenhuis verblijven (Koopman et al. 2014), wat leidt tot hoge zorgkosten. Bij een beroerte wordt een arterie afgesloten door een bloedstolsel waardoor een gedeelte van de hersenen niet meer (voldoende) bloed, en dus zuurstof, krijgt (ischemische beroerte). Voor 15-20% van de ischemische beroertes zijn de bloedstolsels afkomstig van een opengescheurde atherosclerotische plaque in de vertakking van de halsslagader of interne halsslagader (Chaturvedi et al. 2005). Een plaque ontstaat geleidelijk na een ontsteking van de vaatwand en leidt tot versnelde opname van cholesterol, een lokaal stijvere vaatwand (atherosclerose) en afname van de doorstroomopening (stenose).

Om een beroerte of voorbijgaande ischemische aanval (E: transient ischemic attack ofwel TIA) te voorkomen, worden patiënten ofwel alleen medisch behandeld, bijvoorbeeld met cholesterol synthese remmers (statines) en anti-stolling therapie, of wordt aanvullend de atherosclerotische plaque chirurgisch verwijderd: carotis endarteriëctomie (CEA). Op dit moment is de selectie van CEA patiënten voor operatie slechts gebaseerd op de graad van de stenose. Of een operatie gunstig is, is ook afhankelijk van leeftijd en de tijd tussen de ischemische beroerte of TIA en de CEA (Rothwell et al. 2004a; Rothwell et al. 2004b). Eerdere klinische studies hebben laten zien dat patiënten met meer dan 70% stenose vernauwing inderdaad profijt hebben van een CEA. Daarbij moeten minstens 6 patiënten geopereerd worden om één vervolgberoerte te vóórkomen (Rothwell et al. 2003). Alleen mannen met een 50-70% vernauwing profiteren slechts matig van een CEA, vrouwen helemaal niet (Barnett et al. 1998; Rothwell et al. 2003). 15% van de medisch behandelde vrouwen met een matige stenose (50-69%) zou binnen 5 jaar na de eerste beroerte of TIA opnieuw een beroerte in dezelfde hersenhelft krijgen (Barnett et al. 1998). Tegenwoordig is het risico op een vervolgberoerte lager vanwege betere medische behandeling (Park and Ovbiagele 2015), waardoor de relatieve effectiviteit van een CEA mogelijk verslechterd is. Vanwege het operatierisico en de kans op succes zou een betere selectie van patiënten voor een operatie moeten plaats vinden en niet alleen afhankelijk moeten zijn van de mate van vernauwing.

Ischemische beroertes ontstaan voornamelijk door het scheuren van een plaque. De mogelijkheid om het risico op het scheuren van een plaque vast te stellen zou daarom een enorme impact op de klinische besluitvorming hebben en de zorgkosten reduceren. Eerdere studies hebben laten zien dat beeldvormende technieken de potentie hebben om de kwetsbaarheid van een plaque vast te stellen, in overeenstemming met histologische en/of klinische karakteristieken. Echter, deze studies hadden betrekking op een of twee niet-invasieve beeldvormende technieken in relatief kleine patiëntengroepen en leverden niet het nodige bewijs om de huidige klinische richtlijnen te veranderen (Nederlandse vereniging voor Neurologie 2008).

De Plaque At RISK (PARISK) studie is bedoeld om plaques met meerdere niet-invasieve beeldvormende technieken te evalueren zodat patiënten met een hoger risico op een beroerte geïdentificeerd kunnen worden, zelfs voordat de eerste beroerte of TIA heeft plaatsgevonden (Truijman et al. 2014). Patiënten met recentelijk een ischemische beroerte of TIA én een milde tot matige stenose (30-70%) in de interne halsslagader aan dezelfde kant (d.w.z. links of rechts) worden in de studie opgenomen, medisch behandeld en gedurende 2 jaar gevolgd. De kans op een beroerte als gevolg van een instabiele plaque wordt vervolgens afgeleid uit de waarnemingen aan het begin en het eind van de studie in combinatie met het optreden van eventuele volgende beroertes.

Ultrageluid is een beeldvormende techniek die gebaseerd is op de weergave van de echo amplitude (E: brightness- ofwel B-mode) afkomstig van weefselovergangen. Vanwege het relatief goedkope en breed toegankelijke karakter van deze techniek kan deze direct na observatie van klachten worden ingezet. Daarom focust deze thesis op de analyse van echobeelden zoals die met standaard apparatuur kunnen worden opgenomen. Dat laatste is van belang om snel een brede toepassing mogelijk te maken. Om diagnostiek van risicovolle plaques te verbeteren ontwikkelen en valideren we analyseprogramma's voor de bepaling van de morfologische eigenschappen van de halsslagader, zoals wanddikte en diameter, maar ook dynamische/mechanische eigenschappen, zoals de diameterverandering over een hartcyclus (distensie).

Hoofdstuk 2 beschrijft de mogelijkheden (en beperkingen) om met ultrageluid op een niet-invasieve manier informatie over afmetingen en beweging van structuren te verkrijgen. Vanwege de oppervlakkige ligging en oriëntatie (voornamelijk parallel aan de huid) van de gemeenschappelijke halsslagader en zijn vertakking (bifurcatie) in interne en externe halsslagader hebben we gekozen voor een ultrageluidssysteem dat zijn echobeelden opbouwt met parallelle echolijnen (lineair array van transducenten) en een doordringingsdiepte heeft van 3-5 cm.

Aangezien de interne halsslagader (E: internal carotid artery ofwel ICA) tamelijk diep ligt, meestal gebogen is en niet parallel aan de huid ligt, hebben we onze vaatwand detectie methode in eerste instantie gevalideerd voor de relatief rechte gemeenschappelijke halsslagader (E: common carotid artery ofwel CCA). De lokale diameterverandering (distensie) als gevolg van de pulsatiele verandering van de bloeddruk is een belangrijke parameter om slagaderverkalking (atherosclerose) vast te stellen. De distensie wordt meestal bepaald door middel van fase detectie toegepast op de radiofrequente echo signalen. Dit vereist echter een dure en gespecialiseerde ultrageluidmachine die in staat is om meer dan 300 beelden per seconde te genereren (Meinders et al. 2001). Daardoor is een dergelijke toepassing beperkt tot een gelimiteerd aantal gespecialiseerde ziekenhuizen. We laten in **Hoofdstuk 3** zien dat de lokale diameter en distensie ook kunnen worden bepaald uit echo beelden van een standaard echoapparaat met een beeldfrequentie van ongeveer 40 beelden per seconde. Daarbij wordt voor ieder echobeeld de positie van de voor- en achterwand van een bloedvat bepaald. Het onderlinge verschil geeft dan de diameter terwijl uit de verandering daarvan over een reeks van beelden de distensie kan worden afgeleid. In een kleine doch relevante patiënten populatie (N=30) is de CCA distensie, op basis van vaatwand detectie, net zo precies (47 µm precisie)

als de CCA distensie verkregen met radiofrequente fase detectie (44 µm precisie). Omdat in deze technisch moeilijke patiëntengroep onze methode goed functioneert met standaard apparatuur staat niets een brede toepassing van distensie analyse met eenvoudige apparatuur in de weg.

De vaatwand van een halsslagader is grofweg opgebouwd uit een zeer dunne binnenlaag (± 0.02 mm, intima met endotheel laag aan de binnenzijde in contact met het bloed), een elastische middenlaag (media; 0.3-1 mm dik afhankelijk van leeftijd) en een buitenlaag (adventitia) die voornamelijk bindweefsel bevat. De dikte van de intima en media samen neemt geleidelijk met de leeftijd toe (Engelen et al. 2013) en zou indicatief zijn voor het optreden van atherosclerose (Persson et al. 1994; Bonithon-Kopp et al. 1996; Rundek et al. 2015). Op een echobeeld met een goede diepteresolutie zijn, met name van de achterwand, zowel de overgang van de vaatholte (lumen) naar de intima als die van de media naar de adventitia duidelijk te zien als echopieken (Pignoli et al. 1986). De overeenkomstige afstand daartussen is de intima-media dikte (E: intima Media Thickness ofwel IMT). De gemiddelde of maximale IMT zijn ongeschikt gebleken om het risico van toekomstige cardiovasculaire events voor een individuele patiënt te voorspellen (Lorenz et al. 2010; den Ruijter et al. 2013; van den Oord et al. 2013; Bots et al. 2014). Echter, de ontwikkeling van een plaque gaat gepaard met lokale veranderingen van de wanddikte. De spatiele inhomogeniteit van de IMT (een maatstaaf voor een onregelmatige vaatwanddikte; bepaald met de standaard afwijking van de IMT) zou daarom indicatief kunnen zijn voor het risico op cardiovasculaire events. We laten in **Hoofstuk 4** zien dat de gemeenschappelijke halsslagaders met een hoge relatieve IMT inhomogeniteit (>2%) geassocieerd zijn met een hogere graad van ICA stenose (5% groter). Bovendien is, ook na correctie voor traditionele risicofactoren (zoals leeftijd, hoge BMI, roken, diabetes en hoge bloeddruk), de relatieve IMT inhomogeniteit onafhankelijk geassocieerd met de graad van ICA stenose.

De gemiddelde of maximale IMT wordt vaak gebruikt als surrogaat eindpunt in interventie studies. Daarvoor moet men wel een referentie hebben die geldig is voor een brede populatie (mannen/vrouwen, jong/oud) met grote onderlinge verschillen in de afmetingen van de CCA (6-9 mm). Echter, het effect van het normaliseren van de vaatwanddikte op de IMT van een nabijgelegen vaatwand, op de mediaan IMT, of op de diameter is onbekend. Daarnaast is het onduidelijk of IMT inhomogeniteit (**Hoofdstuk 4**) een nuttige voorspeller is naast de vaatwand parameters zoals de maximale IMT, hetzij de absolute waarde daarvan hetzij genormaliseerd op de mediaan IMT of op de (lumen) diameter. In **Hoofdstuk 5** vergelijken we daarom meerdere wanddikte parameters van de CCA in relatie tot de graad van ICA stenose. De aanwezigheid van CCA plaques domineren de associatie met de graad van ICA stenose. Absolute of relatieve IMT inhomogeniteit geeft geen extra informatie bovenop de absolute of relatieve maximale IMT. Een belangrijke bevinding is dat de risicoclassificatie voor het hebben van een matige ICA stenose (>50%) wordt beïnvloed (55 CCAs (15%) worden gereclassificeerd naar een andere risico classificatie waarvan 20 CCAs naar een hoger risico) wanneer de wanddikte relatief t.o.v. de adventitia-adventitia diameter wordt beschouwd in plaats van zijn absolute waarde. Het is derhalve vor de patient relevanter om de maximale IMT te normaliseren op de

eind-diastolische adventitia-adventitia diameter in plaats van op de nabijgelegen IMT omdat de laatste aanzienlijk meer ruis veroorzaakt.

De distensiegolfvorm (distensie als functie van de hartcyclus) heeft grofweg dezelfde vorm als die van de lokale bloeddruk, een snelle stijging van de minimale, diastole, naar de maximale, systole, diameter gevolgd door een geleidelijker afname. Onze echo analyse-techniek geeft voor iedere positie van een arterie segment de distensiegolfvorm en de bijbehorende stijgtijd. De CCA stijgtijd karakteristieken van de distensiegolfvorm worden mogelijk beïnvloed door drukgolfreflecties van ICA plaques. Daarom onderzochten we in **Hoofdstuk 6** de associaties tussen CCA stijgtijd karakteristieken, de graad van ICA stenose en MRI plaque karakteristieken. Met name de CCA stijgtijd-inhomogeniteit (langs het arteriesegment) is significant hoger (verschil 4.4 ms, p=0.001) bij stabiele ICA plaques vergeleken met kwetsbare plaques (vetrijke necrotische kern >10% en dunne/gebroken fibreuze kap). Verassend genoeg was de stijgtijd-inhomogeniteit voor kwetsbare ICA plaques vergelijkbaar met de baseline waarde (beide 14-15 ms) in gevallen waarbij er geen distale plaque was, hetgeen wijst op een dempend effect van de vetrijke necrotische kern op de mate van golfreflectie. Dit biedt mogelijk een niet-invasieve en relatief goedkope methode om de compositie cq de stabiliteit van distale plaques te karakteriseren.

Voor een adequate beoordeling van lokale morfologische en dynamische parameters van een arterie zouden dimensies (en afgeleiden) bepaald moeten worden loodrecht op de as van de arterieholte. Daarom introduceren we in **Hoofdstuk 7** het concept van orthogonale (loodrecht op de as) afstandsmetingen. Voordat we de stap kunnen maken naar orthogonale afstandsmetingen in een gekromde carotis bifurcatie met plaques, hebben we eerst de techniek ontwikkeld voor plaques in de CCA van een relatief klein cohort (N=23). Omdat automatische vaatwand detectie in de aanwezigheid van plaques moeilijk is, worden de vaatwand en CCA plaques handmatig gesegmenteerd. We demonstreerden de haalbaarheid van het bepalen van orthogonale dimensies van de CCA en plaques. Op de plaats van de plaque is de orthogonale lumen diameter significant kleiner dan de lumen diameter langs de echolijnen. Daarentegen blijkt de voorgestelde aanpak, vanwege een te slechte precisie, inadequaat voor de bepaling van diastole-systole plaque compressie. Verassend genoeg vertonen de CCA plaques in onze populatie geen buitenwaartse remodellering, d.w.z. de vaten vertonen geen verwijding van de buitenwand. Daarnaast is de orthogonale relatieve lumen distensie significant lager voor arteriesegmenten met echorijke plaques, wat een indicatie is van een hogere stijfheid, dan voor segmenten met echoarme plaques.

Hoofstuk 8 bevat een discussie van de belangrijkste bevindingen en eindconclusies van de PhD thesis. Daarnaast zijn de mogelijkheden voor een geïntegreerde morfologische en dynamische karakterisatie van plaques beschreven hetgeen mogelijke voorspellers voor het scheuren van een plaque kan opleveren. De voorspellende waarde van vaatwand en plaque eigenschappen voor plaque ontwikkeling en nieuwe beroertes zal worden geëvalueerd in de follow-up fase van de PARISK studie.

Referenties

Barnett HJ, Taylor DW, Eliasziw M, Fox AJ, Ferguson GG, Haynes RB, Rankin RN, Clagett GP, Hachinski VC, Sackett DL, Thorpe KE, Meldrum HE, Spence JD. Benefit of carotid endarterectomy in patients with symptomatic moderate or severe stenosis. North American Symptomatic Carotid Endarterectomy Trial Collaborators. N Engl J Med 1998;339:1415-1425.

Bonithon-Kopp C, Touboul PJ, Berr C, Leroux C, Mainard F, Courbon D, Ducimetiere P. Relation of intima-media thickness to atherosclerotic plaques in carotid arteries. The Vascular Aging (EVA) Study. Arterioscler Thromb Vasc Biol 1996;16:310-316.

Bots ML, Groenewegen KA, Anderson TJ, Britton AR, Dekker JM, Engstrom G, Evans GW, de Graaf J, Grobbee DE, Hedblad B, Hofman A, Holewijn S, Ikeda A, Kavousi M, Kitagawa K, Kitamura A, Ikram MA, Lonn EM, Lorenz MW, Mathiesen EB, Nijpels G, Okazaki S, O'Leary DH, Polak JF, Price JF, Robertson C, Rembold CM, Rosvall M, Rundek T, Salonen JT, Sitzer M, Stehouwer CD, Franco OH, Peters SA, den Ruijter HM. Common carotid intima-media thickness measurements do not improve cardiovascular risk prediction in individuals with elevated blood pressure: the USE-IMT collaboration. Hypertension 2014;63:1173-1181.

den Ruijter HM, Peters SA, Groenewegen KA, Anderson TJ, Britton AR, Dekker JM, Engstrom G, Eijkemans MJ, Evans GW, de Graaf J, Grobbee DE, Hedblad B, Hofman A, Holewijn S, Ikeda A, Kavousi M, Kitagawa K, Kitamura A, Koffijberg H, Ikram MA, Lonn EM, Lorenz MW, Mathiesen EB, Nijpels G, Okazaki S, O'Leary DH, Polak JF, Price JF, Robertson C, Rembold CM, Rosvall M, Rundek T, Salonen JT, Sitzer M, Stehouwer CD, Witteman JC, Moons KG, Bots ML. Common carotid intima-media thickness does not add to Framingham risk score in individuals with diabetes mellitus: the USE-IMT initiative. Diabetologia 2013;56:1494-1502.

Engelen L, Ferreira I, Stehouwer CD, Boutouyrie P, Laurent S, Reference Values for Arterial Measurements C. Reference intervals for common carotid intima-media thickness measured with echotracking: relation with risk factors. Eur Heart J 2013;34:2368-2380.

Koopman C, van Dis I, Vaartjes I, Visseren FLJ, Bots ML. Hart- en vaatziekten in Nederland 2014, cijfers over kwaliteit van leven, ziekte en sterfte. 2014

Lorenz MW, Schaefer C, Steinmetz H, Sitzer M. Is carotid intima media thickness useful for individual prediction of cardiovascular risk? Ten-year results from the Carotid Atherosclerosis Progression Study (CAPS). Eur Heart J 2010;31:2041-2048.

Meinders JM, Brands PJ, Willigers JM, Kornet L, Hoeks AP. Assessment of the spatial homogeneity of artery dimension parameters with high frame rate 2-D B-mode. Ultrasound Med Biol 2001;27:785-794.

Nederlandse vereniging voor Neurologie. Richtlijn Diagnostiek, behandeling en zorg voor patienten met een beroerte. 2008

Park JH, Ovbiagele B. Optimal combination secondary prevention drug treatment and stroke outcomes. Neurology 2015;84:50-56.

Persson J, Formgren J, Israelsson B, Berglund G. Ultrasound-determined intima-media thickness and atherosclerosis. Direct and indirect validation. Arterioscler Thromb 1994;14:261-264.

Pignoli P, Tremoli E, Poli A, Oreste P, Paoletti R. Intimal plus medial thickness of the arterial wall: a direct measurement with ultrasound imaging. Circulation 1986;74:1399-1406.

Rothwell PM, Eliasziw M, Gutnikov SA, Fox AJ, Taylor DW, Mayberg MR, Warlow CP, Barnett HJM. Analysis of pooled data from the randomised controlled trials of endarterectomy for symptomatic carotid stenosis. The Lancet 2003;361:107-116.

Rothwell PM, Eliasziw M, Gutnikov SA, Warlow CP, Barnett HJ. Sex difference in the effect of time from symptoms to surgery on benefit from carotid endarterectomy for transient ischemic attack and nondisabling stroke. Stroke 2004a;35:2855-2861.

Rothwell PM, Eliasziw M, Gutnikov SA, Warlow CP, Barnett HJM. Endarterectomy for symptomatic carotid stenosis in relation to clinical subgroups and timing of surgery. The Lancet 2004b;363:915-924.

Rundek T, Gardener H, Della-Morte D, Dong C, Cabral D, Tiozzo E, Roberts E, Crisby M, Cheung K, Demmer R, Elkind MS, Sacco RL, Desvarieux M. The relationship between carotid intima-media thickness and carotid plaque in the Northern Manhattan Study. Atherosclerosis 2015;241:364-370.

Truijman MT, Kooi ME, van Dijk AC, de Rotte AA, van der Kolk AG, Liem MI, Schreuder FH, Boersma E, Mess WH, van Oostenbrugge RJ, Koudstaal PJ, Kappelle LJ, Nederkoorn PJ, Nederveen AJ, Hendrikse J, van der Steen AF, Daemen MJ, van der Lugt A. Plaque At RISK (PARISK): prospective multicenter study to improve diagnosis of high-risk carotid plaques. Int J Stroke 2014;9:747-754.

van den Oord SC, Sijbrands EJ, ten Kate GL, van Klaveren D, van Domburg RT, van der Steen AF, Schinkel AF. Carotid intima-media thickness for cardiovascular risk assessment: systematic review and meta-analysis. Atherosclerosis 2013;228:1-11.

Valorisation

Valorisation

Relevance

In Europe, around 1.1 million people die annually of stroke, which is the second most common cause of death (Nichols 2012) The estimated total cost for the EU economy due to stroke is over 38 billion Euros a year (Nichols 2012). In the Netherlands, around 6,000 people die annually of ischemic stroke and around 33,000 people are hospitalized annually, excluding day care (Koopman et al. 2014). The high costs of stroke are not only due to healthcare costs but also include substantial productivity losses and informal care of stroke patients.

The most common type of stroke is ischemic stroke, caused by an occluded artery due to thrombosis or embolism. Ischemic strokes (15-20%) predominantly originate from rupture of a vulnerable atherosclerotic plaque in the carotid bifurcation or internal carotid artery (ICA) (Chaturvedi et al. 2005), resulting in the release of thrombogenic material and subsequent thrombus formation. The possibility to assess the risk of rupture of a plaque will have tremendous impact in clinical decision making. Although many studies focus on the assessment of plaques at risk, diagnosing impending plaque rupture is still a problem today.

To prevent the patient from suffering symptoms caused by a vulnerable plaque, the plaque can be removed by a surgeon during carotid endarterectomy (CEA). Despite the overt role of plaque morphology nowadays, clinical guidelines only take the luminal narrowing by a plaque into account to select patients eligible for surgery. Previous studies concluded that it is beneficial to operate patients who (1) have experienced a stroke or transient ischemic attack (TIA), (2) have plaques in the carotid bifurcation, and (3) have a severe stenosis (luminal narrowing >70%). Patients with a mild-to-moderate plaque (30-70%) only have a marginal to moderate benefit from CEA. Therefore, these patients usually are medically treated. Nowadays, the risk of recurrent stroke is lower due to better medical treatment (Park and Ovbiagele 2015), which challenges the effectiveness of CEA demanding the best possible selection of patients for surgery. To reduce health costs and provide a better health care (Buisman et al. 2015), indicators to predict individually the risk of plaque rupture are necessary.

Previous studies have shown a good correlation between non-invasive imaging and histology and/or clinical characteristics. However, these studies employed only one or two imaging techniques in relatively small cohorts and did not deliver the necessary evidence to change the current clinical guidelines (Nederlandse Vereniging voor Neurologie 2008). The PARISK (Plaque At RISK) research program is a longitudinal study (baseline and follow-up after 2 years) aimed to evaluate plaques at risk with multiple non-invasive imaging techniques such as ultrasound, MRI, CT and PET. The main advantage of the PARISK study is the use of multiple non-invasive imaging techniques, thereby enabling comparison. Since patients with mild-to-moderate stenosis only marginally or moderately benefit from CEA, PARISK concentrates on this patient group. The present thesis primarily focuses on ultrasound imaging to detect a vulnerable plaque. The main advantage of ultrasound is that it is affordable and can be used readily after anamnestic assessment of symptoms. Ultrasound provides information about the mechanical and morphological characteristics of a blood vessel or plaque. Furthermore, ultrasound can also provide information about plaque composition due to the grey

values of the plaque. Therefore, it would be beneficial for healthcare and healthcare costs to predict the risk of plaque rupture with ultrasound.

The results of this thesis are of interest for many professionals. The mechanism of plaque development is still unclear, especially shortly after stroke. Ultrasound provides a good platform for repeated examinations within a short time window to observe changes in morphological and functional characteristics of plaques immediately after stroke. Thereby, repeated ultrasound measurements may enhance the understanding of the mechanisms leading to plaque progression and regression. Since this thesis only pertains to the baseline results of the PARISK study, other scientists will have to complete the follow-up study to firmly establish the relationship between plaque progression and clinical endpoints.

Important outcomes

Currently, local distension, i.e., the diameter change over the cycle, is determined with radiofrequency phase tracking applied to recordings obtained at a high frame rate (>300 fps) (Meinders et al. 2001). Because an expensive and dedicate ultrasound machine is necessary for high frame rate recordings, its application is restricted to a limited number of specialized hospitals. We have shown in **Chapter 3** that the local artery distension can be extracted with semi-automatic edge tracking techniques applied to standard B-mode echo recordings (40 fps) as precise and accurate as with radiofrequency phase tracking. We validated our method in an older patient population. Despite curved arteries and motion artifacts, which are common for this population, validation was successful, corroborating that our edge tracking technique will also work adequately in younger patients or those without atherosclerotic disease. Therefore, the edge tracking technique enables the wider use of local distension technique with the standard ultrasound systems available in any hospital.

Commonly, distance and distension measurements are performed along the ultrasound beam. However, in case of plaques or curved vessels, measurements along the ultrasound beam lose their relevance, because of the discrepancy between the light of sight and the true artery orientation. Therefore, in **Chapter 7** we introduced orthogonal distance measurements, i.e., along the radius of the artery. It was shown that orthogonal distance measurements have a direct impact on the morphological evaluation of an artery segment, specifically the lumen and adventitia-adventitia diameter distribution across a stenosis, providing, e.g., the degree of a stenosis.

Previous studies often focused on either mechanical or morphological characteristics of a plaque. An innovative development in this thesis is the integrated assessment of both characteristics to reveal their associations (**Chapter 6 and 7**). For example, in **Chapter 7** we showed associations between the risetime inhomogeneity of distension distribution obtained for the common carotid artery, and the composition of a distal plaque as determined by magnetic resonance imaging. Therefore, the suggested ultrasound technique might simplify assessment of plaque vulnerability.

Future perspectives towards clinical implementation

This thesis focuses on the baseline results of the PARISK study, because the 2-year follow-up study could not be completed within the available time frame. All non-invasive imaging techniques are reapplied in 150 patients 2 years after inclusion. From these follow-up data plaque progression, i.e. change in plaque size, can be extracted and related to the risk factors obtained with the non-invasive imaging techniques (US, MRI and CT). The main endpoint, i.e. which patients endured a recurrent TIA or stroke, will be available at the end of 2016. Since only a few patients will suffer from a recurrent TIA or stroke, the follow-up is extended for another three years.

It would be very interesting to determine the factors, present at baseline, that predict a TIA or stroke. Moreover, the results might establish the relative relevance of the respective imaging techniques including the sequence of application. Preference should be given to techniques that are widely available and can be imminently applied to act as a first screening tool for patient selection. A large randomized trial will be necessary to prove the prediction value of the determined risk factors and to eventually incorporate the new findings in clinical practice. Already, a large longitudinal study (European Carotid Surgery Trial-2) has started which also includes MR and ultrasound plaque imaging.

References

Buisman LR, Tan SS, Nederkoorn PJ, Koudstaal PJ, Redekop WK. Hospital costs of ischemic stroke and TIA in the Netherlands. Neurology 2015;84:2208-2215.

Chaturvedi S, Bruno A, Feasby T, Holloway R, Benavente O, Cohen SN, Cote R, Hess D, Saver J, Spence JD, Stern B, Wilterdink J, Therapeutics, Technology Assessment Subcommittee of the American Academy of N. Carotid endarterectomy--an evidence-based review: report of the Therapeutics and Technology Assessment Subcommittee of the American Academy of Neurology. Neurology 2005;65:794-801.

Koopman C, van Dis I, Vaartjes I, Visseren FLJ, Bots ML. Hart- en vaatziekten in Nederland 2014, cijfers over kwaliteit van leven, ziekte en sterfte. 2014

Meinders JM, Brands PJ, Willigers JM, Kornet L, Hoeks AP. Assessment of the spatial homogeneity of artery dimension parameters with high frame rate 2-D B-mode. Ultrasound Med Biol 2001;27:785-794.

Nederlandse vereniging voor Neurologie. Richtlijn Diagnostiek, behandeling en zorg voor patienten met een beroerte. 2008

Nichols M, Townsend N, Luengo-Fernandez R, Leal J, Gray A, Scarborough P, Rayner M. European cardiovascular disease statistics 2012. European Heart Network, Brussels, European Society of Cardiology, Sophia Antipolis 2012;

Park JH, Ovbiagele B. Optimal combination secondary prevention drug treatment and stroke outcomes. Neurology 2015;84:50-56.

Dankwoord

Dankwoord

Na een tijd hard werken is mijn proefschrift afgerond. Dit had ik natuurlijk niet kunnen bereiken zonder de hulp van een groot aantal personen: van begeleiders tot vrienden en van collegae tot familie. Mijn relaties met deze mensen is heel divers. Het figuur op de pagina hiernaast illustreert (een deel van) mijn persoonlijke en zakelijke netwerk dat ik de afgelopen jaren heb opgebouwd. Dit overzicht laat goed zien welke dwarsverbanden er in dit netwerk aanwezig zijn. Tijdens mijn promotie heb ik me gerealiseerd dat het opbouwen, inzetten en onderhouden van een netwerk erg belangrijk is. Niet alleen voor het werk zelf, maar ook voor de broodnodige ontspanning. Graag wil ik alle mensen in mijn netwerk bedanken voor hun bijdrage of steun, direct of indirect, tijdens mijn promotiewerk.

Het eerste onderdeel van het netwerk rondom mijn promotie is mijn promotieteam. Graag wil ik hen bedanken voor hun steun, vertrouwen en hun geduld tijdens de afgelopen jaren. Geachte prof. W.H. Mess, beste Werner, bedankt voor al je input. In het bijzonder jouw klinische invalshoek was erg waardevol. Onze vergaderingen waren inspirerend en leidde vaak tot nieuwe ideeën. Geachte prof. A.P.G. Hoeks, beste Arnold, ook al ben je wellicht niet officieel onderdeel van mijn promotieteam; zonder jouw begeleiding was dit proefschrift er nooit in deze vorm gekomen. Jouw kennis van ultrageluid evenals de door jouw ontwikkelde analyse methoden maakten mijn promotie een mooie, leerzame tijd. Het omdraaien van redeneringen leidde soms tot verwarring, maar gaf uiteindelijk een dieper inzicht. Koen, je bent pas in een later stadium betrokken geraakt bij mijn promotie. Bedankt voor je ondersteuning tijdens deze laatste loodjes. Evelien, ook jij maakt geen deel uit van mijn officiele promotieteam, maar hoort niet minder in dit rijtje thuis. Ik heb onze discussies altijd erg nuttig en leerzaam gevonden. Bedankt dat je mijn paranimf wilt zijn!

Naast het promotieteam is een belangrijk onderdeel in mijn netwerk de leescommissie. Graag wil ik prof. dr. A.A. Kroon, prof. dr. P. Boutouyrie, prof. dr. C.L. De Korte, prof. dr. G.W.H. Schurink en dr. J. Staals bedanken voor de beoordeling van mijn proefschrift.

Naast het promotieteam hebben mijn collega's van de PARISK studie een belangrijke bijdrage geleverd aan het onderzoek beschreven in mijn proefschrift. Door deze samenwerking zijn er meerdere (toekomstige) proefschriften tot stand gekomen. Martine, Floris, Stefan, en Geneviève bedankt voor jullie inzet en medisch inzicht! Ik heb het erg prettig gevonden om samen een team te vormen en zo elkaar op medisch en technisch gebied verder te helpen. Ook alle activiteiten buiten het werk waren altijd erg gezellig!

Ik heb met veel plezier gewerkt op de afdeling Biomedische Technologie. Op ons "lab" heerste een serieuze, maar gezellige werksfeer. Naast dat iedereen hard werkte aan zijn onderzoek, was er ook meer dan genoeg ruimte voor minder serieuze dingen. Van tafeltennis in de pauzes tot kriek op vrijdagmiddag (bedankt Peter en Lauren!). Tegelijkertijd was er ook altijd iemand bereid om mee te denken over onderzoek of te helpen met software vragen (Bart, Wouter, Sjeng bedankt daarvoor!).

Vrijwel al mijn metingen heb ik uitgevoerd op de afdeling Klinische Neurofysiologie van het MUMC+. Vanaf het begin heb ik me thuis gevoeld op deze afdeling. Ik heb leuke herinneringen aan de Sinterklaasavonden en KNF uitjes. Graag wil ik alle laboranten, in het bijzonder Nathal, Chantal, Odette, en Jos, bedanken voor hun flexibiliteit en inzet bij het uitvoeren van de vele metingen voor mijn proefschrift.

Met behulp van mijn netwerk ben ik inmiddels toegetreden tot het netwerk van Yacht. Mireille en Bram, bedankt voor jullie vertrouwen! Al snel heb ik kunnen beginnen aan een uitdagend project bij Philips Personal Health Solutions. Mieke, Elke, Annelies en Jos, ik werk met veel plezier met jullie samen.

Naast het zakelijke netwerk heeft iedereen natuurlijk ook een privé netwerk. Tijdens mijn studie Biomedische Technologie aan de TU in Eindhoven is er een hechte vriendengroep ontstaan, waarvan het merendeel ook is gaan promoveren. Bedankt voor alle leuke etentjes en uitjes! Het is enerverend om de verschillen, maar zeker ook de overeenkomsten tussen onze promoties te zien. Het is bijzonder dat we nu de verdediging van elkaars proefschriften kunnen meemaken.

Mijn netwerk kan natuurlijk niet zonder mijn familie. Gaia en Yuri, bedankt voor jullie steun en gezellige momenten. Het is interessant om te zien dat wij, als broer en zussen, zulke verschillende persoonlijkheden hebben. Beide opa's en oma's, het is bijzonder en leuk dat jullie mijn promotie kunnen meemaken. Karin, Toine en Krista, bedankt voor jullie steun; we genieten van jullie heerlijke kookkunsten en gezellige bezoekjes!

Netwerken heb ik niet van een vreemde. Mijn beide ouders hebben ook een groot netwerk. Van nature ben ik ook altijd leergierig geweest, iets wat thuis altijd gestimuleerd werd. Graag wil ik mijn ouders, Inge en Maarten, bedanken voor hun steun en adviezen. Maarten, het was erg boeiend (en relativerend) om te horen hoe jij, als ervaren promotor, een promotietraject beleeft. Dit is de eerste promotie waarbij je wel betrokken bent maar toch 'slechts' in de zaal mag plaats nemen tijdens de verdediging.

Raf, zonder jouw hulp en steun was ik nooit zover gekomen. Je bent het zwaartepunt binnen mijn netwerk. Je hebt altijd een luisterend oor en we kunnen goed discussiëren over allerlei onderwerpen, van privé tot werk. We hebben elkaar altijd kunnen helpen als het bij de ander even niet goed lukte. Een promotie schijnt een goede relatie test te zijn en wij hebben allebei onze promoties binnen hetzelfde project van begin tot einde samen gedaan! Werk en privé gaan dus prima samen; ze hoeven niet (strikt) gescheiden te worden. Een bijzonder feit daarbij is dat we, vanaf ons eerste jaar op de TU in Eindhoven, op exact dezelfde dagen onze diploma's hebben gehaald; van onze propedeuse tot onze promoties! Erg bedankt voor je steun en ik verheug me op onze toekomst samen!

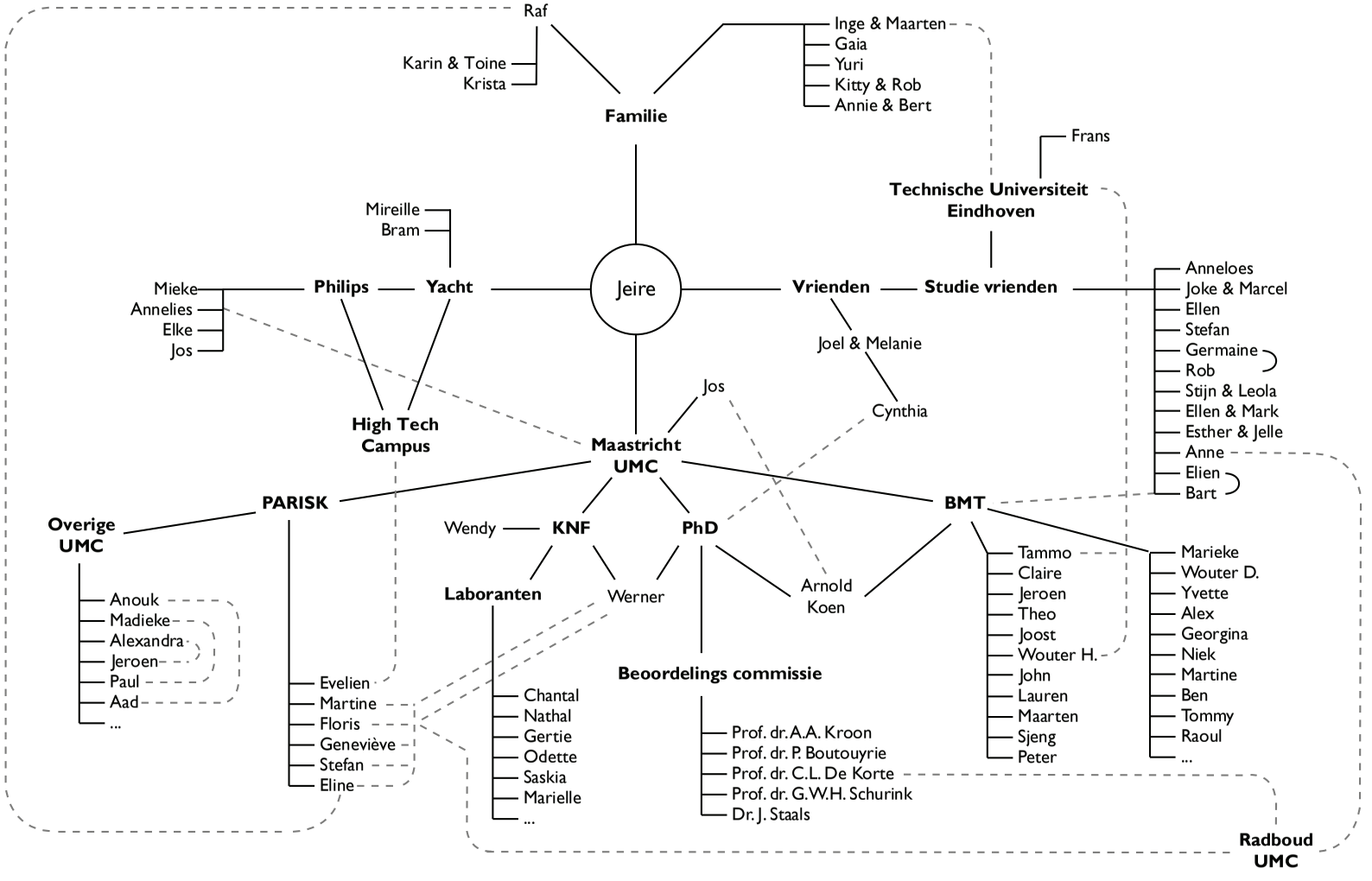
Raf
Karin & Toine
Krista
Familie
Inge & Maarten
Gaia
Yuri
Kitty & Rob
Annie & Bert
Frans
Technische Universiteit Eindhoven
Mireille
Bram
Mieke
Annelies
Elke
Jos
Philips
Yacht
Jeire
Vrienden
Studie vrienden
Anneloes
Joke & Marcel
Ellen
Stefan
Germaine
Rob
Stijn & Leola
Ellen & Mark
Esther & Jelle
Anne
Elien
Bart
Joel & Melanie
Cynthia
Jos
High Tech Campus
Maastricht UMC
PARISK
Overige UMC
Wendy
KNF
PhD
BMT
Anouk
Madieke
Alexandra
Jeroen
Paul
Aad
...
Evelien
Martine
Floris
Geneviève
Stefan
Eline
Laboranten
Chantal
Nathal
Gertie
Odette
Saskia
Marielle
...
Werner
Arnold
Koen
Beoordelings commissie
Prof. dr. A.A. Kroon
Prof. dr. P. Boutouyrie
Prof. dr. C.L. De Korte
Prof. dr. G.W.H. Schurink
Dr. J. Staals
Tammo
Claire
Jeroen
Theo
Joost
Wouter H.
John
Lauren
Maarten
Sjeng
Peter
Marieke
Wouter D.
Yvette
Alex
Georgina
Niek
Martine
Ben
Tommy
Raoul
...
Radboud UMC

About the author

Curriculum Vitae

Jeire Steinbuch was born on January 3rd, 1988 in Heeze, The Netherlands. After obtaining her high school (pre-university) diploma (gymnasium) at the Carolus Borromeus College in Helmond in 2006, she started studying Biomedical Engineering at the Eindhoven University of Technology. In 2009 she received her BSc degree (cum laude). In the same year, she started the Master Medical Engineering at the Eindhoven University of Technology, where she obtained her MSc degree (with great appreciation) in 2011. During her Master she did a 3-month internship at the Mario Negri Institute for Pharmacological Research in Bergamo, Italy under the supervision of ir. S Manini, prof. A Remuzzi and prof.dr.ir. FN van de Vosse. During the internship she investigated the effects of geometric parameters on pressure drop in an arteriovenous fistula. She completed her Master thesis under supervision of dr.ir. W Kroon and prof.dr.ir. FN van de Vosse at the department of Biomedical Engineering at Maastricht University, where she developed a constitutive modelling approach to study in vivo flow-induced structural remodelling of blood vessels. From December 2011 until May 2016 she worked as a PhD student at the department of Biomedical Engineering, Maastricht University under supervision of dr.ir. KD Reesink, prof.dr.ir. APG Hoeks and prof.dr. WH Mess. The PhD research project was part of the Plaque At RISK (PARISK) study within the Center for Translational Molecular Medicine (CTMM) national programme, which aims to evaluate plaques at risk with multiple non-invasive imaging techniques to improve identification of patients at increased risk of stroke. As of October 2016, she works as an interim professional at the Life Science unit at Yacht in Eindhoven/Maastricht. Currently, she is working on an assignment as a Clinical Project Manager at Philips Personal Health Solutions.

Publications

Published publications

Steinbuch J, Van Dijk AC, Schreuder FHBM, Truijman MTB, Hendrikse J, Nederkoorn PJ, Van der Lugt A, Hermeling E, Hoeks APG, Mess WH. Definition of common carotid wall thickness affects risk classification in relation to degree of internal carotid artery stenosis: The Plaque At RISK (PARISK) study. Cardiovasc Ultrasound 2017;15:9.

Steinbuch J, Van Dijk AC, Schreuder FHBM, Truijman MTB, De Rotte AAJ, Nederkoorn PJ, Van der Lugt A, Hermeling E, Hoeks APG, Mess WH. High spatial inhomogeneity in the intima-media thickness of the common carotid artery is associated with a larger degree of stenosis in the internal carotid artery: The PARISK study. Ultraschall Med 2016. (accepted)

Steinbuch J, Hoeks AP, Hermeling E, Truijman MT, Schreuder FH, Mess WH. Standard B-Mode Ultrasound Measures Local Carotid Artery Characteristics as Reliably as Radiofrequency Phase Tracking in Symptomatic Carotid Artery Patients. Ultrasound Med Biol 2016;42:586-595.

Truijman MT, de Rotte AA, Aaslid R, van Dijk AC, Steinbuch J, Liem MI, Schreuder FH, van der Steen AF, Daemen MJ, van Oostenbrugge RJ, Wildberger JE, Nederkoorn PJ, Hendrikse J, van der Lugt A, Kooi ME, Mess WH. Intraplaque hemorrhage, fibrous cap status, and microembolic signals in symptomatic patients with mild to moderate carotid artery stenosis: the Plaque at RISK study. Stroke 2014;45:3423-3426.

Submitted publications

Steinbuch J, Schreuder FHBM, Truijman MTB, Hendrikse J, Nederkoorn PJ, Van der Lugt A, Kooi ME, Hoeks APG, Mess WH. Spatial inhomogeneity of diastolic-systolic risetime of the distension waveform in the common carotid artery is associated with lipid-rich necrotic core in distal plaques: The Plaque At RISK (PARISK) study.

Steinbuch J, Schreuder FHBM, Reesink KD, Hoeks APG, Mess WH. Carotid plaques do not modify orthogonal adventitia-adventitia diameter while relative lumen distension is negatively associated with plaque echogenicity.

Abstracts

Steinbuch J, Schreuder FHBM, Truijman MTB, de Rotte AAJ, Liem MI, Hermeling E, Hoeks APG, Mess WH. The inhomogeneity of diastolic-systolic rise time of the distension waveform distribution in the common carotid artery is associated with lipid presence of distal plaques. Artery 15. Krakow, Poland 2015; oral presentation

Steinbuch J, Schreuder FHBM, Hermeling E, Van Dijk AC, Truijman MTB, Hoeks APG, Mess WH. Spatial inhomogeneity in distension and intima-media thickness. Artimino ultrasound conference, Glumslöv, Sweden 2015; oral presentation

Steinbuch J, Hermeling E, Schreuder FHBM, Truijman MTB, Hoeks APG, Mess WH. Artery distension detection with B-mode echo-tracking and radio-frequency phase-tracking have similar absolute values and precision. Artery 14, Maastricht, Netherlands 2014; poster presentation

Steinbuch J, Truijman MTB, Hermeling E, Hoeks APG, Mess WH. Spatial characterization of common carotid artery inhomogeneities in patients with plaques in the bifurcation. Artimino, Lake Rosseau, Canada 2013; oral presentation

Steinbuch J, Truijman MTB, Hoeks APG, Mess WH. Spatial inhomogeneities in intima-media thickness of the common carotid artery are associated with the degree of stenosis in the internal carotid artery. Artery 13, Londen, United Kingdom 2013; oral presentation

Awards and grants

Young Investigator Presentation Award (3rd place), Artery 15, Krakow, Poland, 2015

Student educational bursary, Artery 15, Krakow, Poland, 2015

Brigitte Laloux bursary award, Artery 13, London, United Kingdom, 2013

Erasmus grant, Eindhoven University of Technology, Eindhoven, Netherlands, 2010

BEST/e Grant Eindhoven University of Technology, Eindhoven, Netherlands, 2009